University of Alberta

Tissue engineering therapies for cleft palate reconstruction

By

Nesrine Abdel Hady Zakaryia Mostafa

A thesis submitted to the Faculty of Graduate Studies and Research

in partial fulfillment of the requirements for the degree of

Doctor of Philosophy

in

Medical Sciences - Dentistry

Fall 2013

Edmonton, Alberta

Dedication

I would like to dedicate this thesis to

My dear husband, Mostafa and my lovely children Logean and Mohamed who joined me during the whole process and helped me in every way with their love, support and patience

My beloved parents (A. Mostafa and F. El-Sayed), my dear sister Nermine and my dear brothers (Sameh and Hany), who gave me hope and strength throughout my entire life

Abstract

This thesis was intended to develop two tissue engineering approaches for cleft palate reconstruction. One approach focused on developing a cell-based therapy *in vitro*, using osteogenically induced mesenchymal stem cells (MSCs). The other approach focused on the delivery of bone morphogenetic protein-2 (BMP-2) in a scaffold designed to provide sustained release after *in vivo* implantation.

To develop a cell-based therapy, MSCs were cultured with combinations of dexamethasone, vitamin-D3, basic fibroblast growth factor (b-FGF), and BMP-2. A comparison between osteogenesis and adipogenesis was pursued to investigate the best combination. An optimal condition was obtained at dexamethasone (10 nM) and BMP-2 (500 ng/mL) for mineralization without increasing adipogenesis-related markers. BMP-2 and dexamethasone were found to be essential for mineralization of MSCs. The b-FGF mitigated osteogenesis and enhanced adipogenesis. Vitamin-D3 appeared essential for calcification only in the presence of b-FGF.

Rodent models of both surgically induced and spontaneous cleft palate are available, but are subject to several limitations. Hence, we modified the dimension of the two published rodent models of cleft palate (mid palate cleft "MPC", and alveolar cleft "AC") and assessed bone healing by micro-computed tomography (μCT) and histology. Virtual planning was performed to determine the accurate design of MPC and AC defects based on preoperative μCT images. Planned dimensions were similar to dimensions reproduced surgically. There was no significant difference in percent bone filling between MPC group and AC

group at weeks 4 and 8. The presented modifications for AC and MPC cleft models made them more reliable and clinically relevant. However, the MPC defect had less anatomical challenges and larger residual defect volume as compared to AC defect, therefore this model was used for subsequent studies.

A nanofiber (NF) based scaffold with collagen (ACS) backbone impregnated with BMP-2 was prepared and implanted in the MPC defect. Five treatments were evaluated: no scaffold, ACS alone, ACS+BMP-2, NF+ACS, and NF+ACS+BMP-2. Constructs containing BMP-2 demonstrated enhanced bone healing as compared to other groups. Based on histologic evaluations, both H&E and trichrome staining, together with cross-sectional and 3D reconstructed μCT images, NF+ACS+BMP-2 treatment resulted in better and more consistent bone healing when compared to ACS+BMP-2 group.

In conclusion, osteogenically induced MSCs and BMP-2 loaded in a NF based scaffold are promising bone tissue engineering therapies for cleft palate reconstruction.

Acknowledgment

It is indeed a great pleasure and a moment of great satisfaction for me to express a deep sense of gratitude toward:

Dr. Paul W. Major for his patience, guidance and endless support that helped me to successfully complete my doctoral dissertation. His commitments, obligations and busy schedule did not prevent him to provide me with all the help that I needed throughout the PhD program.

Dr. Michael Doschak for giving me the opportunity to pursue my studies in his lab. In addition to the scientific knowledge and training, the learning experience under his supervision included an emphasis on developing collaborative relationships with peers, and the ability to work both independently as well as part of a team.

Dr. Larry D. Unsworth and his group for the productive discussions leading to the development of the nanofiber hydrogel

Dr. Reena Talwar for dedicating a lot of time and energy into the animal studies. Her expertise, guidance and encouragement considerably improved my graduate research experience and increased the clinical relevance of my PhD project.

Dr. Anthea Senior and **Dr. Seema Ganatra** for their incredible support during my teaching in Radiology

All my lab mates (Dr. Neel Kaipatur, Mr. Arash Panahifar, Dr. Madhuri Newa, Ms.YuChin Wu, Ms. Kathy Tang, Dr. Yang Yang, and Mr. Imran Khan) for creating a pleasant work environment in the lab

Mrs. Pat La Pointe for her help to facilitate all the administrative work need for my graduate studies.

Prosthodontics' lab team: Mr. Youssef Sleiman, Mr. Paul Ladell, Ms. Zenona Kawecka, and Mr. Anthony Sawchuk for the development of the surgical template.

Finally, I gratefully acknowledge the funding sources that made my work possible:

- Department of Dentistry, University of Alberta (Fund for Dentistry)
- Faculty of Graduate Studies and Research, University of Alberta
- Canadian Institutes of Health Research (CIHR)
- Alberta Innovates- Health Solutions (AIHS)
- Graduate Students' Association, University of Alberta

Table of Contents:

List of Tables

List of Figures

List of abbreviations

ACS	Absorbable collagen scaffold
ALP	Alkaline phosphatase
ANOVA	Analysis of Variance
ATP	Adenosine triphosphate
BMP	Bone morphogenetic protein
BMPR	Bone morphogenetic protein receptor
BSP	Bone sialoprotein
C/EBP	Ccaat-enhancer-binding proteins
CBCT	Cone-beam computed tomography
CFU	Colony-forming unit-fibroblasts
DMEM	Dulbecco's Modified Eagle Medium
DMSO	Dimethyl sulfoxide
DNA	Deoxyribonucleic acid
ECM	Extracellular matrix
EDTA	Ethylene Diamine Tetra Acetic acid
FBS	Fetal bovine serum
FDA	Food and drug administration
FGF	Fibroblast growth factor
FITC	Fluorescein isothiocyanate
GAPDH	Glyceraldehyde 3-phosphate dehydrogenase
HA	Hydroxyapatite
HBSS	Hank's Balanced Salt Solution
ICC	Intraclass correlation coefficient
MPC	Mid palate cleft
MSCs	Mesenchymal stem cells
NFAT	Nuclear factor of activated T cells
NPP	p-nitrophenol phosphate
OPN	Osteopontin
PBS	Phosphate buffer saline

PCL	Poly(ε-caprolactone)
PCR	Polymerase chain reaction
PDGF	Platelet derived growth factor
PDL	Periodontal ligament
PLA	Poly(lactide)
PLGA	Poly(glycolic acid)
PMCB	Particulate marrow cancellous bone
PPAR	Peroxisome proliferator-activated receptor gamma2
PRM	Placental resorbable membrane
RCT	Randomized controlled trial
RGD	Arginine-Glycine-Aspartic acid
RNA	Ribonucleic acid
ROI	Region of interest
TCP	Tricalcium phosphate
TGF	Tumour growth factor
TNF	Tumour necrosis factor

Chapter 1

General Introduction

1.1 STATEMENT OF THE PROBLEM

Clefts of lip and palate are common birth defects that have a worldwide frequency of 1·7 per 1000 live born babies with interesting racial predilections. North Americans are affected with incidence of 1 per 700 births, Mongolians, 0.55–2.50 per 1000 births, Negroids, 0.18–0.82 per 1000 births, and Caucasians, 0.69– 2.35 per 1000 births.[1]

Clefts can involve the lip with or without the palate or can involve the palate alone. Based on anatomy, the palate can be divided into primary and secondary palates. Primary palate comprises structures located anterior to the incisive foramen (lip and alveolus) while, secondary palate involves structure posterior to the incisive foramen (hard and soft palates). Thus clefts could involve the primary palate, secondary palate, or both. A cleft of the primary palate can be further divided into unilateral or bilateral.[2] Clefts of the primary palate occur due to incomplete fusion between medial nasal and maxillary processes. While, clefting of the secondary palate results from incomplete fusion of the palatine shelves.[3]

Clefts can be further classified into isolated and syndromic clefts. Isolated clefts occur in approximately 50-70% of cleft cases while, 15% of the cases have been identified as a feature in more than 300 syndromes. Individuals with isolated clefts have no other related health problems. But in syndromic clefts, the individual has a set of physical, developmental, and sometimes behavioural features that occur together.[4]

In general, children with cleft defects need multidisciplinary health care from birth till adulthood including surgery, speech therapy, dental care and psychological support.[5] Hence, the expected average lifetime treatment cost is ~100,000 US per oral cleft patient in North America which imposes a large psychosocial and economic burden on affected families and society.[6, 7] Cleft patients are associated with several health problems and complications leading to reduced quality of life. This population has higher morbidity rate as compared to unaffected individuals.[8]

Surgical management of patients with cleft palates involves a well-established

protocol. Primary soft tissue closure is performed at 3-5 months of age to correct the associated feeding and speech problems without interfering with maxillary growth.[9] The principal factors in defining the time of secondary grafting of bony cleft defect, which is performed at 5-6 years of age, are maxillary growth and dental age of the patient. Generally, bone grafting is more successful if it is performed before permanent canine eruption.[10] The objectives of alveolar bone grafting include maxillary arch stabilization, closure of the oronasal fistula, facilitating tooth eruption, supporting the alar base and improving nasal symmetry.[11] It also provides adequate alveolar bone for prosthodontic rehabilitation of the edentulous segment.[12]

In selecting the ideal bone grafting material to achieve a successful clinical outcome, three specific properties are desired: osteogenesis (new bone formation by living bony cells in the graft), osteoinduction (stimulation and recruitment of *in situ* osteoprogenitor cells to graft site), and osteoconduction (inward migration of osteoprogenitor cells and vascular tissue into scaffold).[13] Autograft is the only graft that contains all these properties and hence it is the current gold standard therapy for cleft palate reconstruction.[14] Autogenous bone grafts can be acquired from the iliac crest, mandibular symphysis, rib, tibia or calvarium, with each donor site having its benefits and drawbacks.[10] Irrespective of the donor site, several complications were associated with the procedure such as postoperative pain, infection and scarring at the donor site that hamper the desired therapeutic outcomes.[15] Therefore, several studies evaluated the efficacy of different artificial bone grafting materials including demineralized bone matrix, hydroxyapatite, cadaveric bone grafts and methylmethacrylate. These biomaterials have the osteoconductive property and provide adequate structural support, but they do not provide the bioactivity needed to stimulate tissue regeneration and are more susceptible to infection.[16] To overcome these limitations, bone tissue engineering has been proposed as a viable alternative.[5] In this approach, appropriate cells (osteogenic) and/or osteoinductive molecule are combined with osteoconductive biomaterial scaffolds until a suitable bone graft is achieved.

The ideal cell source should have no immune rejection, no tumorigenicity, no graft *versus* host disease, controlled cellular proliferation, reliable osteogenic potential, and controlled integration into the adjacent tissues.[17] Embryonic stem (ES) cells are potential cell source for cell-based therapies for repairing craniofacial defects. ES cells have the capability to differentiate into any cell type.[18] However, ethical issues, dysregulation of ES cell differentiation, and immune rejection may limit their applicability in the near future.[19] Therefore, mesenchymal stem cells (MSCs) from autologous bone marrow (i.e., bone marrow stromal cells) are considered an ideal source of cells for bone tissue engineering constructs, as they are readily available from the host, can be easily expanded in standard culture conditions, high proliferative potential, and have predictable osteogenic potential without possibility of immune rejection or tumorigenicity.[17] Successful use of MSCs for augmentation of bone mass and repair requires these cells to be stimulated down the osteogenic pathway *in vitro* before *in vivo* transplantation. Among several molecules used for inducing the osteogenic commitment of MSCs are bone morphogenetic proteins (BMPs), basic fibroblast growth factor (b-FGF), vitamin D3 (Vit-D3), and dexamethasone (Dex).

BMPs are arguably the most studied growth factors in bone regeneration. BMPs are part of the transforming growth factor beta (TGF-β) protein family. Among the BMPs, BMP-2 is best known for its osteoinductive capacity and it is clinically used for bone regeneration. It acts as a chemotactic agent (attracting stem cells to implantation site)[20] and as a morphogen (causing osteogenic differentiation of stem cells) if placed in the appropriate environment.[21]

The delivery of MSCs and/or BMPs to cleft palate defects requires the utilization of a carrier to maximize therapeutic outcomes. The osteoconductive scaffold should mimic the extracellular matrix (ECM), and control bone formation in the desired contour and position. Collagen is a clinically inspired biomaterial as it forms the backbone of native bone tissue (~ 90% of extracellular matrix is composed of collagen type I).[22] Absorbable collagen scaffold (ACS) has low

antigenicity, low toxicity and is biodegradable.[23] It also contains RGD (Arginine-Glycine-Aspartic Acid) and non RGD domains that facilitate cell migration, attachment, proliferation, and differentiation.[24, 25] Therefore, the Food and Drug Administration (FDA) has approved BMP-2 loaded Absorbable Collagen Sponge (ACS) for specific surgical indications in humans.[26] Despite successful bone formation through simple adsorption of BMP-2 on collagen scaffold, burst release of growth factors with fast reduction of biological activity and the lack of controlled release limits its utility.[27] As bone growth is temporal, the appropriate cells may not be attracted to the defect area until after considerable diffusion of BMP-2 from the site.[28] Therefore, an effective delivery system is still needed to localize and maintain the proper dose of BMP-2 at the defect site for longer time. Self-assembling peptide nanofiber (NF) based hydrogel RADA16-I (Arginine-Alanine-Aspartic Acid- Alanine) is a hydrated 3D insoluble network that has been used for protein delivery. It provides timed release for growth factors and good diffusion properties along with its biocompatibility and low toxicity.[29] It is made from natural amino acids, which can be metabolized naturally and safely by the body.[30] Studies reported that NF based scaffolds supported proliferation and osteogenic differentiation of osteoprogenitor cells, suggesting possible application for bone tissue engineering.[31, 32]

Towards this end, this thesis focused on the development of two tissue engineering approaches for cleft palate repair. In the first approach, osteogenically induced MSCs were utilized to develop a cell-based therapy. While, the second approach focused on the development of NF based collagen scaffold for sustained BMP-2 delivery. The efficacy of this scaffold was then evaluated *in vitro* and *in vivo* in a rodent model of cleft palate. The applicable clinical and social benefits of these innovative therapies include reduction in donor site morbidity, hospital stay duration and overall procedure cost, when compared to autologous bone grafts.

1.2 SPECIFIC AIMS

Aim 1: To elucidate the mechanism(s) of action of different osteogenic supplements on the *in vitro* differentiation of MSCs.

Our long-term aim is to determine the appropriate combination(s) of osteogenic supplements needed for developing a cell-based therapy for bone regeneration in cleft defects.

Aim 2: **Developing an appropriate scaffold for *in vivo* delivery of BMP-2 for effective bone formation in a cleft palate model.**

This was achieved through the following outline:

- **Specific Aim 2.1:** To develop a reliable cleft defect rodent model suitable for cleft palate research.
- **Specific Aim 2.2:** To design a novel carrier for sustained BMP-2 release and to evaluate its effectiveness for *in vivo* bone formation in the developed cleft palate model.

1.3 THESIS HYPOTHESIS

Hypothesis 1: Combining the optimal dose of BMP-2 and b-FGF, along with Vit-D3 and Dex, will result in synergistic effects that may further augment osteogenic differentiation of MSCs.

Hypothesis 2: Bio-absorbable scaffolds that retard the burst release kinetics of doped BMP-2 will enhance *in vivo* local delivery of BMP-2 and produce more effective bone formation in a cleft palate defect.

- **Hypothesis 2.1:** A reliable and clinically relevant surgical critical size cleft defect will be developed in rodents based on careful assessment with micro-computed tomography (μCT).
- **Hypothesis 2.2:** The designed NF scaffold will offer a sustained release of BMP-2 over extended period of time and will enhance *de novo* bone formation after *in vivo* implantation into the developed model of cleft palate.

1.4 SCOPE OF DISSERTATION

The introduction of this thesis consists of three chapters (a general introduction, a literature review, and an evidence-based review). Subsequently, three chapters were structured to address all the objectives and to test the research hypotheses with final chapter for general discussion and conclusion.

Chapter 1 (the present chapter) summarized epidemiology, etiology, current treatments, and alternative therapies for cleft palate patients. Bone tissue engineering was emphasized with special attention to the characteristics of appropriate scaffolds, cell source, and signalling molecules. Then, thesis objective and hypothesis were discussed. Finally, the scope of the thesis was presented.

An overview of cell-based and protein-based tissue engineering modalities for cleft palate reconstruction is detailed in **Chapter 2**. Critical observations from both *in vitro* and *in vivo* studies utilizing MSCs and BMP-2 for cleft palate reconstruction were emphasized. Moreover, molecular basis of osteogenic differentiation of MSCs as well as mechanism of bone healing following bone grafting were summarized. Finally, major concerns regarding the application of tissue engineering in children and challenging cleft defects were discussed.

In **Chapter 3**, an evidence-based review was conducted to specifically address the effectiveness of BMP-2+ACS for cleft palate reconstruction. Comprehensive searches of 5 databases were conducted to identify all articles using BMP-2+ACS for cleft palate reconstruction in humans. Selected articles were classified based on different levels of evidence published by Oxford Centre for Evidence-based Medicine. Characteristics of the reviewed studies were summarized. The clinical outcomes as well as adverse events following BMP-2+ACS grafting were compared to the standard autologous bone grafting therapy to provide complete picture on the effectiveness of the therapy. Contraindications for BMP-2+ACS graft were also reviewed. Finally, future considerations were discussed to help improving the quality of future research in this area.

Developing cell-based therapy for bone regeneration was elaborated in

Chapter 4. The studies were conducted using human MSCs with a main focus on optimal approach for *in vitro* modification of the cells in order to assess their potential for developing cell-based therapy but no *in vivo* transplantations were done (to maintain project focus). A step-by-step approach was taken to clarify the role of specific osteogenic supplements, namely dexamethasone (Dex), vitamin D3 (Vit-D3), basic fibroblast growth factor (b-FGF), and BMP-2 on MSC differentiation. Osteogenic and adipogenic differentiation were evaluated concurrently in MSCs cultures exposed to range of concentrations and combinations of those osteogenic supplements. Osteogenesis was assessed by alkaline phosphatase (ALP) activity, mineralization, and gene-expression of ALP, Runx2, bone sialoprotein (BSP), and osteonectin (ON). Adipogenesis was characterized by Oil Red O staining, gene-expression of peroxisome proliferator-activated receptor (PPARγ2) and adipocyte protein-2 (aP2).

An appropriate animal model of cleft palate is necessary to test the efficacy of new biomaterials for secondary bone grafting. Therefore, **Chapter 5** is focused on developing a reliable rodent model of cleft palate. Two main rodent models of gingivoperiosteoplasty are published namely mid palate cleft (MPC) model[33] (9×5×3 mm^3) and alveolar cleft (AC) model[34] (7×4×3 mm^3). But both models had limitations: one was not a critically sized defect[33] and the other failed when utilized for testing bone grafting therapies based on BMP-2.[34, 35] Therefore, this chapter critically assessed and compared the current rodent models of cleft palate to identify the most reliable model. This was achieved through a series of successive experiments. In the pilot study we attempted to reproduce the 7×4×3 mm^3 AC model in 8 weeks old Sprague Dawley rats but this resulted in significant injury of the surrounding structures. The same dimensions were then reproduced in 16 weeks old Sprague Dawley rats and damage to adjacent structures was observed again. Then, we compared the anteroposterior and transverse dimensions of the maxilla in non operated 16 weeks old Sprague Dawley vs. Wistar rats. Subsequently, virtual planning for the appropriate design of MPC and AC defects was performed in 16 weeks old Wistar rats. Finally, we

conducted a comparative study to assess bone healing of the modified MPC and AC defects in 16 weeks old Wistar rats over 8 weeks. Modified defects were designed to be at least 1 mm away from roots of the incisors to avoid damage to PDL, 1 mm away from the palatine foramen and 1 mm away from the zygomatic arch. Bone healing in the two models was assessed by "*in vivo*" μCT (weeks 0, 4, and 8) and histology (week 8) to confirm the critical size nature of the modified defects.

The second bone tissue engineering approach based on the delivery of BMP-2 in a properly designed scaffold was elaborated in **Chapter 6**. NF based scaffold with ACS backbone was prepared to provide the necessary sustained release of BMP-2 after *in vivo* implantation. The choice of the appropriate NF density is an important factor that determines the release profile and the overall success of the delivery system *in vivo*. Therefore, the release profile of BMP-2 from scaffolds with different NF densities was characterized *in vitro*. Subsequently, the designed scaffold with the appropriate NF density was implanted into the modified MPC model ($7\times2.5\times1$ mm^3) previously described in Chapter 5 and bone formation was assessed using "*in vivo*" μCT and histology. This study was aimed to provide the necessary "proof-of-principle" for developing and transferring this technology to the clinical setting, with the objective of improving the quality of life of patients with cleft palate.

Collectively, the work presented in this thesis was explored based on the hypothesis that combining appropriate scaffold with osteogenically induced MSCs, which is characterized by its high regenerative potential, or osteoinductive protein, such as BMP-2, will provide viable therapies for cleft palate reconstruction. In **Chapters 4-6**, two tissue engineering approaches for cleft palate repair were developed and detailed: cell-based therapy and BMP-2 based therapy. **Chapter 7** was dedicated to general discussion, conclusions and future directions, where additional studies were recommended to further enhance the clinical outcomes of tissue engineering therapies for cleft palate reconstruction.

Chapter 2

Tissue engineering Therapies for cleft palate reconstruction

2.1 BACKGROUND

Cleft palate is a common congenital abnormality, which could be isolated clefts or a part of syndromes.[36, 37] Etiology is incompletely understood, but both genetic and environmental factors are thought to play role during embryological development. Cleft defect could involve either primary or secondary palate or both. Clefts of the primary palate are due to failure of the fusion between medial nasal and maxillary processes. While, clefts of the secondary palate are due to failure of the palatine shelves to fuse because of inability of the tongue to descend into the oral cavity.[5] Current therapy for cleft palate patients involves rotation of adjacent soft tissues into the defect site and secondary bone grafting into the cleft defect. Autogenic bone is considered an ideal bone graft as it provides osteogenic, osteoconductive, and osteoinductive environment needed to support bone regeneration in the cleft defect.[38] Reconstruction of palate defect facilitates the eruption of the permanent incisor or canine naturally or with the assistance of orthodontics. It will also provide appropriate alveolar contour for prosthetic rehabilitation of the edentulous spaces. However, donor site (tibia, mandible, ilium, cranium, rib) morbidity remains to be the main limitation in the cleft palate reconstruction when considering autografts.[5] Clearly, tissue engineering application could provide sufficient bone formation similar to autologous bone grafting but with reduced donor site morbidity.

Engineering bone tissue requires appropriate cell source, osteoinductive biomolecule and biodegradable scaffold as the basic elements. Mesenchymal stem cells (MSCs) are considered a promising source of cells for regenerating alveolar bone, due to their reliable osteogenic differentiation potential. They are readily available, can be easily expanded in standard culture, with no risk of immune rejection or tumorigenicity.[17] Osteogenesis in pluripotent cells can be achieved using osteoinductive factors, such as bone morphogenetic proteins (BMPs). But, the delivery of MSCs and/or BMPs to the cleft defect necessitates the utilization of the appropriate carrier/scaffold to maximize the induced osteogenic effect.

This review discussed two main bone tissue engineering therapies that could

considerably impact alveolar bone regeneration following cleft palate reconstruction namely cell-based therapy and protein-based therapy. A critical evaluation of MSC's and BMP's potential and limitations for cleft palate reconstruction were elaborated. Moreover, molecular basis of osteogenic differentiation of MSCs as well as mechanism of bone healing following bone grafting were summarized. Finally, major concerns regarding the application of tissue engineering in children and challenging cleft defects were discussed.

2.2 MSCs

MSCs are considered potential candidates for cell-based therapies for cleft palate reconstruction. Utilizing those cells necessitate harvesting bone marrow aspirate from the patient's sternum or iliac crest and expanding the plastic-adherent cell population.[39] Colony-forming unit-fibroblasts (CFU-f) assay is considered to be one of the gold standards and is utilized to isolate adherent cells from bone marrow aspirates. Isolated cells are known to have multipotent potential, i.e. can differentiate into osteoblasts, adipocytes, and chondrocytes.[40] However, successful use of MSCs for alveolar bone grafting would require those cells to be osteogenically differentiated before transplantation. Osteogenesis in pluripotent cells can be achieved using several agents including BMPs.

2.3 BMPs

BMPs are part of transforming growth factor β (TGF-β) superfamily. Although more than 20 BMPs have been discovered, only BMP-2, -4, -6, -7, and -9 were proven to induce osteogenic differentiation of multipotent cells in culture.[41] BMP-2 is best known for its osteoinductive potential and is the most studied growth factor for bone regeneration.[5] *In vitro*, BMP-2 alone induced poor osteogenic commitment of h-MSCs, but it improved dexamethasone-induced osteogenesis of MSCs.[42, 43] However, high dexamethasone concentrations were reported to stimulate adipogenesis in MSC cultures. We recently reported an

optimal condition (10 nM Dexamethasone and 500 ng/mL BMP-2) for osteogenic differentiation of MSCs without increasing adipogenesis.[44]

In vivo, BMP-2 alone can induce *de novo* bone formation when implanted into bony defects. Both preclinical and clinical reports have demonstrated the effectiveness of BMP-2 for *de novo* bone formation.[45] Therefore, Food and Drug Administration (FDA) approved BMP-2 loaded absorbable collagen sponge (ACS) for given human surgical indications.[26] BMP-2 acts as a chemotactic agent (attracting cells host cells *in situ*) and as a morphogen (causing stem cells to differentiate to an osteogenic lineage).[20] It also mediates mesenchymal condensations and stimulates bone growth by a mechanism recapitulating the intramembranous and endochondral ossification that happens *in utero*.[46] Extensive research was done to better clarify the molecular basis of BMP-2 mediated osteogenesis, which is highlighted below.

2.4 INSIGHTS INTO MOLECULAR OSTEOGENIC EFFECTS OF BMPS ON MSCS

Runt-related transcription factor-2 (Runx-2), osterix (Osx) and canonical Wnt signaling promotes osteogenic differentiation of MSCs into bone forming cells (**Figure** 2-1). BMP activates Smads, which interact with Runx-2 to induce expression of osteogenic genes.[47] Runx-2 maintains osteoblasts in immature stage and negatively controls osteoblast terminal differentiation.[48] While, Osx is the downstream gene of Runx-2, which promotes the differentiation of pre-osteoblasts to immature osteoblasts.[49] Osx forms a complex with the nuclear factor of activated T cells (NFAT). Then NFAT activates the Wnt signaling pathway, which controls osteoblastogenesis and bone mass (**Figure** 2-2).[50]

During osteogenic differentiation of MSCs, alternative differentiation pathways are also blocked. Runx-2 inhibits adipogenic differentiation of MSCs through blocking Ccaat-enhancer-binding proteins (C/EBP) family and peroxisome proliferator-activated receptor gamma2 (PPAR-γ_2). Runx-2 and canonical Wnt signalling inhibit the chondrogenic differentiation of MSCs by

inhibiting Sox5, Sox6, and Sox9.[47] Moreover, Wnt signalling stimulates differentiating osteoblasts to secret osteoprotegerin, an osteoclast differentiation inhibitor.[51]

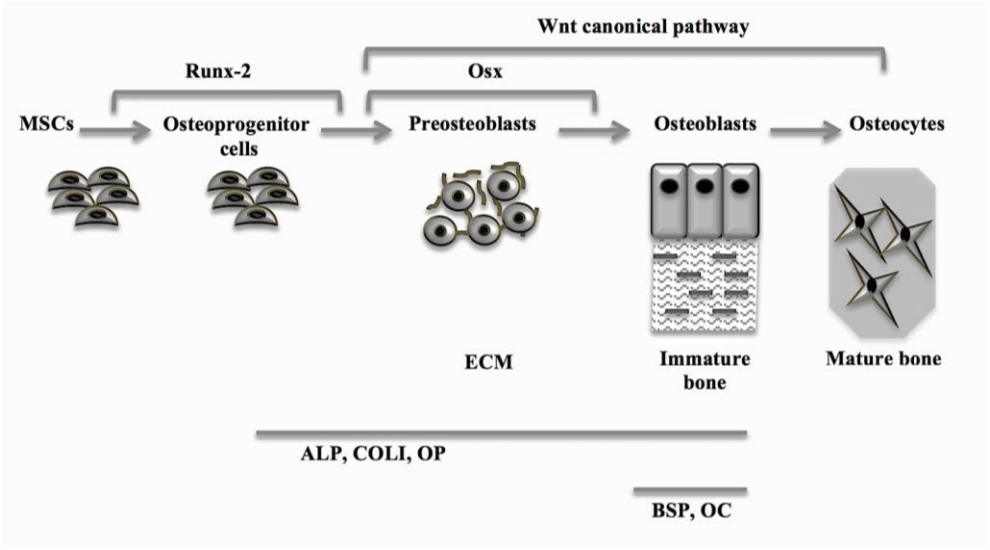

Figure 2-1: Role of transcription factors in the osteogenic differentiation of MSCs. Bone formation starts with the differentiation of MSCs into mature osteoblast, and ends with osteoblast apoptosis.

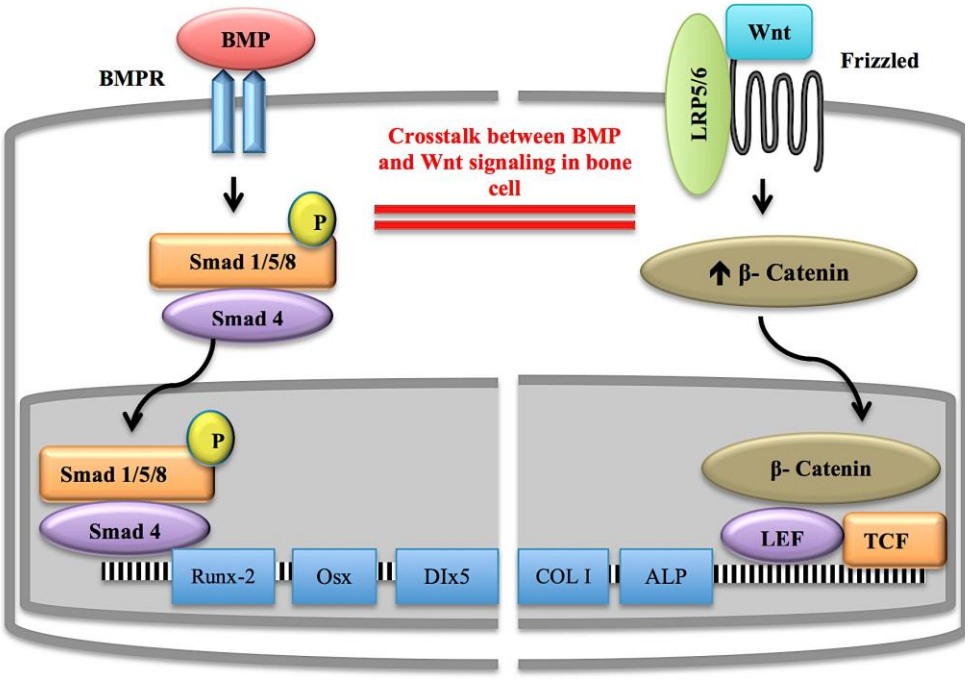

Figure 2-2: BMP-2 signalling during MSCs osteogenesis.

2.5 MECHANISM OF BONE HEALING FOLLOWING CLEFT PALATE RECONSTRUCTION

Bone healing is a complex process that is coordinated by different mechanisms based on the biophysical environment. It starts with the migration of inflammatory cells to the repair site and hematoma formation. When platelets are activated, they secrete growth factors to recruit inflammatory cells to the injury site. Cells involved in repair include fibroblasts, MSCs and osteoprogenitor cells. Growth factors produced during bone regeneration include platelet derived growth factor (PDGF), tumour necrosis factor (TNF), insulin-like growth factors (IGFs), fibroblast growth factor-2 (FGF-2) and BMPs.[52]

Based on histological features, bone repair can be classified into four categories: endochondral, primary, direct, and distraction osteogenesis. Mesenchymal and/or surface osteoblasts are responsible for bone formation in various types of repair. Endochondral bone repair takes place in an environment of interfragmentary space and mobility, where cartilage initially forms the soft callus followed by formation of woven and lamellar bone. While, primary bone repair (direct contact repair) occurs in an environment of no interfragmentary space with rigid fixation where bone repair is facilitated without soft callus formation. Osteoclast cells resorb necrotic bone at the edges of the fracture or osteotomy and osteoblast cells forms lamellar bone along the long axis of bone; therefore no bone remodelling is required. On the other hand, direct bone repair (gap repair) occurs when the interfragmentary space is larger than 0.1 mm with rigid fixation. It is also mediated without formation of a soft callus where woven and lamellar bone is formed perpendicular to the long axis of the bone and then remodelled to be parallel to the long axis. Finally, distraction osteogenesis (callotasis) occurs in slow widening gap where woven and then lamellar bone is synthesized parallel to the long axis of the bone.[53] Bone healing in cleft defect is expected to follow direct bone repair (gap repair) model. Placement of bone

grafts mediates bone healing in the defects through providing framework that enhances cell migration, attachment and proliferation (osteoconduction).

2.6 MSCS BASED THERAPIES FOR CLEFT PALATE RECONSTRUCTION

MSCs are potential candidates for bony reconstruction of cleft defects with less donor site morbidity as compared with autologous bone. Autologous MSCs are considered a safe therapeutic option with no reported immunological reaction or tumour development over ~ 11 years of follow up after transplantation.[54]

In animals, there are no data on utilizing MSCs in cleft palate reconstruction, but there is adequate evidence in other craniofacial critical-sized defects.[55, 56] Addition of growth factors to MSCs/biomaterial construct was reported to further enhance bone formation *in vivo*.[57]

In human patients, Gimbel et al.[58] conducted a randomized controlled trial (RCT), where cleft defects were reconstructed with marrow aspirates seeded on ACS (n=21), traditional iliac autograft (n=25), or minimally invasive iliac autografts. This study only assessed postoperative pain and did not provide any quantitative assessment of bone healing at defects sites. In contrast, Behnia et al.[59] implanted MSCs with demineralized bone mineral/calcium sulphate scaffold in 2 patients (case series) and reported 25-35% bone fill after 4 months. It is important to note that both studies employed MSC with no osteogenic conditioning. Hence, the reported bone filling percentages in these studies were likely suboptimal and might require second grafting surgery. On the other hand, osteogenic conditioning of the implanted MSCs prior to *in vivo* transplantation was reported to significantly enhance the outcome of cell-based therapies for bone regeneration.[60] This is consistent with Hibi et al. *study*,[61] which employed osteogenically induced autologous MSCs for alveolar cleft repair in a 9 year old patient (case report), and reported ~79% bone fill after 9 month post-operatively with successful eruption of lateral incisor and canine. Additionally, Behnia et al.[62] implanted autologous MSCs seeded on hydroxyapatite–tricalcium phosphate (HA-TCP) and mixed with PDGF in four alveolar defects. Mean bone filling was ~51.3% at 3 months

postoperative. It is important to note that osteogenic conditioning in this study[62] was done using patients' plasma, whose osteogenic effects are difficult to dissect due to its various constituents. Employing purified growth factors might be a superior approach as it can further control the potency and reproducibility of cellular differentiation. These approaches could potentially provide alternative therapies for autologous bone grafting.

2.7 BMP-2 BASED THERAPIES FOR CLEFT PALATE BONE RECONSTRUCTION

Several studies demonstrated efficacy of BMP-2 for reconstruction of cranial defect,[63-66] mandibular defects,[67, 68] and sinus augmentation.[69-72] However, its efficacy for cleft reconstruction remains understudied. To our best knowledge, there are four articles in total on BMP-2 in cleft palate reconstruction in animals. One study was done in monkeys,[73] one study in dogs,[74] one study in rabbits,[75] and one study in rodents.[35] Summary of these studies is presented in **Table** 2-1. Boyne et al.[73] reconstructed alveolar cleft defects created in Macaca mulatta monkeys and reported significant bone healing following BMP-2+ACS and autologous bone grafting, while ACS group demonstrated minimal bone formation. Another study in dogs[74] compared the effectiveness of BMP-2 plus PLGA (poly(lactic-co-glycolic acid)), PLGA+autologous blood, and autograft for alveolar cleft reconstruction. Autograft treated group had more bone healing as compared to other treatments at 2 months, however by 4 months there was no significant difference between treatments except PLGA+autologous blood treated group demonstrated the least amount of bone. While, Sawada et al.[75] created maxillary osseous defects of 6×6 mm^2 and implanted gelatin hydrogel containing BMP-2, gelatin hydrogel, or BMP-2 solution while control group was left untreated. Utilization of controlled release system (gelatin hydrogel) for BMP-2 delivery resulted in significant bone regeneration after four week post-implantation as compared to other groups. Finally, Nguyen et al.[35] created surgical alveolar defects of 7×4×3 mm^3 were in Sprague Dawley rats and reconstructed them with

one of the following treatments: ACS, BMP-2+ACS, HA-TCP, BMP-2+HA-TCP, and empty defect (control). ACS and HA-TCP induced more bone formation than untreated controls. The addition of BMP-2 to ACS failed to demonstrate significant effect on bone formation over 12 weeks postoperative while addition of BMP-2 to HA-TCP added a small but significant osteogenic advantage to HA-TCP scaffold. Authors explained this due to burst release kinetics of BMP-2 from ACS as well as incompletely sealed oral tissue post-operatively.

Unfortunately, the available animal models have several limitations. Although, primate studies have the highest relevance to human beings because of the primates' size as well as anatomical and physiological similarity to humans,[46] it is not essential to use subhuman primates for critical-sized defect studies.[76] Now it is also difficult to obtain institutional ethical approval for using primates in research since the scientists must provide a strong justification for the need of the primate models rather than other animals. High husbandry and operational expenses limit the use of large animal models (primates, dogs, and rabbits). Although rodent models are the most commonly used animals in biomedical research for testing the efficacy of new therapies, there was only one study done in rats.[35] Another drawback of the existing animal models is the presence of clear communication between the created cleft defects and surrounding anatomical structures such as nasal cavity, incisive foramen, and/or palatine foramen that could result in substantial loss of BMP-2 with subsequent suboptimal BMP-2 concentration at the recipient site.[35, 73, 74] One model also deemed to be a non critical size defect.[74] Presently, there is no reliable, reproducible and cost-effective animal model suitable for testing new bone grafting alternatives, which could explain the delays for developing alternative therapies for secondary bone grafting.

In humans, only seven studies were found on BMP-2+ACS grafting in cleft palate patients. Three studies were RCTs,[77-79] one retrospective cohort study,[80] one case series study,[81] one case report,[82] and one expert opinion.[83] Characteristics of the reviewed studies are discussed in the previous chapter in details. Current evidence lacks high quality RCTs and current studies are limited

by inappropriate study designs and diverse outcome measurements. The main benefit of BMP-2+ACS is to provide bone formation similar to autologous bone grafting, but with greatly reduced donor site morbidity, hospital stay, and procedure cost. However to obtain therapeutic outcomes when ACS is utilized, milligram doses of BMP-2 are required. Such high protein concentration (1-1.5 mg/ml) was optimized in spine research however; the appropriate concentration for maxillofacial applications could be different.[45] A recent study utilized a chemically cross-linked hydrogel and reported moderate bone quantity at a much lower BMP-2 concentration (250 μg/ml).[84] However, severe gingival swelling and initial exposure of BMP-2+hydrogel was evident in the two cleft patients involved in the study and the study was prematurely terminated. This study also did not have BMP-2+ACS comparison group. Decreasing the effective BMP-2 dose needed for bone formation is appealing, as it will reduce toxicity and cost of the therapy. But, appropriate carrier is also necessary to maximize the clinical outcomes and to reduce morbidity. An appropriate delivery system is expected to recapitulate the role of BMP-2 in directing condensation of precursor MSCs and modulating intramembranous bone formation. Therefore, reducing the amount of BMP-2 needed for optimal therapeutic effect. The potential of new delivery systems needs to be optimized in appropriate animal models before efficacy testing in clinical trials in human subject.

Table 2-1: Analysis of animal studies employing BMP-2 for cleft palate reconstruction

	Primate Model[73]	Dog Model[74]	Rabbit model[75]	Rat Model[35]
Sample	Macaca Mulatta Monkeys 1.5 years old (n=4 defects/group) Bilateral defects	Skeletally mature Foxhound dogs 55-60 Ib (n= 6 defects/group at each time point) Bilateral defects	New Zealand white rabbits 20 weeks old (n=3 defects/group) Bilateral defects	Sprague Dawley rats 8 weeks old (n= 4 rats/group at each time point). Unilateral defect
Defect size	8 mm wide defect extending from nasal aperture over lateral side of maxillae, through the alveolar ridge and narrowing in width (6 mm) toward incisive foramen	1 cm wide defect extending from nasal floor to palatine foramen	6×6 mm^2 osseous defect created on the lateral side of the maxilla and 5 mm distal to incisor teeth	7×4×3 mm^3 alveolar defects were created on the lateral side of the maxilla
BMP-2 dose	430 μg	200 μg	17 μg	4.2 μg
Carrier	ACS	PLGA	Gelatin hydrogel	ACS or HA-TCP
Treatment groups	- BMP-2+ACS - ACS control - Autologous particulate marrow cancellous bone (PMCB)	- BMP-2+PLGA plus autologous blood - PLGA plus autologous blood - Autograft - Empty defect (control)	- Gelatin hydrogel with BMP-2 - Gelatin hydrogel with PBS (phosphate buffered saline) - BMP-2 solution - Untreated control	- ACS - BMP-2+ACS - HA-TCP - BMP-2+HA-TCP
Assessment method	- Macroscopic exam - 2D Radiographs - Histology	- 2D Radiographs - Histology	- 3D microCT - Histology	- 3D microCT - Histology
Follow up	3 months	2 and 4 months	4 weeks	4, 8, and 12 weeks
Outcomes	No significant difference in bone formation between BMP-2 and PMCB treatments. ACS group had minimal bone formation	Autograft promoted more bone healing than other treatments at 2 months. After 4 months, PLGA group had the least quantity of bone with no differences between the rest of treatments	Gelatin hydrogels plus BMP-2 resulted in significant bone healing as compared with other groups	ACS and HA-TCP scaffolds enhanced bone healing as compared to untreated controls. But, the addition of BMP-2 failed to demonstrate significant effect on bone formation over 12 weeks postoperative
Limitations	- Cleft defects were designed to communicate with the incisive foramen, which could potentially damage the nerve - In the mid portion of the palate, BMP-2+ACS and PMCB were in close proximity that could result in potential leakage of BMP-2 into the contiguous autograft side	- Spontaneous bone healing of the defect (i.e. not critical size defect) - Suboptimal effect of BMP-2 could be due to inability of PLGA scaffold to retain BMP-2 at the recipient bed or communication with palatine foramen leading to early loss of BMP-2	- Small sample size - Although utilized microCT scans for outcome assessment, they did not report quantitative measurement	Suboptimal effect of BMP-2 could be due to difficulty maintaining BMP-2 within surgical defect due to: - Communication with palatine foramen and nasal cavity - Incompletely sealed oral mucosa - Burst release of BMP-2 from ACS and HA-TCP scaffolds leading to substantial early loss of BMP-2

2.8 APPROPRIATE CARRIER

Biomaterial scaffold plays a vital role in the success of bone grafting approaches. The ideal tissue-engineered construct will need to be designed to accommodate bone growth overtime together with minimum scarring and local adverse events. The primary scaffold properties of concern are: 1) Biocompatibility; 2) Biodegradability; and 3) Cell adhesiveness and interconnectivity. ACS carrier fulfill these three criteria.[23] But, it relies on simple adsorption of the protein to scaffold through soak loading. This results in burst release of the protein with fast reduction of biological activity and the lack of controlled release limits its utility.[27] As bone growth is temporal, the appropriate cells may not be attracted to the defect area until after considerable diffusion of BMP-2 from the site.[28] Therefore, an effective delivery system is essential to localize and maintain the proper dose of BMP-2 at the defect site for longer time.

Several biomaterials have been developed for BMP-2 delivery such as poly(lactic acid) (PLA), polyglycolide (PLG) and their copolymers, and poly ε-caprolactone (PCL), and other biomaterials including alginate, agarose, collagen gels, etc.[85] These biomaterials have significantly enhanced our understanding of cell-material interactions and promoted a new field of tissue engineering. However, these scaffolds are made of microfibers with diameters of ~10-100 microns which are variable in size, porosity, surface interaction, and concentration relative to the native ECM (extracellular matrix) and cells interacting with it. Therefore, they did not mimic the nanoscale dimension and chemical features of ECM. In order to reproduce 3-D microenvironment, the fibers should be significantly smaller than cells so that cells are surrounded by a scaffold, similar to native extracellular environment.[86]

Self-assembling peptide nanofiber (NF) based hydrogel RADA16-I (Arginine-Alanine-Aspartic Acid- Alanine)$_4$ is a novel class of self-assembling peptide biomaterials has been discovered and established in the context of cell culture, stem cell biology and tissue engineering.[31, 32, 86, 87] It is made from natural amino acids, which can be metabolized naturally and harmlessly by the body. It does not require chemical cross-linkers to initiate gel formation and spontaneously form

stable β-sheet structure in water.[88] NF scaffold is similar to the natural ECM with fiber diameter of ~10 nm and pore size between 5–200 nm so it creates 3-D microenvironment similar to native extracellular matrix.[30] It provides timed release for growth factors and good diffusion properties along with its biocompatibility and low toxicity.[29] Moreover, the release profiles of proteins within NF hydrogel can be adjusted by altering peptide concentrations. Thus, lower peptide concentrations form lower density NF with larger pores, while, higher peptide concentrations form higher density NF with smaller pores.[88]

Several studies utilized PuraMatrix (commercially available system based on RADA16-I) for osteogenesis *in vitro* and *in vivo*. *In vitro*, PuraMatrix (PM) did not only promote the differentiation capacity of mouse embryonic stem cells (mESCs) and mouse embryonic fibroblasts (MEFs) but also stimulated the generation of a stem cell–like niche in mESCs grown in 3D cultures.[89]

In vivo, PM was compared with Matrigel (Basement Membrane Matrix) on bone regeneration in calvarial mouse defects (3 mm). PM increased quantity and strength of the newly formed bone as compared with Matrigel treated defects.[90] Moreover, PM supported the osseointegration of dental implants in mandibular defects created in dogs.[87] In this study, addition of autologous MSCs to PM further improved bone to implant contact after 4 weeks post-operatively. However, the main concern related to the clinical use of PM/RADA16-I is it is strength. It was reported that PM in combination with ACS scaffold (PM+ACS) was more convenient to handle and displayed enhanced mechanical and hemostatic properties compared to PM alone.[91] Another study developed cage from polyetheretherketone to support PM for bone regeneration in rat femur defects (load bearing bone) and demonstrated significant bone healing after 28 days.[92] Hence, the establishment of the appropriate microenvironment would be adequate to induce bony defects to regenerate. To our best knowledge no study employed NF with/without BMP-2 for bony reconstruction of cleft defects. Therefore, the potential of NF+BMP-2 based scaffold need to be further evaluated in animal models of cleft palate prior to efficacy testing in clinical trials for cleft palate reconstruction.

2.9 CHALLENGES OF TISSUE ENGINEERING THERAPIES IN PAEDIATRIC POPULATION

Cleft palate is a birth defect and is ideally treated early in life; hence most cleft palate patients are children. However, there are numerous aspects that should be considered before utilizing bone tissue engineering therapies in children. BMP-2 demonstrates a great potential for cleft palate reconstruction, but safety concerns limits its widespread clinical application. Despite of the reported short half-life of BMP-2 *in vivo*,[93] it is necessary to monitor the potential long-term effects of BMPs on local and distant tissues/organs before expanding it clinical use in cleft palate population. Additionally, the manufacturer of BMP-2+ACS construct (INFUSE Bone Graft) cautioned the use of the product in children or skeletally immature patients because of the potential of premature fusion of the epiphyseal plates in response to transient exposure to BMP-2. It is not also recommended for pregnant patients because of the reported risk of the production of anti BMP-2 antibodies.[46] Therefore, its use should be limited to skeletally mature patients. Consequently, autologous bone grafting is considered the best option for skeletally immature patients. Autologous bone grafting is mostly successful in children of 6-10 years of age.[77, 94] This is based on the fact that children have superior bone healing potential as compared to adults which could be due to the increased proliferative capacity of younger cells.[95] However, sometimes the amount of autologous bone available for grafting is limited. Therefore, MSC based therapies could be considered for those children. Since children have higher number of MSCs in their bone marrow which decrease as a function of donor age.[96] Transplantation of Autologous MSCs is considered safe therapy with no reported immunological reaction or tumour development over ~ 11 years of follow up.[54] Moreover, number of MSCs is 1 out of every 10,000 bone marrow cells in neonates, then it drops to 1:100,000 in teenagers, 1:400,000 in 50-year-olds, and 1:200,000 in 80-year-olds.[96] But, utilizing MSCs for cleft palate reconstruction necessitate *ex-vivo* amplification and osteogenic induction before implantation in bony defects. Therefore, concerns related to tissue engineering in

children must be addressed and strategies optimized *in vitro* and *in vivo* before efficacy testing in clinical setting.

2.10 EFFECT OF CLEFT SIZE AND SURGICAL TIMING ON THE OUTCOMES OF BONE GRAFTING

The fate of the bone grafting therapies depends on many factors including patient age and cleft size, which may directly or indirectly influence graft failure. Increased age during secondary grafting is associated with having deficient or failed grafts.[97] Although, older patients could benefit from autologous bone grafting; but it is associated with several complications such as reduced healing, graft exposure, recurrent fistula, and failure of tooth eruption.[77] Cleft width is another factor that could influence the fate of the bone grafting. Long et al.[98] reported that presurgical width has little or no effect on the success of bone grafting. Conversely, another study[99] reported weak but significant relation ($P = 0.04$) between cleft width and the success of the bone graft, meaning that wider clefts are more prone to failure. There are numerous reasons for this conclusion. Revascularization of the central portion of the graft in wider clefts is more likely to fail. Furthermore, the amount of autologous bone may be insufficient. Collapse of the soft tissue flaps with subsequent graft exposure and loss of stability may also occur more frequently in wider clefts.[99] Therefore, addition of MSCs to BMP-2 delivered in appropriate carrier could improve treatment outcomes for those patients. Inclusion of angiogenic factors to the construct could further promote robust bone formation. However, additional investigations are required to explain what works for whom, in all circumstances and conditions, rather than failed ways of responding to problems in a 'one-size-fits-all' manner. Clinical studies optimizing dose, delivery systems, and conditions for stimulation of bone growth will bring about a new era; the ability to predictably enhance bone regeneration using BMP-2 and/or MSCs technologies is becoming a reality and will strongly influence the dental practice.

Chapter 3

Efficacy Of Bone Morphogenetic Proteins In Alveolar Clefts Reconstruction: Current Evidence

3.1 BACKGROUND

Cleft palate is a relatively common congenital anomaly.[1] It imposes a large economic burden on affected families and society.[100] Estimated average lifetime healthcare cost per oral cleft patient in North America is ~100,000 US.[6, 7] Grafting autologous bone is currently the preferred method for cleft palate reconstruction. Autogenous bone could be obtained from: iliac crest, calvarium, mandibular symphysis, and tibia.[15] Bone grafting is needed to support permanent teeth eruption and to provide adequate bone for prosthodontic rehabilitation of the edentulous segment.[12] However, autologous bone grafting is limited by donor site morbidity, pain, wound infection, paresthesia, and poor mobility. To overcome these limitations, INFUSE® Bone Graft have been utilized for cleft palate reconstruction. It consists of osteoconductive collagen scaffold (to promote bone growth and integration) and bone morphogenetic protein-2 (BMP-2) which is a well-known osteoinductive agent (i.e. it influence mesenchymal cells to differentiate into pre-osteoblasts).

BMP-2 stimulates *de novo* bone formation if placed in the appropriate environment. It attracts host stem cells at the implantation site and induces their differentiation into bone forming cells.[83] Both preclinical and clinical reports have demonstrated the effectiveness of BMP-2. Therefore, BMP-2 loaded Absorbable Collagen Sponge (ACS) is approved by Food and Drug Administration (FDA) for selected human surgical indications.[26] However, further research is required to expand its clinical use in cleft palate patients. Detailed literature reviews on the subject remain sparse, and are needed in order to summarize current evidence to facilitate knowledge translation.

Two systematic reviews recently evaluated artificial bone grafting therapies for cleft palate reconstruction, including BMP-2+ACS.[101, 102] No definitive conclusions could be drawn regarding the most effective grafting technique, due to poor quality of reviewed studies. Both reviews included a total of three studies (two clinical trials and one retrospective study). Systematic reviews usually rely on the hierarchy of evidence for article selection, which ranks different study designs according to their scientific validity. In this model, randomized clinical

trial (RCT) is considered the best evidence since it is the only design that adequately controls for confounding variables and biases. Therefore, systematic reviews mostly include RCTs.[103] However it is important to note that there are two drawbacks of supporting this rigid hierarchy of evidence: the first drawback relates to the lack of high quality RCTs on the efficacy of BMP-2+ACS for alveolar cleft reconstruction. The second drawback is related to the downgrading of other study designs, such as cohort or case series studies, which might be helpful to evaluate therapeutic effectiveness. It is important to understand that there are different levels of evidence, i.e. that not all forms of evidence can be considered of equal value. Therefore, Slavin[104] proposed the best evidence synthesis as an alternative to both systematic and traditional reviews. The main idea behind this approach is to add to the traditional literature review the application of rational, systematic search and selection of the included studies. There are different grading systems to evaluate the levels of evidence such as Oxford Centre for Evidence-based Medicine system, GRADE system, and US Preventive Services Task Force (USPSTF) system. In this review we utilized Oxford Centre for Evidence-based Medicine for evidence-based classification because of its simplicity and logical judgments of quality of evidence.

Therefore, this evidence-based review is aimed to characterize the current evidence and evaluate the effectiveness of BMP-2+ACS for bone grafting in cleft patients to help improving the quality of future research in this area.

3.2 METHODS

Literature searches examined five electronic databases (Medline (1948-present), Embase (OVID), Scopus, Web of Science, and Biomed central). Specific search terms were truncated and combined according to the database being searched with the help of a senior librarian specialized in database searches for health sciences. Search terms used for the condition included “cleft palate”, “cleft alveolus”, “alveolar process”, or “alveolar clefts” and for the therapy: “bone morphogenetic protein 2” or “BMP 2”. Similar search terms were used in different databases when possible. The last database search was conducted April

10, 2013. Two authors reviewed all of the titles and abstracts independently for article inclusion. Discrepancies were resolved through discussion and consensus. All English language papers on bone grafting for alveolar clefts using BMP-2+ACS in humans including clinical trials, cohort studies, case reports, and case series were considered. Full articles of all potentially adequate abstracts were retrieved for further methodological evaluation. Reference lists of all selected articles were then searched for any article that might have been missed in the database searches. Following full article screening, reviewed studies were categorized based on different levels of evidence published by Oxford Centre for Evidence-based Medicine (**Table** 3-1).[105]A flow diagram of the literature search and selection process is summarized in **Figure** 3-1.

Table 3-1: Oxford Centre for Evidence-based Medicine - Levels of Evidence

Level	Therapy/Prevention/Etiology/Harm:
1a	Systematic reviews (with homogeneity) of randomized controlled trials
1b	Individual randomized controlled trials (with narrow confidence interval)
1c	All or none randomized controlled trials
2a	Systematic reviews (with homogeneity) of cohort studies
2b	Individual cohort study or low quality randomized controlled trials (e.g. <80% follow up)
2c	"Outcomes" Research; ecological studies
3a	Systematic review (with homogeneity) of case-control studies
3b	Individual case-control study
4	Case series (and poor quality cohort and case-control studies)
5	Expert opinion without explicit critical appraisal, or based on physiology, bench research or "first principles"

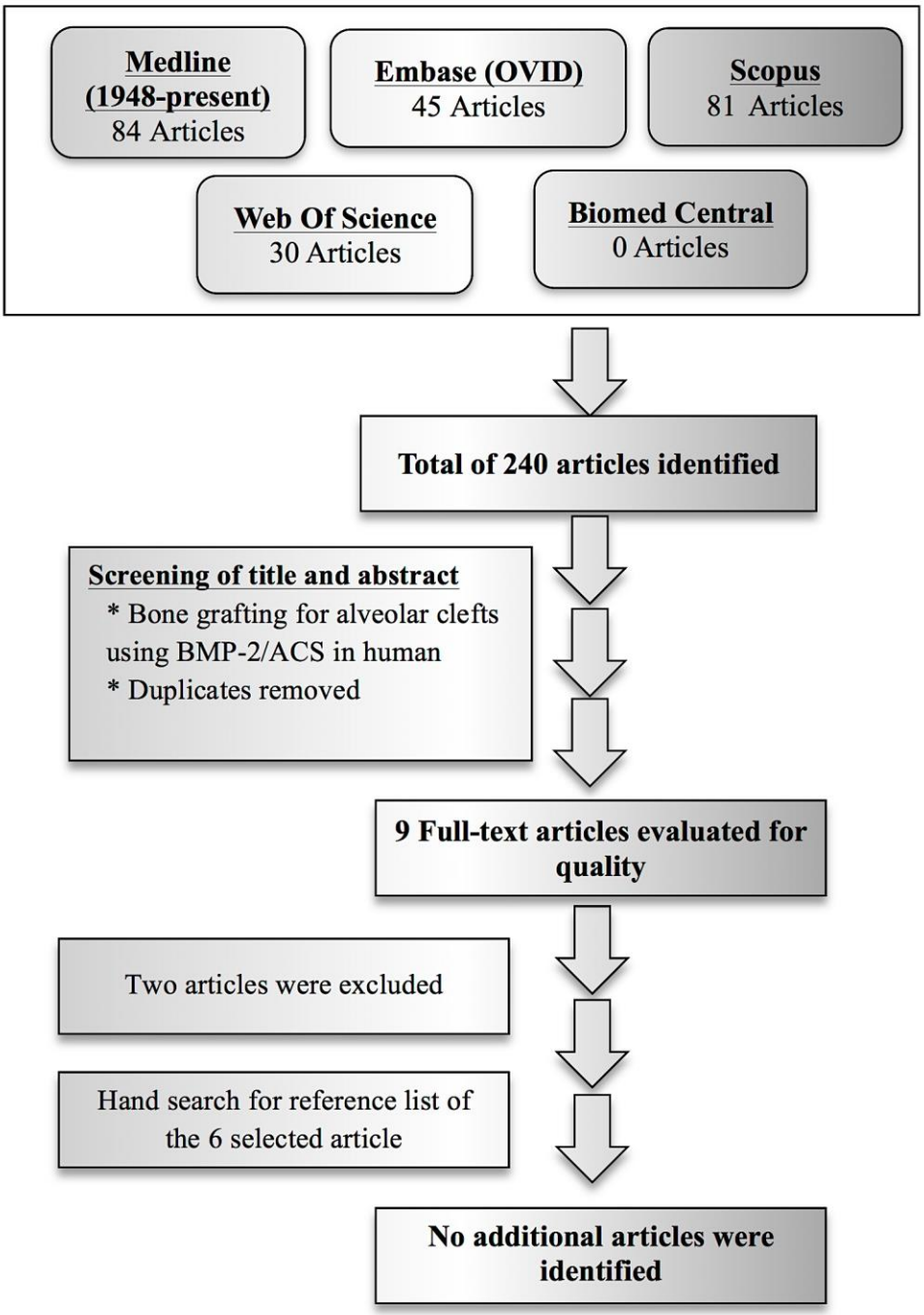

Figure 3-1: Flowchart demonstrating the articles selection process

3.3 RESULTS

3.3.1 Search results

Using the search terms as outlined above, a total of 240 articles were identified (84 in Medline, 45 in Embase, 81 Scopus, 30 in Web of Science and 0 in Biomed Central). Based on titles and abstracts, we found 9 articles investigating BMP-2+ACS grafting for alveolar clefts in humans. Following methodological evaluation of the full articles, two articles were excluded[106, 107] as they constituted expert opinions or discussion articles. Further searching of the reference lists of the selected articles did not reveal any further relevant studies. Characteristics of the selected studies are presented in **Table** 3-2.

Table 3-2: Finally selected studies' key methodological information

	Dickinson [77]	Alonso [78]	Canan[79]	Herford [80]	Fallucco [81]	Chin [83]	Herford[82]
Design	RCT	RCT	RCT	Retrospective cohort	Retrospective case series	Case series	Case report
Sample size	BMP-2+ACS: 9 Control: 12	BMP-2+ACS: 8 Control: 8	BMP-2+ACS: 6 Control:6 Periosteoplasty: 6 (this group was discontinued due to low bone formation)	BMP-2+ACS: 10 Control: 2	BMP-2+ACS: 17 clefts (number of participants was not reported) Control: N/A	BMP-2+ACS: 50 clefts in 43 patients Control: N/A	BMP-2+ACS: 1 Control: N/A
Cleft type	Unilateral	Unilateral	Unilateral	Unilateral	Not clear	30 unilateral, 7 bilateral, 4 midline and 2 lateral facial	Unilateral
Patient age	15-18 years	8-12 years	8-15 years	7-11 years	Not reported	6-14 years	6 years
Exclusion criteria	Skeletally immature, previous surgery, had contraindication to BMP-2 therapy (i.e., history of neoplasm), or had incomplete records.	Previous surgery, canine eruption, presence of comorbidities, or incomplete records	Not reported	Not reported	Not reported	Not reported	Not reported
Follow up	12 months	6 and 12 months	3, 6, and 12 months	4 months	6 months	Inconsistent	Not reported
Method of evaluation	CT, panorex, periapical films	CT	CT	CT	CT	Inconsistent (periapical, panoramic, occlusal ,CT).	CT, periapical films
Outcome assessors	- 3 blinded assessors - Inter-rater reliability: Done - Intra-rater reliability: Not reported	- Single blinded assessor - Intra-rater reliability: Done - Inter-rater reliability: N/A	- Single assessor - Intra-rater reliability and blinding: Not reported	- Single blinded assessor - Intra/inter-rater reliability: Not reported	- 2 blinded assessors - Intra/inter-rater reliability: Not reported	- No clear information regarding number and blinded assessors - Intra/inter-rater reliability: Not reported	- No clear data regarding number and blinded assessors - Intra/inter-rater reliability: Not reported
Radiographic assessment	**Bone filling %:** **6 month:** BMP-2+ACS (95%), control (63%) **Bone height (vs. cleft tooth roots):** **12 month:** BMP-2+ACS (85%), control (70%)	**Bone filling %:** **6 month:** BMP-2+ACS (59.6%), control (75.4%) **12 month:** BMP-2+ACS (74.4%), control (80.2%) **Bone height:** **6 month:** BMP-2+ACS (53.3%), control (83.8%) **12 month:** BMP-2+ACS (65.0%), control (86.6%)	**Bone filling %: 3 month:** BMP-2+ACS (72.6%), control (75.6%). **6 month:** BMP-2+ACS (73.7%), control (76%)**. 12 month:** BMP-2+ACS (75.1%), control (78%) **Bone height: 3 month:** BMP-2+ACS (55.4%), control (61.4%). **6 month:** BMP-2+ACS (58.9%), control (64%). **12 month:** BMP-2+ACS (58%), control (64%) **Bone density:** No differences between BMP-2+ACS and control at any time point	**Bone filling %:** **4 month:** BMP-2+ACS (71.7%), control (78.1%)	**Bone density:** -Trabecular bone was defined as HUs > 226 -16 of the 17 clefts showed bone formation both vertically and transversely - Bone height and defect volume were not reported	Subjective assessment based on the clinical judgment only without any quantitative measurement for bone formation.	Subjective assessment based on the clinical judgment only without any quantitative measurement for bone formation
Postoperative complications and adverse events	**BMP-2+ACS:** prolonged pain (1 patient), no ectopic bone formation **Control:** significant pain at day1 (12 patients), partial graft loss (5 patients), complete graft loss (1 patient), oral fistula (3 patients)	**BMP-2+ACS:** - 37.5% postoperative swelling **Control:** - 87.5% donor site morbidity	Not reported	**BMP-2+ACS:** - Postoperative swelling, - 2 patients with >25% bone fill of the cleft defect	Not reported	- No systemic adverse effects - No ectopic bone formation beyond normal contours - No adverse effect on teeth adjacent to cleft	Not reported

3.3.2 Evidence-based classification for selected articles

Following methodological analysis, articles were classified based on the levels of evidence. Studies were classified as follows: three RCTs[77, 78] (level-2b), one retrospective cohort study[80] (level-4), one case series study[81] (level-4), one case report,[82] and one expert opinion[83] (level-5).

RCTs conducted by Dickinson et al.,[77] Alonso et al.,[78] and Canan et al.,[79] were well designed studies with subjective and objective analysis of bone healing and postoperative complications. However, they contained several methodological defects and therefore they were classified as level-2b. Firstly, although the groups were randomly allocated, the sequence generation was not explained. Secondly, both studies did not discuss the allocation concealment method. Thirdly, both studies did not report prior sample size calculations.

Herford et al. study[80] is a retrospective cohort and therefore, the level of evidence is lower than RCTs. Although they provided detailed description of baseline characteristics and blinded assessment, there was short follow up (4 months); and the study did not report intra-rater reliability. Due to those limitations, it was considered as level-4 evidence.

Fallucco et al.[81] study is a retrospective case series (level-4). Selective data reporting was evident in that study; they did not provide information for the finally included participants, such as age and cleft type (unilateral or bilateral). Additionally, they did not fully report data outlined in the methods section, such as bone density preoperative and 6 months postoperative.

Chin et al.[83] study was reported as a case series of 50 clefts repaired in 43 patients that was divided into three groups based on the cleft severity. Surprisingly, the authors presented treatment outcomes of only one case in each group. The study presented excellent clinical and radiographic images, but outcome assessment was subjective and follow up time was not clear/consistent. Blinding and independent assessment for outcome were not reported (high bias risk). Therefore, it was considered as expert opinion and classified as level-5.

Herford et al.[82] is a case report (level-5). Although, this study evaluated bone formation with computed tomography, but outcome assessment was subjective

and follow up time was not clear. Blinding and independent assessment for outcome were not reported.

3.3.3 Full article analysis

All studies used the same BMP-2 kit (Infuse® Bone Graft) for clefts reconstruction in the experimental group. Four studies included autologous graft from iliac crest as the control group.[77-80] The remaining studies did not have control group.[81-83]

Timing for alveolar reconstruction varied between the studies. Alveolar clefts were reconstructed in children and early adolescents in all studies except Dickinson et al.,[77] who performed cleft reconstruction in skeletally mature patients, whilst Fallucco et al.[81] did not report the age of participants.

Exclusion criteria were reported in just two studies.[77, 78] Dickinson et al.[77] excluded patients who were skeletally immature, had previous surgery, had contraindication to BMP-2 (i.e., history of neoplasm), or had incomplete records. Alonso et al.[78] excluded patients with previous surgery, canine eruption, presence of comorbidities, or incomplete records.

Mean size of the preoperative alveolar cleft was 1.052 cm^3 in the control group vs. 0.975 cm^3 in the BMP-2+ACS group in Alonso et al.,[78] 5.1 cm^3 vs. 5.6 cm^3 in Dickinson et al.,[77] 0.657 cm^3 vs. 0.472 cm^3 in Canan et al.,[79] and 17.86 cm^3 vs. 10.55 cm^3 in Herford et al.[80] Although Chin et al.,[83] Fallucco et al.,[81] and Herford et al.[82] utilized CT scans for outcome assessment, they did not report cleft size.

3.3.4 Assessment of outcomes

Blinded assessors evaluated the outcomes of bone grafting in all the studies except Chin et al.,[83] Canan et al.,[79] and Herford et al.[82] studies. Inter-/intra- rater reliability was only reported in Dickinson et al.[77] and Alonso et al.[78] studies.

Length of the follow up differed between the six studies. Dickinson et al.,[77] Alonso et al.,[78] and Canan et al.[79] reported one-year follow up, Fallucco et al.[81] reported 6 month follow up, and Herford et al.[80] reported 4 months follow up; whereas, Chin et al.[83] and Herford et al.[82] did not clearly indicate the length of the follow up.

3.3.4.1 Radiographic assessment of postoperative bone formation

3.3.4.1.1 Quantity of bone formation

Four studies performed volumetric analysis for the defect site.[77-80] Dickinson et al.[77] reported significant increase in the percentage of bone fill in the BMP-2+ACS group (95%) as compared to the control group (63%) at the 6 month follow up. Conversely, Alonso et al.[78] reported significantly higher percentage of bone fill in the control group (75.4%) as compared to BMP-2+ACS group (59.6%) after 6 months, but at 12 months this difference (80.2 % for control vs. 74.4% for BMP-2+ACS group) was no longer significant. While, Canan et al.[79] reported no differences in bone healing between BMP-2+ACS and control group at 3, 6 and 12 months difference (75-78% for control vs. 72.6-75.1% for BMP-2+ACS group). Similarly, Herford et al.[80] did not detect any significant difference in bone formation after 4 months in BMP-2+ACS group (71.1%) as compared to the control group (78.1%).

Fallucco et al.[81] defined trabecular bone formation in the cleft defect as Hounsfield units (HUs) of more than 226. They reported radiographic evidence of dental arch fusion in 16 out of 17 alveolar clefts and only 1 case failed to meet the assigned radiographic criteria. However, Chin et al.[83] and Herford et al.[82] did not provide any quantitative measures for postoperative bone healing.

Three studies assessed bone height.[77-79] Dickinson et al.[77] assessed bone bridge formation between cleft tooth roots by a four-point grading system (0-4), where 0 represented absence of bony bridge and 4 represented complete bone healing. The mean scores on this scale were converted to percentage to facilitate easy comparison with the other studies. Alonso et al.[78] provided percentage of bone height (postoperative height/preoperative height) and Canan et al.[79] provided percentage of height on the cleft side/normal maxilla height. Dickinson et al.[77] reported higher bone height vs. tooth roots of the cleft in BMP-2+ACS group (85%) as compared to control group (70%). While, Alonso et al.[78] reported significantly shorter bone in the BMP-2+ACS group vs. the control group (6 months: 53.3% vs. 83.8% and 12 months: 65.0% vs. 86.6% vs. preoperative bone height). Canan et al.[79] revealed no significant differences between BMP-2+ACS

group vs. the control group (55.4-58% vs. 61.4-64.2%)

3.3.4.1.2 Quality of bone formation

Dickinson et al.[77] reported successful osseointegration around dental implants placed in 1 of 12 patients in the control group and 2 of 9 patients in the BMP-2+ACS group. Alonso et al.[78] reported successful tooth eruption through the reconstructed clefts in both groups. No information was provided on orthodontic tooth movement into the cleft area or periodontal conditions in any study.

3.3.4.2 Assessment of postoperative complications and adverse events

Dickinson et al.[77] reported substantial donor site pain, increased healing problems, longer hospital stay, and greater surgery cost in the control group. Alonso et al.[78] reported donor site pain in the control group (87.5%) and local swelling in the BMP-2+ACS group (37.5%). Moreover, Chin et al.[83] reported no systemic adverse effects, no ectopic bone formation beyond normal contour, and no adverse effect on the teeth adjacent to the cleft following BMP-2+ACS therapy. However, the rest of the studies[79-82] did not report complications.

3.4 DISCUSSION

The evidence-based classification is intended to assist the surgeons to recognize the limitations of reviewed articles and to identify the gaps where further studies could be performed. There were only six studies on BMP-2+ACS grafting in cleft palate patients. Three studies were RCTs[77-79] (level-2b), one retrospective cohort study[80] (level-4), one case series study[81] (level-4), and one case report[82] and one expert opinion[83] (level-5). Additionally, two systematic reviews recently evaluated different bone grafting procedures for cleft palate repair, including BMP-2+ACS.[101, 102] Both reviews correctly concluded based on their methodological approach that further well designed RCTs are needed for providing definitive treatment recommendations for cleft palate patients. However, they did not discuss the safety of using BMP-2 in cleft palate population and especially children.

It is important to mention that BMP-2+ACS is FDA approved for limited human applications in adults including lumbar spinal fusion, tibial long bone fracture, sinus elevation, and alveolar defects associated with extraction sockets.[26] Therefore, the utilization of BMP-2+ACS graft in cleft population in the papers reviewed was done at the discretion of some surgeons in an "off-label" capacity.

BMP-2+ACS graft is contraindicated in patients with hypersensitivity to BMP-2, collagen Type I (bovine) or to other components of the formulation. It is also contraindicated for patients who are skeletally immature, pregnant, patients with an active malignancy or patients undergoing treatment for a malignancy, or in patients with an active infection or tumour at the operative site.[108] Surprisingly, all reviewed studies except Dickinson et al.[77] did not consider those contraindications in the participants selection. Alveolar clefts were reconstructed in children and early adolescents in all reviewed studies. Only Dickinson et al.,[77] utilized skeletally mature patients, whilst Fallucco et al.[81] did not report the age of participants.

The current evidence is limited by the lack of high quality RCTs and inadequate study designs. Selective reporting was also evident; most of the studies did not fully report the data outlined in the method sections. Prior sample size calculation was not done in all the review papers and the sample sizes were considered inadequate, which may result in a high risk of bias. Moreover, there was a huge discrepancy in the size of the cleft between the studies. Herford's[80] patients had much greater preoperative volume of maxillary defects. This could be due to the preoperative orthodontic expansion of the maxillary segments done in Dickinson et al.[77] and Alonso et al.[78] studies. While, the difference in the cleft volume between Dickinson et al.[77] and Alonso et al.[78] could be due to the age difference between the participants at the surgery time. The mean defect size in Canan et al.[79] study was much smaller. This could be due to variation in the measurement method, different anatomical landmarks and inter-operator variation between the different studies.

Treatment outcomes should be assessed using reliable and valid scales. Three scales (Bergland, Kindelan, and Chelsea scales) for radiographic assessment of

successful secondary alveolar bone grafting have been developed and validated for two-dimensional "2D" radiography.[109-111] Nightingale et al.[112] compared the validity and reproducibility of these scales and showed that the three scales were equally valid and reproducible. Therefore, it is recommended to utilize those scales for radiographic assessment of bone grafting.

Recently, cone-beam computed tomography (CBCT) partially replaced 2D radiography. 2D radiographs are limited by: superimposition of structures, magnification, and distortion. CBCT has overcome all these disadvantages.[113] As compared to conventional CT, CBCT provides images of high diagnostic quality and lower radiation dosages at lower costs.[114] The effective dose of CBCT is 10-75 uSv (one jaw scan) compared with 250-560 uSv for CT (one jaw scan), 60 uSv for full mouth periapical view, and 30 uSv for a panoramic film. [115, 116]

Assessment of postoperative complications is another essential aspect for evaluating BMP-2+ACS efficacy as it helps to clarify benefits for patients and clinicians. Local complications following BMP-2+ACS grafting were reported in three studies,[77, 78, 107] but, the rest of the studies[79-82] did not report complications. None of the studies addressed systemic complications reported in the spine applications such as cancer risk, systemic toxicity, reproductive toxicity, immunogenicity, and effects on distal organs.[117]

3.5 EFFECTIVENESS OF THE THERAPY

The main benefit of BMP-2+ACS is to provide sufficient bone formation similar to autologous bone, but with greatly reduced postoperative complications. Despite successful formation of mineralized bone with this approach, conclusive knowledge regarding appropriate BMP-2 dosage, time course and release profile remains to be clarified and presents opportunities for improvement for widespread clinical use.

Following injury, local BMP-2 produced in tissues has relatively low concentrations (ng-µg) and is maintained over prolonged time period, resulting in physiological bone healing and minimal side effects. While, INFUSE® Bone Graft relies on direct administration of high BMP-2 concentration (mg) on ACS

carrier to maintain therapeutic level over time even with initial burst release and fast clearance of the protein. Such high BMP-2 concentrations may be detrimental for bone formation and may increase side effects including postoperative swelling, ectopic bone formation, and cancer risk.[118] It is also reported that ACS lacks structural stability leading to soft tissue collapse in the grafted area.[78] Therefore, new scaffolds offering longer BMP-2 release and greater structural stability in the grafted area could address some of the shortfalls of ACS delivery system. Kinetics of prolonged/sustained BMP-2 release may better mimic natural protein production during bone healing,where relatively constant amount of growth factor is released overtime. Thus allowing investigators to test decreased BMP-2 concentrations needed to induce robust bone formation with minimal side effects. Furthermore, longer follow up is essential for evaluating local and systemic adverse events associated with BMP-2 therapies.

3.6 CONCLUSION

Using BMP-2+ACS in place of traditional bone grafting could be a promising therapy for cleft reconstruction. However, the important question is whether BMP-2+ACS can be safely used in humans and particularly in children. The FDA considered BMP-2+ACS to be contraindicated in children, since its safety has not been demonstrated. Therefore, its use should be limited to skeletally mature patients. Current evidence is inconclusive and additional data is needed to clarify associated benefits and complications when utilizing BMP-2+ACS for cleft palate population. The presented outcomes propose possibility for future research but not clinical practice.

Chapter 4

Osteogenic Differentiation of Human Mesenchymal Stem Cells Cultured with Dexamethasone, Vitamin D3, basic Fibroblast Growth Factor and Bone Morphogenetic Protein-2 [1]

[1] A version of this chapter has been previously published in: N. Mostafa, R. Fitzsimmons, P. Major, A. Adesida, N. Jomha, H. Jiang, H. Uludag˘. Osteogenic Differentiation of Human Mesenchymal Stem Cells Cultured with Dexamethasone, Vitamin D3, Basic Fibroblast Growth Factor, and Bone Morphogenetic Protein-2. Connective Tissue Research, 2012, 53(2): 117–131.

4.1 INTRODUCTION

Bone deficiencies and defects due to congenital anomalies such as cleft palate are quite common in the clinic setting.[119] Despite significant variations in the nature of defects, autologous bone grafting is currently the front-line treatment for bone augmentation in a wide range of defects. However, there are numerous shortcomings to autologous bone grafting. In addition to donor site morbidity, other complications such as pain, wound infection, paresthesia, local tissue injury and poor mobility, hamper the desired therapeutic outcomes.[5] To overcome the limitations related to bone harvesting and grafting, bone tissue engineering has been proposed as an alternative solution to prepare clinically useful bone grafts. In this approach, appropriate cells are cultivated in culture with biomaterials scaffolds and/or osteogenic supplements until a suitable bone graft is achieved. The tissue engineering approach, however, is often hampered by the need for large quantities of tissue-specific cells.[120] Human mesenchymal stem cells (h-MSCs) from autologous bone marrow (i.e., bone marrow stromal cells) are the leading candidate for the source of cells in tissue engineering constructs, as they are readily available from the host, can be easily expanded in standard culture conditions, and have reliable osteogenic potential with no risk of immune rejection or tumorigenicity.[17] Successful use of h-MSCs for augmentation of bone mass and repair requires these cells to be stimulated down the osteogenic pathway *in vitro* before transplantation. Among numerous agents used for inducing the osteogenic commitment of MSCs are bone morphogenetic proteins (BMPs), dexamethasone (Dex), basic fibroblast growth factor (b-FGF), and vitamin D3 (Vit-D3).

The BMPs are multifunctional growth factors that are part of the transforming growth factor beta (TGF-β) protein family. Among the BMPs, BMP-2 and BMP-7 are best known for their osteoinductive potential and they are clinically used for bone repair and augmentation along with biomaterial implants. BMP-2 was proposed to require Dex to effectively induce osteogenic differentiation of rat MSCs.[42] Similarly, BMPs alone induced poor osteogenic commitment of h-MSCs, but they improved Dex-induced osteogenesis of h-MSCs, as measured by

the alkaline phosphatase (ALP) induction and calcification *in vitro.*[43, 121] Other studies also demonstrated that Dex in combination with ascorbic acid (AA) and ß-glycerophosphate (GP), induced osteogenic differentiation of h-MSCs based on enhanced ALP activity, expression of osteocalcin (OC) as well as *in vitro* calcification.[122] The growth factor b-FGF is another protein that has been shown to augment the osteoinductive potential of BMP-2. b-FGF is a prototypical mitogen which supports angiogenesis *in vivo*. Combinations of BMP-2 and b-FGF demonstrated synergistic effects in osteogenic differentiation of MSCs *in vitro* and enhanced bone formation *in vivo.*[123, 124] Subcutaneous implants supplemented with b-FGF demonstrated enhanced ALP activity and calcification, since the presence of b-FGF induced faster and stronger invasion of capillaries into implanted scaffolds, presumably resulting in an influx of osteoprogenitor cells from the enhanced vascular network.[125] It was also reported that b-FGF and BMP-2 has a biphasic effect on osteoinduction; the stimulatory effect of b-FGF was obtained at low b-FGF doses, while b-FGF exerts an inhibitory role in osteoinduction at high doses.[126]

In addition to the protein growth factors, the active form of Vit-D3 has been shown to play an important role in skeletal homeostasis, as it displays anabolic effects on osteoblasts, resulting in increased bone formation.[127] *In vitro* studies demonstrated that treatment of h-MSCs with Vit-D3 induced expression of both early as well as late stage osteogenic markers including ALP, bone sialoprotein (BSP), osteopontin (OPN), and OC.[43, 128] Moreover, Vit-D3 improved Dex-induced osteogenic differentiation of human pre-osteoblasts and MSCs, resulting in increased ALP activity and matrix mineralization.[43, 128, 129]

Taken together, we hypothesized that combining the optimal dose of BMP-2 and b-FGF, along with Vit-D3 and Dex, will result in synergistic effects that may further augment osteogenic differentiation of h-MSCs. To test this hypothesis, h-MSCs were cultured with different concentrations of these osteoinductive reagents to explore the optimal combination(s) that will lead to robust osteogenesis *in vitro*. Our long-term aim was to determine the appropriate combination(s) of osteogenic supplements needed for developing a cell-based

tissue engineering therapy for regeneration in bone defects. Towards this goal, this study took the first step by delineating the culture conditions that provided robust osteogenesis with minimal adipogenesis.

4.2 MATERIALS AND METHODS

4.2.1 Materials

Dulbecco's Modified Eagle Medium (DMEM; high glucose with *L*-glutamine), Hank's Balanced Salt Solution (HBSS) and penicillin-streptomycin (10,000 U/mL-10,000 μg/mL solutions) were from Invitrogen (Grand Island, NY). Master mix (2X) used for quantitative polymerase chain reaction (q-PCR) was developed by the Molecular Biology Service Unit (MBSU) in the Department of Biological Science at the University of Alberta (AB, Canada). The master mix contained Tris (pH 8.3), KCl, $MgCl_2$, Glycerol, Tween 20, DMSO, dNTPs, ROX, SYBR Green, and the antibody inhibited Taq polymerase-Platinum Taq. Fetal bovine serum (FBS) was obtained from Atlanta Biologics (Lawrenceville, GA). RNeasy kit was obtained from Qiagen (Valencia, CA) and Agilent RNA 6000 Nano LabChip kit from Agilent Technologies (Santa Clara, CA). Oligo$(dT)_{18}$ primer was obtained from Fermentas (Burlington, ON, Canada). Primers were purchased from Integrated DNA Technologies (Coralville, IA). CyQUANT cell proliferation kit and SYBR Green were from Molecular Probes (Portland, OR). ALP substrate p-nitrophenol phosphate (p-NPP), 8-hydroxyquinoline, o-cresolphthalein, 2-amino-2-methyl-propan-1-ol (AMP), Dex, GP, AA, and Oil Red O were obtained from Sigma (St. Louis, MO). Recombinant human b-FGF was obtained from the Biological Resource Branch of NCI-Frederickton (Bethesda, MD). Recombinant human BMP-2 was obtained from an E-coli expression system, and its activity has been extensively reported in the literature.[130, 131] The BMP-2 stock solution was reconstituted in ddH_2O.

4.2.2 Isolation and Culture of h-MSCs

The bone marrow aspirates were isolated from three (15-48 year old) patients undergoing routine orthopeadic surgical procedures under a protocol approved by

the institutional Health Research Ethics Board. The cells were cultured in a growth medium containing DMEM, 10% FBS, 100 U/mL penicillin, and 100 µg/mL of streptomycin supplemented with 5 ng/mL b-FGF for a total of 2 passages according to a published procedure.[132] Upon confluence, the cells were split 1:3 using 0.05% trypsin/0.04% EDTA. One day before the addition of osteogenic supplements, h-MSCs at passages 3 to 6 were seeded in 24-well plates in a basic medium (BM: DMEM with 10% FBS, 50 mg/L AA, 100 U/mL penicillin and 100 g/L of streptomycin). The cultures were incubated at 37 ^{o}C with 5% CO_2.

4.2.3 Osteogenic Treatment

Two series of experiments were conducted in this study. We first investigated the effect of different osteogenic supplements by exposing h-MSCs to the BM containing combinations of one concentration of the following supplements: 10 mM GP, 10 nM Dex, 10 ng/mL b-FGF and 1 µg/mL BMP-2. The control group was treated with BM only without any supplements. The h-MSCs were then analyzed for cell proliferation (DNA assay) and differentiation (specific ALP activity) at days 7 and 11. In a second experiment, the dose- and time-dependent changes in osteogenesis of h-MSCs were investigated with the addition of different concentrations of Dex, b-FGF, BMP-2 and Vit-D3. The effects of 36 possible treatments were investigated with all possible combination of Dex (10 and 100 nM), BMP-2 (0, 200 and 500 ng/mL), Vit-D3 (0, 10 and 50 nM) and b-FGF (0 and 10 ng/mL), all in the presence of 10 mM GP. The control group was treated with BM alone without any supplements. After 15 and 25 days, the h-MSCs were analyzed for total DNA content and specific ALP activity. Calcification (total Ca^{++} content) and adipogenesis (Oil Red O stain) were also assessed after 25 days of treatment. After 15 days, q-PCR was performed with a select group of treated h-MSCs.

4.2.4 Specific ALP Assay

The effects of the osteogenic supplements on ALP activity of h-MSCs were measured as this enzyme is a critical predictor for mineralization.[133] Cultured h-MSCs were washed with HBSS and lysed with an ALP buffer (0.5 M 2-amino-2-

methylpropan-1-ol and 0.1% (v/v) Triton-X100; pH=10.5). After two hours, 100 µL of cell lysates were added into 96-well plates, and an equal volume of 2 mg/mL ALP substrate p-NPP solution was added to each well. The absorbance was periodically measured (once every 90 seconds) at 405 nm for 10 minutes. The ALP activity was normalized with the DNA content in each lysate to obtain the specific ALP activity (ALP/DNA).[134]

4.2.5 DNA Assay

To quantify the total DNA content in the wells, the remaining cell lysates from the ALP assay were frozen at -20 ºC and measured at the end of the experiment to minimize differences. DNA content of h-MSCs was analyzed using the CyQUANT DNA kit according to the manufacturer's instructions and measured with a fluorescent plate reader ($\lambda_{excitation}$ at 480 nm and $\lambda_{emission}$ at 527 nm). A DNA standard supplied with the kit was used to calculate the DNA concentrations in the cell lysates.[134]

4.2.6 Calcium Assay (Total Ca++ content)

The wells containing h-MSCs lysate from the DNA assay were rinsed (x2) by HBSS and 0.5 mL of 0.5 M HCl was then added to dissolve the mineralized matrix overnight. On the following day, 20 µL of aliquots from each well were added to 50 µL of a solution containing 0.028 M 8-hydroxyquinoline and 0.5% (v/v) sulfuric acid, plus 0.5 mL of solution containing 3.7×10^{-4} M o-cresolphthalein and 1.5% (v/v) AMP. The absorbance was quantified at 570 nm. A standard curve was developed using Ca^{++} standards obtained from Sigma and used to convert the obtained absorbance values into Ca^{++} concentrations (in mg/dL).[134]

4.2.7 Oil Red O Staining

After 25 days of treatment with the indicated supplements, h-MSCs were fixed in 10% formalin for 1 hour, washed with 60% isopropanol and left to dry completely. Cultured h-MSCs were then stained with 0.21% (w/v) Oil Red O solution for 10 min, washed 4 times with dH_2O and examined by microscopy.

4.2.8 Comparison of Osteogenic and Adipogenic Potential of h-MSCs

The extent of calcification was classified based on the obtained Ca^{++} content in cultures: (a) - : no calcification where $0<[Ca^{++}]<3$ mg/dL, (b) -/+ : poor calcification where $3<[Ca^{++}]<8$ mg/dL, (c) + : moderate calcification where $8<[Ca^{++}]<13$ mg/dL, and (d) ++ : significant calcification where $[Ca^{++}]>13$ mg/dL. Adipogenesis was also classified with a similar semi-quantitative scale, based on the amount of positively stained lipid vacuoles for Oil Red O in the treated cultures: (a) - : no staining, (b) -/+ : poor staining with only a few areas (<10%) of stain, (c) + : moderate areas (10-40%) of staining, and (d) ++ : significant (>50%) areas of staining.

4.2.9 q-PCR

The q-PCR was performed on h-MSCs from 3 donors that were cultured for 15 days in BM and the three media formulations that gave the most osteogenesis (i.e. groups which resulted in the highest calcification in previous studies). The study groups were: **1.** BM (control), **2.** Dex (10 nM) + BMP-2 (500 ng/mL), **3.** Dex (100 nM) + Vit-D3 (10 nM) + BMP-2 (500 ng/mL), and **4.** Dex (100 nM) + Vit-D3 (50 nM) + BMP-2 (500 ng/mL). After washing the monolayers with HBSS, RNA was extracted and purified with an RNeasy kit using QIAshredders and an RNase-free DNase set for on-column digestion of genomic DNA. RNA concentration was determined by a GE NanoVue spectrophotometer, and sufficient RNA quality was confirmed by an Agilent 2100 Bioanalyzer using an Agilent RNA 6000 Nano LabChip kit. All samples were deemed acceptable (RIN $\geq$ 6.9) with the exception of group 4 of one of the three donors and was excluded from this study.

Each cDNA synthesis reaction was performed in 20 µL volume with 300 ng total RNA using M-MLV reverse transcriptase, as per the manufacturer's instructions. Moreover, a combination of 0.5 µL random primers and 0.5 µL oligos (dT_{18}) were also used to synthesize cDNA template.

The q-PCR was performed as SYBR Green assays using an Applied Biosystems 7500 Fast Real-time PCR System. Cycle conditions were set to 2 min of 95 ^{o}C, followed by 40 cycles of 20 sec at 95 ^{o}C, 1 min at 60 ^{o}C and ending in a

default dissociation step. Primers for the experiment were designed using Primer Express 3.0 (Applied Biosystems). All 10 μL q-PCR reactions consisted of 2.5 μL of cDNA template, 2.5 μL of 3.2 μM primers (combined concentration), and 5 μL of a proprietary 2X master mix (Tris, KCl, $MgCl_2$, Glycerol, Tween 20, DMSO, dNTPs, ROX, SYBR Green, and the antibody inhibited Taq polymerase-Platinum Taq; pH = 8.3).

Prior to the q-PCR experiment, stable expression of glyceraldehyde 3-phosphate dehydrogenase (GAPDH) was confirmed for each group. All primer sets (**Table** 4-1) were validated with a four-sample 1/5 to 1/625 dilution series of a mixed cDNA sample composed of cDNA from each treatment; primer efficiency (ΔC_t / log(dilution)) was found to be stable for each primer set for cDNA dilutions 1/25-1/625.

Each sample from the 3 donors was analyzed in triplicate for each target gene using a cDNA dilution of 1/60. Data were analyzed by the $\Delta\Delta C_t$ method using group1 (BM) of one of the donors as a calibrator and normalizing to GAPDH. Hence data is reported as fold change compared to group1: BM (**Figure** 4-7).

Table 4-1: Sequence of the forward and reverse primers used for the q-PCR

Target Gene (NCBI Ref. #)	Forward Primer (5' to 3')	Reverse Primer (5' to 3')
GAPDH NM_002046.3	ACCAGGTGGTCTCCTCTGACTTC	GTGGTCGTTGAGGGCAATG
PPARγ NM_015869.4	AGACATTCAAGACAACCTGCTACAA	GGAGCAGCTTGGCAAACAG
BSP NM_004967.3	AAGCTCCAGCCTGGGATGA	TATTGCACCTTCCTGAGTTGAACT
aP2 NM_001442.2	CATAAAGAGAAAACGAGAGGATGATAAA	CCCTTGGCTTATGCTCTCTCA
ON NM_003118.2	TCCGTACGGCAGCCACTAC	GCATGGCTCTCAAGCACTTG
Runx2 NM_004348.3	TCAGCCCAGAACTGAGAAACTC	TTATCACAGATGGTCCCTAATGGT
ALP NM_000478.4	AGAACCCCAAAGGCTTCTTC	CTTGGCTTTTCCTTCATGGT

4.2.10 Statistical Analysis

All assays were performed in triplicate for each donor, for a total of 3 cell donors. The results were expressed as mean and standard deviation (SD). Data were analyzed by one-way analysis of variance (ANOVA) using SPSS version 18.0 software package (SPSS, Chicago, IL, USA). Intergroup variations were analyzed using 'Tukey HSD' testing. Statistical significance was determined by p-values < 0.05.

4.3 RESULTS

4.3.1 Initial Response of h-MSCs to Osteogenic Supplements

The DNA and specific ALP activity of h-MSCs were investigated in short time culture (7 and 11 days) in BM (control) and medium supplemented with b-FGF, BMP-2 and b-FGF+BMP-2 combination. The summary of the DNA analysis is provided in **Figure** 4-1**A** (day 7) and **1B** (day 11). At day 7, h-MSCs treated in the absence of growth factors did not show any differences in DNA content with different media, indicating no effect of GP, Dex, and GP+Dex combinations on cell proliferation. In the presence of b-FGF, the combination of BM+GP+Dex significantly enhanced DNA content as compared to control cultures (BM only) and cultures treated with BM+GP ($p<0.05$), while BM+Dex demonstrated higher DNA amount as compared to BM only ($p<0.05$). The h-MSCs treated with BMP-2 did not show a significant variation in DNA content among the treatment groups. In the presence of the b-FGF+BMP-2 combination, the h-MSCs cultured in BM+Dex and BM+GP+Dex demonstrated higher DNA content as compared to h-MSCs cultured in BM alone and BM+GP ($p<0.05$).

On day 11, there was no effect for b-FGF, BMP-2, or b-FGF+BMP-2 groups in terms of total DNA content for h-MSCs cultured in BM (**Figure** 4-1**B**). On the other hand, BMP-2 treated h-MSCs gave increased DNA content when cultured in BM+Dex and BM+GP+Dex as compared to cells treated with BM+GP ($p<0.05$), but not as compared to BM alone ($p>0.05$).

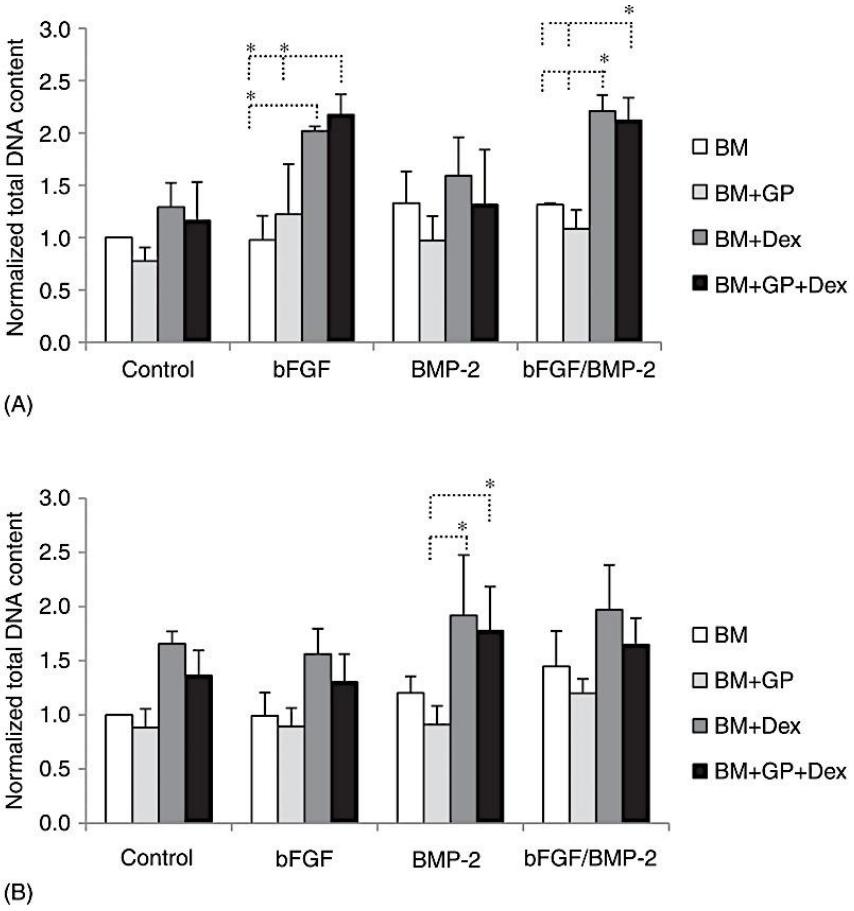

Figure 4-1: Effect of different osteogenic supplements (GP "10 mM", Dex "10 nM", b-FGF "10 ng/mL", and BMP-2 "1 µg/mL") on total DNA content of the h-MSCs. The analysis was conducted on day 7 (A) and day 11 (B). The data is a summary from three cultures of h-MSCs derived from three different donors. Due to significant variations in the DNA amounts of different donors, all samples were normalized with the control treatment of individual donors (i.e., h-MSCs treated with BM alone; indicated to be equivalent to 1.0). The significantly different groups are indicated (*: $p<0.05$).

The summary of the specific ALP activity is provided in **Figure** 4-2**A** (day 7) and **2B** (day 11). At day 7 in the absence of growth factors, h-MSCs cultured with BM+Dex and BM+GP+Dex gave significantly elevated ALP activity as compared to the cells cultured in BM alone and BM+GP ($p<0.001$). A similar effect was also evident in the presence of b-FGF, BMP-2 and b-FGF+BMP-2 combination; cells cultured in BM+Dex and BM+GP+Dex showed higher ALP activity as compared to cells cultured in BM or BM+GP ($p=0.05$). However, the specific ALP responses obtained from the BM+Dex and BM+GP+Dex cultured h-MSCs

were generally attenuated in the presence of growth factors ($p<0.005$), compared to the cells treated with no growth factors. Addition of GP failed to enhance ALP activity under all conditions, and Dex addition was essential for such a response.

The specific ALP activity was generally elevated in all cultures on day 11 (**Figure** 4-2**B**). In the absence of growth factors, or presence of b-FGF and BMP-2 alone, the ALP activity was again elevated in cells cultured in BM+Dex or BM+GP+Dex, as compared to BM and BM+GP cultured h-MSCs ($p=0.005$). Among the cells treated with the b-FGF+BMP-2 combination, h-MSCs cultured in BM+Dex gave higher ALP activity as compared to BM and BM+GP cultures ($p=0.005$). Addition of b-FGF alone or in combination with BMP-2 significantly decreased the ALP activity obtained in BM+Dex and BM+GP+Dex media, as compared to similar cultures in the absence of growth factors ($p<0.05$).

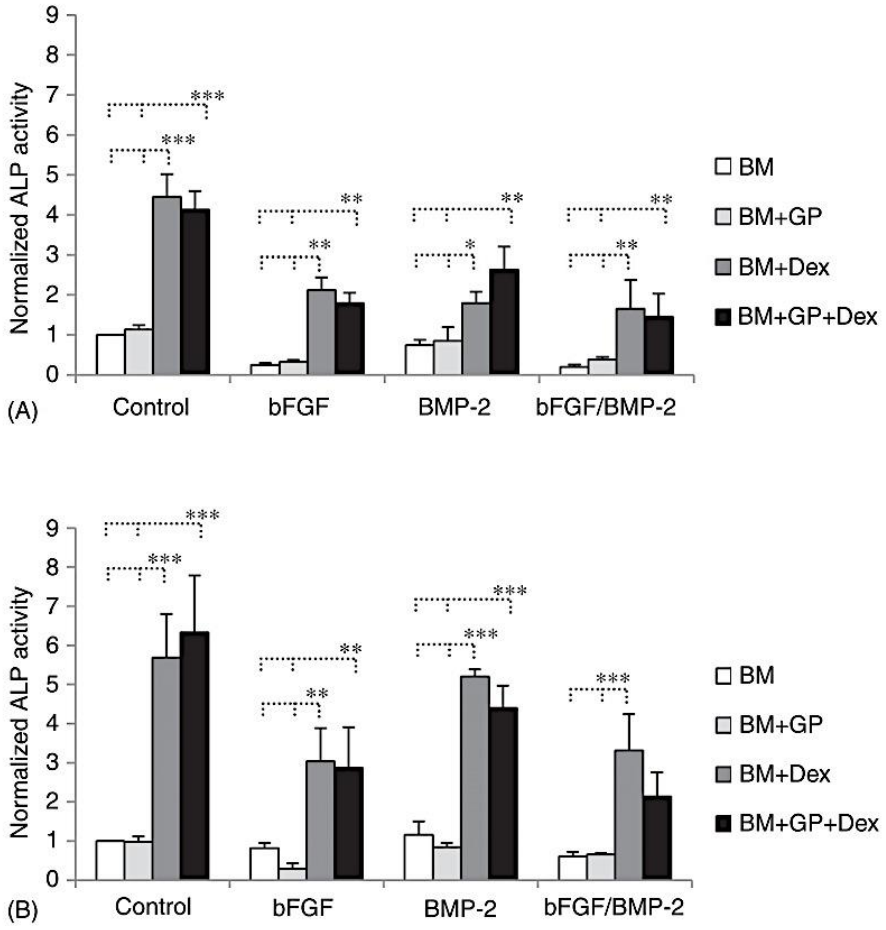

Figure 4-2: Effect of different osteogenic supplements (GP "10 mM", Dex "10 nM", b-FGF "10 ng/mL", and BMP-2 "1 µg/mL") on specific ALP activity of h-MSCs. The analysis was conducted on day 7 (A) and day 11 (B). The data is a summary from three cultures of h-MSCs derived from three different donors. Due to significant variations in the ALP activity of different donors, all samples were normalized with the control treatment of individual donors (i.e., h-MSCs treated with BM alone). The significantly different groups are indicated (*: p<0.001**: p<0.005, and *: p<0.05 as compared to cultures treated with BM and BM+GP).**

4.3.2 Dose Dependent Response of h-MSCs to Dex, BMP-2, Vit-D3 and b-FGF

Longer term osteogenesis of h-MSCs was then investigated by culturing the cells in BM containing GP (10 mM) and in the presence of various concentrations of supplements. The GP was added to media since this supplement is known to be essential for *in vitro* mineralization. The control group was treated with BM without any supplements. As before, the DNA content and specific ALP activity were determined in addition to *in vitro* calcification.

4.3.2.1 DNA Content

The DNA content of the treatment groups was generally lower on day 15 (**Figure** 4-3**A**) than the control BM group without supplements. The DNA content of h-MSCs treated with 10 nM Dex+0 nM Vit-D3+0 ng/mL BMP-2 was significantly higher than h-MSCs treated with 10 nM Dex +50 nM Vit-D3+0 ng/mL BMP-2 ($p<0.005$). Similarly, cultures treated with 10 nM Dex+0 nM Vit-D3+500 ng/mL BMP-2 demonstrated higher DNA content as compared to similar cultures treated with 10 nM ($p<0.05$) and 50 nM ($p<0.001$) Vit-D3. On the other hand, the b-FGF significantly increased the total DNA content of h-MSCs treated with 100 nM Dex+0/50 nM Vit-D3+500 ng/mL BMP-2, as compared to similar treatments without b-FGF ($p<0.001$). Increasing Dex and BMP-2 concentrations did not show any detrimental effects on the DNA content of h-BMC cultures.

In longer cultures (day 25), there was no significant effect of increasing Dex or Vit-D3 on the DNA content of the treated h-MSCs (**Figure** 4-3 **B**). Addition of b-FGF, however, increased DNA content of cultures treated with 10/100 nM Dex+0 nM Vit-D-3+500 ng/mL BMP-2 as compared to similar cultures treated in the absence of b-FGF ($p<0.05$).

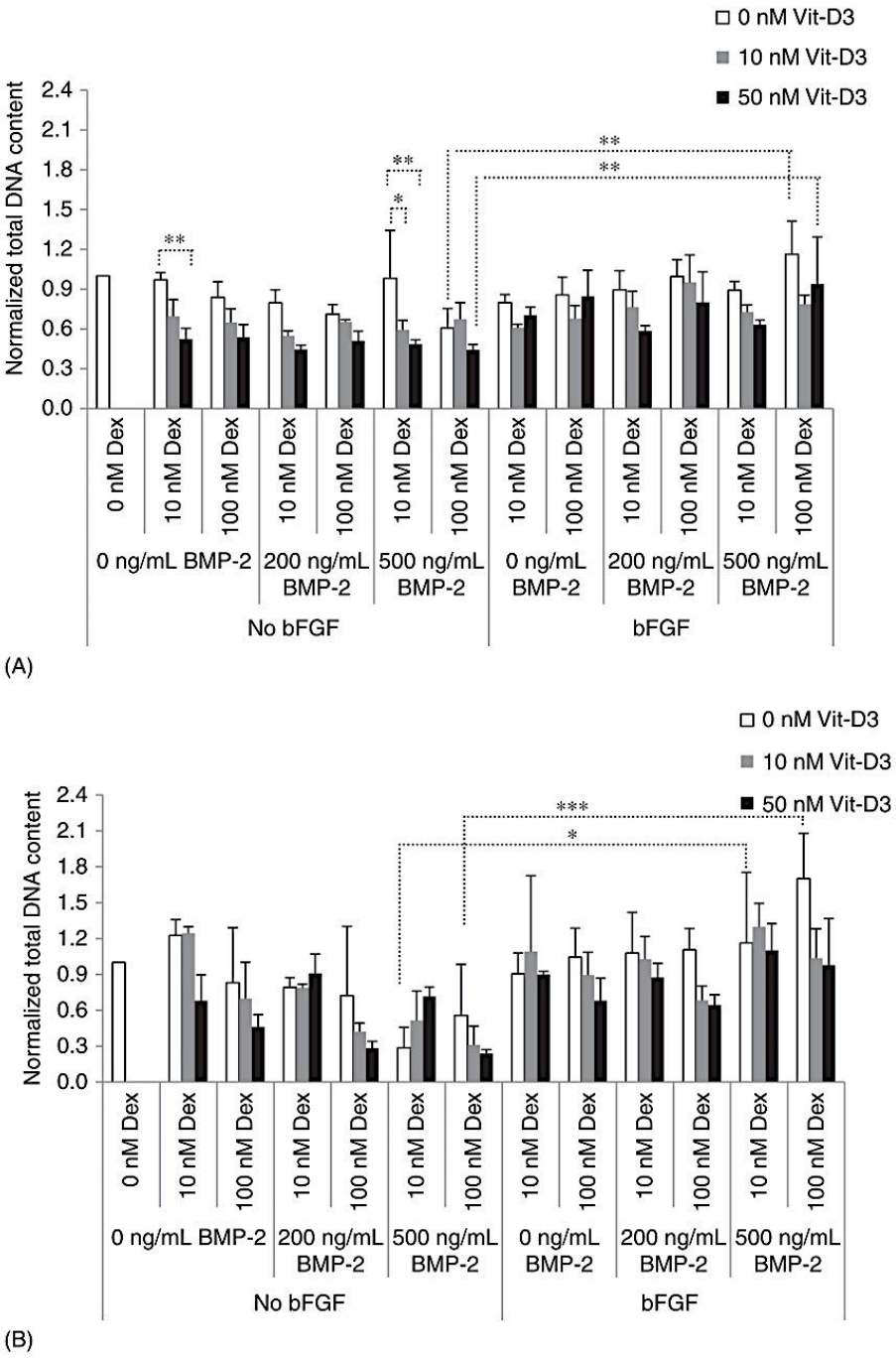

Figure 4-3: Effect of different osteogenic treatments on total DNA content of the h-MSCs. The analysis was conducted on day 15 (A) and day 25 (B). The data is a summary from three cultures of h-MSCs derived from three different donors. Due to significant variations in the DNA amounts of different donors, all samples were normalized with the control treatment of individual donors (i.e., h-MSCs treated with BM alone). The significantly different groups are indicated (*: p<0.001, **: p<0.005, and *: p<0.05).**

4.3.2.2 Specific ALP activity

On day 15, the specific ALP activities of h-MSCs were generally higher without b-FGF treatment (**Figure** 4-4 **A**). In the absence of b-FGF, Vit-D3 (50 nM) had a stimulatory role in specific ALP activity, which was considerably increased by treatments with 100 nM Dex+0 ng/mL BMP-2, 100 nM Dex+200 ng/mL BMP-2 and 10 nM Dex+500 ng/mL BMP-2 ($p<0.05$) as compared to control cultures. The specific ALP activity was also stimulated in cultures treated with 50 nM Vit-D3+100 nM Dex+200 ng/mL BMP-2 as compared to cells treated similarly but without Vit-D3 ($p<0.05$). In the presence of b-FGF, cells treated with 100 nM Dex+50 nM Vit-D3+200 ng/mL BMP-2 displayed reduced specific ALP activity ($p<0.005$) as compared to similar cultures treated in the absence of b-FGF. Although there was a general trend of increasing specific ALP activity with increasing Vit-D3 concentration in the presence of b-FGF, there were no significant differences among the groups on day 15. Increasing Dex and BMP-2 concentrations did not appear to change the specific ALP activity of treated h-MSCs in this time frame.

On day 25, there was a general reduction in the specific ALP activity among the groups (compare scales in **Figure** 4-4 **A** and **4B**). Vit-D3 again appeared to increase specific ALP activity, as evident by the increased ALP activity in 100 nM Dex+50 nM Vit-D3+0 ng/mL BMP-2, 100 nM Dex+10 nM Vit-D3+200 ng/mL BMP-2, 100 nM Dex+50 nM Vit-D3+200 ng/mL BMP-2, 10 nM Dex+50 nM Vit-D3+500 ng/mL BMP-2, and 100 nM Dex+50 nM Vit-D3+500 ng/mL BMP-2 groups as compared to control group ($p<0.05$ in all cases). The specific ALP activity was also stimulated in cultures treated with 50 nM Vit-D3+100 nM Dex+0 ng/mL BMP-2 and 50 nM Vit-D3+100 nM Dex+200 ng/mL BMP-2 as compared to cells treated similarly but without Vit-D3 ($p<0.05$). Increasing Dex concentration from 10 nM to 100 nM in cultures treated with 50 nM Vit-D3 and 200 ng/mL BMP-2 significantly increased the ALP activity ($p<0.05$). Addition of b-FGF to 100 nM Dex+50 nM Vit-D3+200 ng/mL BMP-2 decreased ALP activity in treated cells as compared to cells exposed to similar conditions but

without b-FGF ($p<0.05$). There was no effect of increasing BMP-2 concentration (from 0 to 500 ng/mL) on specific ALP activity of h-MSCs at this time point.

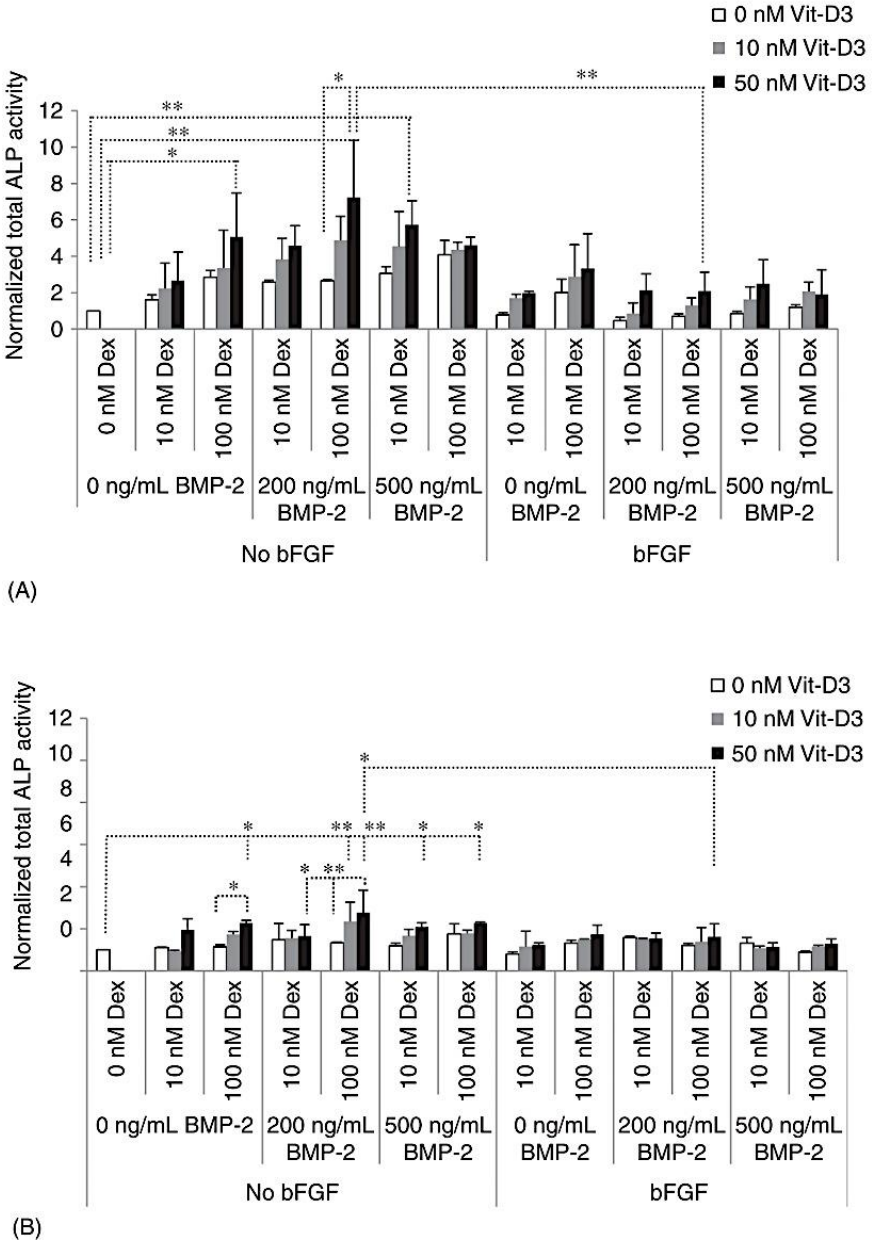

Figure 4-4: Effect of different osteogenic treatments on specific ALP activity of the h-MSCs. The analysis was conducted on day 15 (A) and day 25 (B). The data is a summary from three cultures of h-MSCs derived from three different donors. Due to significant variations in the DNA amounts of different donors, all samples were normalized with the control treatment of individual donors (i.e., h-MSCs treated with BM alone). The significantly different groups are indicated (: $p<0.005$, and *: $p<0.05$).**

4.3.2.3 Calcification

There was a lack of calcification for h-MSCs on day 15 (not shown), but calcification was evident on day 25 (**Figure** 4-5). Cells cultured in BM without any supplements did not yield any calcified deposits over the 25 days, indicating a lack of dystrophic calcification under our experimental conditions. In the absence of any growth factors, calcification was evident with increasing Dex concentration from 10 to 100 nM ($p<0.05$). In the absence of b-FGF, increasing Dex concentration from 10 to 100 nM also enhanced calcification of h-MSCs treated with Vit-D3 (10 or 50 nM) and BMP-2 (200 and 500 ng/mL) ($p<0.01$ in all cases). In the presence of b-FGF, increasing Dex concentration from 10 to 100 nM also enhanced calcification only in h-MSCs treated with Vit-D3 (10 or 50 nM) and BMP-2 (0 and 500 ng/mL) ($p<0.01$ in all cases).

The effect of Vit-D3 on the calcification of h-MSCs was dependent on other supplements. In the absence of b-FGF, a detrimental effect of Vit-D3 (50 nM) was seen for cultures treated with 10 nM Dex and 200 or 500 ng/mL BMP-2 ($p<0.05$) as compared to similar cultures treated without Vit-D3. In the presence of b-FGF, only h-MSCs treated with 100 nM Dex and, 10 and 50 nM Vit-D3 showed significant calcification irrespective of the BMP-2 concentration ($p<0.01$).

In the absence of b-FGF, BMP-2 was stimulatory for calcification; for example, increasing BMP-2 concentration from 0 to 500 ng/mL in cultures with 10 nM Dex+0 or 10 nM Vit-D3, and 100 nM Dex+10 or 50 nM Vit-D3 showed a BMP-2 dose dependent increase in calcification ($p<0.05$). Addition of b-FGF resulted in significant reduction in mineralization in all cultures treated with the highest BMP-2 concentration (500 ng/mL) except one culture (10 nM Dex+50 nM Vit-D3) as compared to similar cultures without b-FGF ($p<0.05$ in all cases). Cultures treated with 100 nM Dex+0 nM Vit-D3+200 ng/mL BMP-2 and in the presence of 10 ng/mL b-FGF demonstrated inhibition of calcification as compared to cultures exposed to the same treatment but without b-FGF ($p<0.005$).

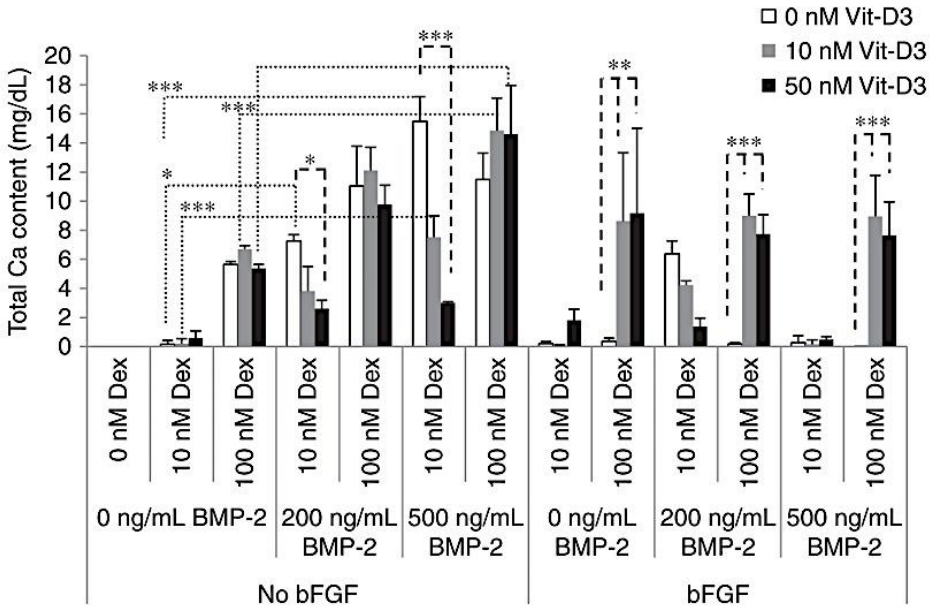

Figure 4-5: Effect of different osteogenic supplement combinations on calcification of h-MSCs on day 25. Each bar represents the mean + SD from 3 donors and no normalization was employed in this analysis (*: p<0.005, **: p<0.01, and *: p<0.05). Lines indicate significant changes in calcification due to Vit D3 (dashed line) and BMP-2 (dotted line).**

4.3.3 Comparison of Osteogenic and Adipogenic Response of h-MSCs

Following treatment of h-MSCs with different supplements, some cultures gave lipid droplet-like deposits in cells, which were positively stained with Oil Red O, whereas h-MSCs grown in BM did not produce such results. A comparison between calcification (osteogenesis) and Oil Red O staining (adipogenesis) in treated h-MSCs was then pursued to investigate the best supplement combination for enhanced osteogenesis without adipogenesis. Adipogenesis was characterized based on Oil Red O staining and classified into "No", "Poor", "Moderate" and "High" based on the amount of positively stained lipid vacuoles (**Figure** 4-6), as well as specific changes in molecular markers (**Figure** 4-7). Calcification from **Figure** 4-5 was used as a measure of osteogenesis for comparison purposes and summarized in **Figure** 4-6.

(A)

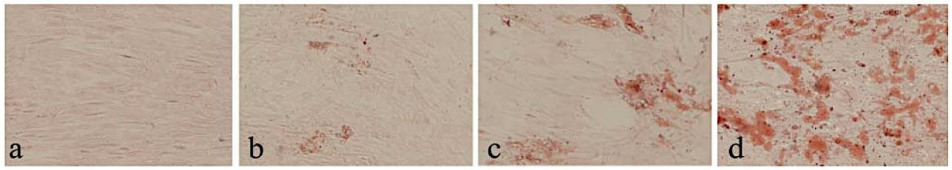

(B)

			Adipogenesis (D15)		Adipogeneis (D25)		Osteogeneis (D25)	
			10 nM Dex	100 nM Dex	10 nM Dex	100 nM Dex	10 nM Dex	100 nM Dex
No b-FGF	0 ng/mL BMP-2	0 nM Vit D3	–	–	–	–	–	–/+
		10 nM Vit D3	–	–/+	–	–/+	–	–/+
		50 nM Vit D3	–	+	–	+	–	–/+
	200 ng/mL BMP-2	0 nM Vit D3	–	–/+	–	+	–/+	+
		10 nM Vit D3	–	–/+	–	+	–/+	+
		50 nM Vit D3	–	–/+	–/+	+	–	+
	500 ng/mL BMP-2	0 nM Vit D3	–	–	–	–/+	++	+
		10 nM Vit D3	–	–/+	–	–/+	–/+	++
		50 nM Vit D3	–	+	–/+	+	–	++
b-FGF	0 ng/mL BMP-2	0 nM Vit D3	–	–	–	–	–	–
		10 nM Vit D3	–	–	–	–/+	–	+
		50 nM Vit D3	–	–	–	–/+	–	+
	200 ng/mL BMP-2	0 nM Vit D3	–	–/+	–	++	–/+	–
		10 nM Vit D3	–/+	+	–/+	–/+	–/+	+
		50 nM Vit D3	–/+	+	–/+	–/+	–	–/+
	500 ng/mL BMP-2	0 nM Vit D3	–/+	–/+	–/+	++	–	–
		10 nM Vit D3	–/+	+	–/+	+	–	+
		50 nM Vit D3	–/+	±	–/+	+	–	–/+

Figure 4-6: Adipogenic differentiation in h-MSCs based on Oil Red O staining. Adipogenesis was classified based on the amount of positively stained lipid droplets in treated cultures. (A) Typical spectrum of adipogenesis seen in cultures (a) - : no staining, (b) -/+ : poor staining with only a few areas (<10%) of Oil Red O stain, (c) + : Moderate areas (10-40%) stained with Oil Red O Stain, and (d) ++ : significant (>50%) areas of Oil Red O stain. (B) Summary of adipogenesis in h-MSCs after 15 and 25 days of treatment with different osteogenic supplements. Calcification from Figure 4-5 was summarized and was used as a measure of osteogenesis for comparison purposes and summarized in Figure 4-6 as follow: - : no calcification (Ca++= 0-3 mg/dL), -/+ : poor calcification (Ca++= 3-8 mg/dL), + : moderate calcification (Ca++= 8-13 mg/dL) and ++ : significant calcification (Ca++> 13 mg/dL).

Based on Oil Red O staining, Dex appeared to be most influential in adipogenesis. At day 15, in the absence of b-FGF, 10 nM Dex did not demonstrate any adipogenesis in any culture, but the adipogenesis was evident as the concentration of the Dex was increased to 100 nM in all groups, except the 0 nM Vit-D3+0 ng/mL BMP-2 and 0 nM Vit-D3+500 ng/mL BMP-2 groups. Stronger adipogenesis was seen in the presence of b-FGF; 10 nM Dex gave some adipogenesis in all groups treated in the presence of BMP-2 (200 and 500 ng/mL) irrespective of Vit-D3 concentration (except 0 nM Vit-D3+200 ng/mL BMP-2). All 100 nM Dex groups treated in the presence of BMP-2 (200 and 500 ng/mL) demonstrated adipogenesis, which increased in the presence of Vit-D3 irrespective of its concentration (10 or 50 nM).

At day 25, in the absence of b-FGF, 10 nM Dex gave some adipogenesis with 200 and 500 ng/mL BMP-2 with 50 nM Vit-D3, but the level of adipogenesis was increased as the Dex concentration was increased to 100 nM. Stronger adipogenesis was seen with the addition of b-FGF; almost all 100 nM Dex groups (except 0 nM Vit-D3+0 ng/mL BMP-2) and 10 nM Dex groups treated with BMP-2 (except 0 nM Vit-D3+200 ng/mL BMP-2) gave adipogenesis. The strongest adipogenesis was seen in the presence of b-FGF (10 ng/mL) plus 100 nM Dex+0 nM Vit-D3+200 /500 ng/mL BMP-2. In b-FGF treated groups, Vit-D3 addition had a negative effect on the adipogenesis activity of h-MSCs in some cases (in the presence of BMP-2), but a stimulatory effect in others (in the absence of BMP-2).

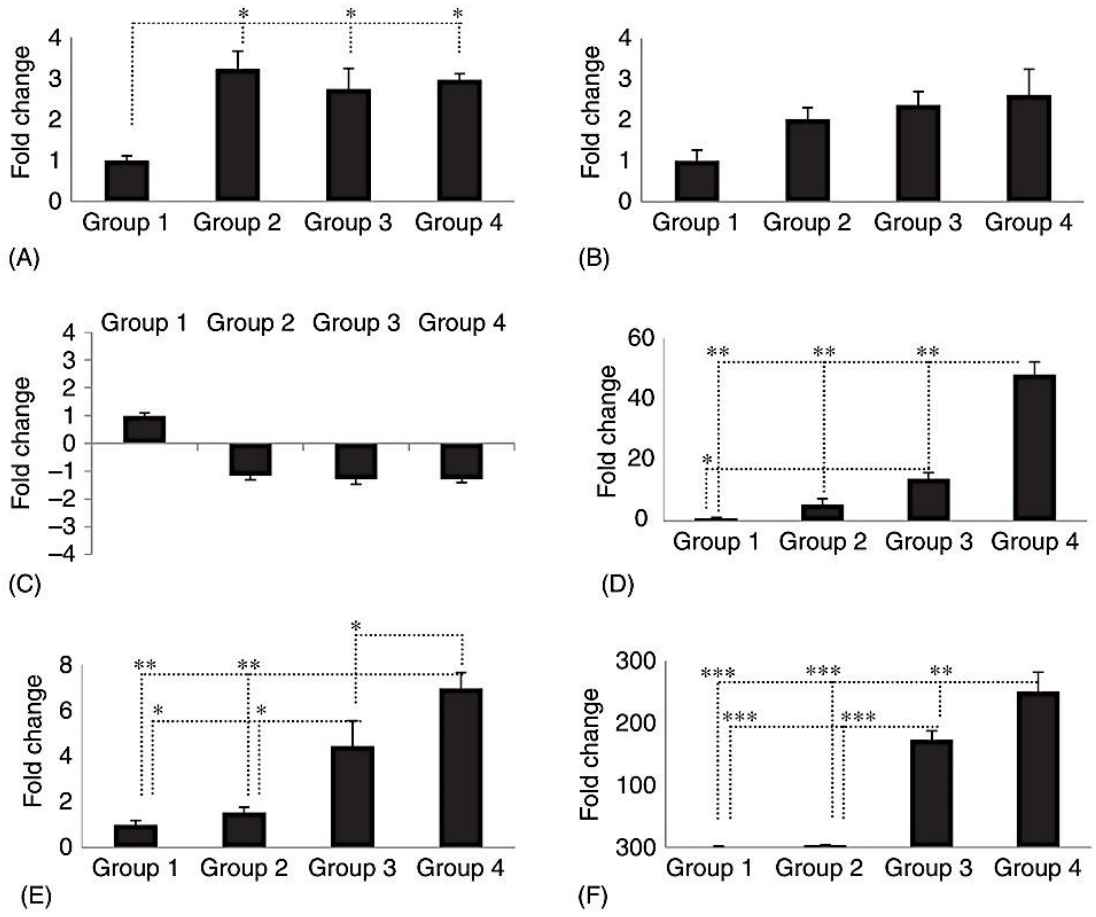

Figure 4-7: Quantitative analysis of osteogenic and adipogenic gene markers at day 15. The specific groups were: 1. BM (control), 2. Dex (10 nM) and BMP-2 (500 ng/mL), 3. Dex (100 nM), Vit-D3 (10 nM) and BMP-2 (500 ng/mL), and 4. Dex (100 nM), Vit-D3 (50 nM) and BMP-2 (500 ng/mL). (A) ALP, (B) Runx2, (C) ON, (D) BSP, (E) PPARγ2, and (F) aP2. Data represent mean ± SD from 3 donors. (*: p=0.000, **: p<0.001, and *: p<0.05).**

The q-PCR results for the expression levels of osteogenic and adipogenic markers are summarized in **Figure** 4-7. Only cells cultured in BM (control) and the three most osteogenic media were assessed for osteogenic and adipogenic gene-expression. The ALP expression level was increased 2.7-3.0 fold ($p<0.05$) in h-MSCs exposed to osteogenic treatments compared to control cultures (**Figure** 4-7**A**). The specific ALP activity (as measured by colorimetric assay on day 15) and ALP mRNA levels (as measured by q-PCR on day 15) gave comparable responses in h-MSCs under these treatments. The expression of Runx-2 in all osteogenic groups was 2.0-2.6 fold higher as compared to the cultures in BM (**Figure** 4-7**B**). ON was slightly decreased in osteogenic media as compared to control; however, this difference was not significant (**Figure** 4-7 **C**). BSP expression was pronouncedly increased in groups 3 and 4 by ~14 fold ($p<0.05$ as compared to control) and ~48 fold ($p<0.001$ as compared to all groups), respectively (**Figure** 4-7 **D**). The adipogenic genes PPARγ2 and aP2 were significantly up-regulated in groups 3 and 4, but not in group 2 (**Figure** 4-7 **E**). The PPARγ2 expression was 4.4-fold increased in group 3 ($p<0.05$ as compared to all groups) and ~7 fold in group 4 ($p<0.05$ as compared to all groups). Moreover, the expression of aP2 was increased by ~172 fold in group 3 ($p<0.000$ as compared to group 1 and 2) and by ~250 fold in group 4 ($p<0.001$ as compared to all groups) (**Figure** 4-7 **F**).

4.4 DISCUSSION

In tissue engineering based cellular therapies, one will rely on osteogenic cells cultivated in designer scaffolds to create a viable bone tissue in a bony defect site. It is desirable to use h-MSCs and induce them into osteogenic pathway during *in vitro* culture before implantation. Therefore, the aim of this study was to investigate the effects of Dex, BMP-2, Vit D3 and b-FGF on h-MSC osteogenesis *in vitro* to determine their potential for developing a cell-based therapy. Although there is extensive literature on *in vitro* osteogenic differentiation of h-MSCs, there were no studies that simultaneously investigated osteogenesis and adipogenesis with a wide range of concentrations and combinations of different supplements

(16 treatments in initial experiments and 37 treatments in subsequent experiments presented in our study). Most of the previous reports on differentiation of h-MSCs focused on either osteogenic or adipogenic differentiation of h-MSCs exposed, respectively, to osteogenesis or adipogenesis inducing media. We avoided this approach and evaluated the osteogenic and adipogenic differentiation concurrently in h-MSC cultures to provide a complete picture in clarifying the role of the supplements Dex, Vit-D3, b-FGF, and BMP-2. To the our best knowledge, most reports focused on osteogenic differentiation and lacked adipogenesis data in h-MSCs cultures exposed to osteogenic media containing BMP-2, Vit-D3 or b-FGF, which might explain some of the reported deleterious effects of these agents on osteogenic differentiation in h-MSCs.[135-137] Jaiswal et al.[122] extensively studied the osteogenic effects of Dex at 1-1000 nM, GP at 1-10 mM, and AA at 0.01 to 4 mM on h-MSCs and did not observe any adipogenesis with different doses of Dex (1-1000 nM) based on Oil Red O staining, but they did not studied the associated adipogenic gene-expression at the mRNA level. Moreover, Piek et al.[138] extensively studied osteogenic differentiation induced by Dex (100 nM), BMP-2 (250 ng/ml), and Vit-D3 (10 nM) and identified the role of the proto-oncogene c-MYC as a regulator of osteogenesis, however they did not explore the effects of these supplements on the adipogenic differentiation of h-MSCs. On the other hand, our study presented balanced osteogenesis and adipogenesis data for several combinations of supplements and presented optimal conditions for osteogenesis with minimal induction of adipogenesis based on ALP activity, calcification and expression of specific osteogenic and adipogenic markers. Our study reported similar responses in h-MSCs derived from the three different donors, so that our findings could be generally applicable to a wider population, although the latter extrapolation will require further investigation with additional cell sources.

The studies performed here initially relied on DNA content and ALP activity to investigate the response of h-MSCs to the supplements. The total DNA content was used as a measure of cell mass and to detect any detrimental effects of osteogenic supplements on cell proliferation. ALP is considered to be an early marker for osteoblastic differentiation that becomes up-regulated *in vitro* within

two weeks of osteogenesis.[139] It promotes mineralization through hydrolysis of pyrophosphate and ATP (an inhibitor of mineralization), and it is essential for phosphate production at local sites needed for the hydroxyapatite crystallization.[133] The specific ALP activity (as measured by a colorimetric assay on day 15) and ALP mRNA levels (as measured by q-PCR on day 15) demonstrated comparable responses in h-MSCs, suggesting that the ALP activity colorimetricly measured throughout this study could be linked to gene-expression. Our results demonstrated that GP alone did not affect cell viability (i.e., DNA content) and failed to promote ALP activity at any time point, but the addition of Dex was essential for the desired ALP response. Dex exposure additionally induced cellular proliferation of h-MSCs in early culture (day 7 and 11). Our data were similar to the study by Jaiswal et al.,[122] who demonstrated a significant increase in ALP activity and mineralization in h-MSCs exposed to osteogenic media containing 10 nM Dex, unlike cells grown with GP (10 mM) alone.

We expected the prototypical morphogen BMP-2 with its ability to induce *de novo* bone to impart significant osteogenesis in h-MSCs. On the contrary, Jorgensen et al.[43] reported that BMP-2 alone did not affect ALP activity and poorly induced *in vitro* calcification by h-MSCs. We made a similar observation in this study where, based on ALP activity as a measure of osteogenic differentiation, the BMP-2 effect was enhanced when h-MSCs were additionally exposed to BM+Dex or BM+GP+Dex combinations, so that these supplements might be needed for a strong BMP-2 effect in culture. The b-FGF, on the other hand, acted to increase cellular mass under numerous culture conditions in this study, while reversing osteogenesis. This was consistent with the literature on the mitogenic effects of b-FGF on MSCs,[140, 141] and anti-osteogenic effects mediated by b-FGF in human and rat MSCs.[136, 141]

We subsequently investigated dose dependent responses of the cultured h-MSCs to the supplements. Unlike the early time points, Dex did not change cellular proliferation or ALP activity of h-MSCs at late time points (days 15 and 25), but it enhanced mineralization in a dose dependent manner, as noted earlier.[122] However, increased mineralization of h-MSCs at higher Dex

concentrations also resulted in significant appearance of Oil Red O-stained cells. Increased adipogenesis was confirmed under select conditions, based on elevated expression of the adipogenic markers PPARγ2 and aP2. PPARγ2 is an early stage marker [142] and aP2 is a late stage marker of adipogenic differentiation.[143] The expression of aP2 is limited to adipocytes *in vitro* and *in vivo*, and an adipose-specific enhancer component was identified in the 5' flanking region of the gene.[144] In contrast, Jaiswal et al.[122] did not observe any adipogenesis in h-MSCs treated with different doses of Dex (1-1000 nM) based on Oil Red O staining, but they did not study the associated adipogenic gene-expression at the mRNA level. This might be due to different isolation protocol and/or variability in the cell source. Having adipogenesis in the induced cells is not desirable, since it might reduce the osteogenic cell pool at the transplant site, and it is imperative to minimize this activity for cultures destined for clinical application.

The influence of Vit-D3 on osteogenesis was previously investigated with h-MSCs;[135] Vit-D3 (10 nM) markedly inhibited cellular proliferation, enhanced ALP activity and reduced mineralization in Dex (10 nM) treated h-MSCs. In our hands, increasing Vit-D3 concentration from 0 to 50 nM in the presence of Dex resulted in reduced DNA content and mineralization in cultures treated in the absence of b-FGF, which is in accordance with others' observations. Reduced mineralization might be due to reduced cell proliferation induced by increasing Vit-D3 concentration. The addition of Vit-D3 was stimulatory for adipogenesis in h-MSCs used in our study, in line with observations in the rat calvarial cells cultured with similar concentrations of the supplements,[145] where adipogenesis was increased in a dose dependent manner for Vit-D3 (from 0.1 to 100 nM) and Dex (from 1 to 100 nM). A synergistic effect for Vit-D3 and Dex on adipogenesis was evident in h-MSCs (this study) and rat calvarial osteoblasts.[145] Interestingly, addition of Vit D3 (10 or 50 nM) plus Dex (100 nM) significantly enhanced calcification of h-MSCs after 25 days only in the presence of 10 ng/mL b-FGF, irrespective of the BMP-2 concentration. It is likely that the Vit-D3 and Dex inhibited b-FGF induced adipogenesis and supported osteogenesis in h-MSCs as

evidenced by reduction in lipid formation concurrent with a significant increase in mineralization at this time point.

The BMP-2 gave dose dependent mineralization in h-MSCs, consistent with other studies on the activity of this morphogenetic protein on rat and h-MSCs.[137, 141] Conversely, the highest BMP-2 concentration (500 ng/mL) reduced cell mass of cultured h-MSCs at day 25, which was significantly improved by co-treatment with b-FGF. It is likely that cell mass (as measured by the DNA content) might have been reduced due to enhanced extracellular mineralization caused by BMP-2. In parallel with osteogenesis, BMP-2 also gave enhanced adipogenesis in some cases, for example in combination with Dex (100 nM) and b-FGF (10 ng/mL). Previous studies reported negative effects of Dex on osteogenesis as a result of preferential adipogenic differentiation in rat calvarial cells (based on Oil Red O staining), in cells treated with 10 nM Dex and 100 ng/ml BMP-2.[146] BMP-7 (100 ng/mL) also gave elevated expression of adipocyte specific genes aP2, adiponectin and lipoprotein lipase in h-MSCs in osteogenic media (10 mM GP, 50 µg/mL AA, and 100 nM Dex).[147] BMP-7 (50-200 ng/mL) was also capable of inducing adipogenesis in h-MSCs cultured in conditions favoring chondrogenic differentiation in the absence of TGF-ß3.[148] Therefore, there seems to be consistent data in the literature that the presence of BMPs might stimulate adipogenesis under 'osteogenic' culture conditions.

Combinations of BMP-2 and b-FGF demonstrated synergistic osteogenic effects during differentiation of h-MSCs and bone formation *in vivo*.[149] The BMP-2+b-FGF co-treatment used in our experiment was intended to investigate this synergistic action, but no such synergistic effects were evident on osteogenic responses of h-MSCs. In fact, b-FGF treatment consistently deteriorated BMP stimulated osteogenic differentiation in h-MSCs, in line with previous studies on h-MSCs.[136] However the latter studies did not investigate adipogenesis. The stronger adipogenesis seen in h-MSCs cultured in the presence of b-FGF in this study might explain the reduction in osteogenesis in treated h-MSCs. It is likely that b-FGF increased the population of other cell lineages as they share the same multipotent precursors in the bone marrow.[150] Conversely, Akita et al.[149]

demonstrated significant enhancement of ALP activity following treatment of h-MSCs with b-FGF (2.5 ng/mL) and BMP-2 (50 ng/mL) for 4 days after 6 days of osteogenic treatment with Dex (100 nM), AA (0.05 mM) and GP (10 mM). Sequential addition of the media supplements and the lower concentration of BMP-2 and b-FGF used in Akita`s study might lead to increased ALP activity and presumably osteogenesis, unlike our results.

Osteogenesis in our strongly mineralizing cultures was also confirmed based on specific changes at the mRNA levels of ALP, BSP, ON, and Runx-2. Runx-2 is expressed in pre-osteoblasts, immature osteoblasts, and early mature osteoblasts.[151] ON is involved with the onset of crystal nucleation.[152] BSP indicates a late phase of osteoblast differentiation and an initial phase of mineralization.[153] Our study reported considerable enhancement of *in vitro* calcification in cultures enriched with the highest concentration of BMP-2 and Dex (i.e., cultures treated with 100 nM Dex+10 nM Vit-D3+500 ng/mL BMP-2, and 100 nM Dex+50 nM Vit D3+500 ng/mL BMP-2) more than the lower concentrations. This was confirmed with increased expression of ALP, Runx-2 and BSP as compared untreated control cells. Unlike other markers, ON expression was not significantly changed in h-MSCs and we note a similar observation in a previous independent study.[132] Adipogenesis in these cultures paralleled osteogenesis, given by significant up-regulation of the adipogenic markers PPARγ2 and aP2. Our results are consistent with a previous report,[147] which indicated enhanced expression of osteogenic markers (ALP, Runx-2, osteopontin, and osteocalcin) as well as adipogenic markers (aP2, adiponectin, and lipoprotein lipase) in h-MSCs exposed to similar osteogenic media (10 mM GP, 100 nM Dex, but with 100 ng/mL BMP-7). A critical issue is to identify culture conditions that optimize osteogenesis with no or minimal adipogenesis. In our hands, this condition was attained at 10 nM Dex, 500 ng/mL BMP-2, and without Vit-D3 and b-FGF. It must be stated that this conclusion is based on addition of media supplements to h-MSCs simultaneously. It is likely that sequential addition of the media supplements might alter this picture and lead to different results. This was considered beyond the scope of the current study. We

can envision employing conditions that do not support osteogenesis initially (e.g., culture in BM + b-FGF supplementation) following by exposure to osteogenic supplements (e.g., Dex and BMP-2) when sufficient cell expansion occurs.

The concept of reconstructing craniofacial defects with MSCs from bone marrow was successfully validated in different animal models,[55, 154] with osteogenically induced cells yielding better bone induction in animal models.[155] However, the use of h-MSCs for bone regeneration in humans is rare. Gimbel et al.[58] implanted collagen scaffolds seeded with bone marrow aspirates into human cleft defects and reduced morbidity compared to autologous grafts, but they did not report any quantitative measurement of bone formation at defects. Behnia et al. [59] implanted h-MSCs combined with a demineralized bone mineral/calcium sulphate scaffold to obtain <50% bone fill. Both studies employed h-MSCs with no osteogenic conditioning. Hibi et al.,[61] on the other hand, employed osteogenically induced h-MSCs to repair an alveolar cleft in a 9 year old patient, which resulted in ~79% bone fill after 9 month post-operatively with successful eruption of lateral incisor and canine. The conditioning was attempted with platelet-rich plasma, whose osteogenic effects are difficult to dissect due to its various constituents. No attempts have been made to optimize the osteogenic conditioning of the cells using purified supplements (such as the ones used in this study) before transplantation. Employing purified reagents might be a better approach since it can provide better control over the potency and reproducibility of cellular differentiation. The outcome of cell-based therapies for bone regeneration could be accordingly optimized with such an approach, potentially providing a superior alternative for autologous grafts. Our studies delineated the conditions for phenotypic differentiation of h-MSCs and it will be important to explore *in vivo* potential of phenotypically differentiated h-MSC for translation into clinics.

In conclusion, Dex was found to be most essential for osteogenesis of h-MSCs *in vitro*, but high concentrations of Dex (100 nM) also enhanced adipogenesis of h-MSCs. Vit D3 appeared to be essential for calcification only in the presence of b-FGF. But in the absence of b-FGF, increasing Vit-D3 in culture (e.g., from 0 to

50 nM) did not have any additive effect on mineralization and, in fact, increased adipogenesis in some cases. BMP-2 demonstrated a dose dependent increase in mineralization as its concentration increased from 0 to 500 ng/mL, but its effect was more pronounced in the presence of Dex. Although b-FGF (10 ng/mL) was beneficial in enhancing DNA content in some cases, it deteriorated osteogenic and enhanced adipogenic features of the cultured h-MSCs. Our results indicated that under appropriate priming with the optimal Dex and BMP-2 concentrations, h-MSCs could be stimulated for osteogenesis with minimal adipogenesis. These studies provide a framework for obtaining optimal osteogenesis with h-MSCs and this will be indispensable for clinical tissue engineering efforts that will rely on conditioned cells to induce a viable bone tissue in desired repair sites.

Chapter 5

Reliable critical-sized defect rodent model for cleft palate research

5.1 BACKGROUND

Repair of Alveolar clefts defects remains a challenging surgical procedure. Few treatment options are considered for cleft patients including gingivoperiosteoplasty and secondary bone grafting. The gingivoperiosteoplasty technique is utilized to permit bone healing by creating a periosteal tunnel between the cleft alveolar segments.[156] Together with preoperative orthodontic alveolar molding, the alveolar gap is reduced and adequate alveolar bone regeneration was reported in approximately 60% of treated patients.[157] Grafting autologous bone from patients' iliac crest is another treatment modality. However, donor site morbidity, persistent pain, nerve injury, infection, fracture, scarring, and paraesthesia may hamper this method.[158] Therefore, developing innovative grafting therapies based on artificial bone grafts would have a tremendous impact on cleft palate reconstruction. The main benefits of these artificial bone grafts are reduced donor site morbidity, hospital stay duration, and overall procedure cost.

An appropriate animal model is essential for testing new bone grafting therapies. Available animal models of cleft palate include both congenital and surgical clefts. Teratogenic and transgenic cleft models were established. Teratogenic pharmaceuticals (phenytoin and corticosteroids) or genetic mutations (Twirler gene (Tw/Tw) in mice) are utilized to develop cleft palate with either unilateral or bilateral clefts lip.[159-162] These models significantly enhanced our understanding of etiology and morphogenetic factors contributing to cleft development, but they were not utilized for development of new grafting therapies.[34] This could be due to the small maxilla size in mice models as well as the variability in cleft size and anatomical location. Therefore, surgical cleft models were considered more suitable for efficacy testing for new biomaterials for bone grafting. The created surgical defects should be critically sized i.e. bony voids of a size that cannot heal spontaneously during the lifespan of the animal.[163]

Surgical clefts were produced in primates,[73, 164] dogs,[74] and rabbits.[75, 165] But these models are limited by high operational and husbandry cost. This led to the development of rodent models of gingivoperiosteoplasty namely mid palate cleft model (MPC) and alveolar cleft model (AC). In 2000, Mehrara et al.[33] developed

the MPC model (9×5×3 mm^3) and demonstrated complete bone healing by 12 weeks. However this study did not report strain, age, or weight for the tested rat model. It also provided semi-quantitative assessment of bone formation based on anterioposterior and mediolateral radiographs that are limited by: superimposition of structures, variable magnification, and distortion. This led to the development of the AC model (7×4×3 mm^3) by Nguyen et al.[34] in 8 week old Sprague Dawley rats.[8] Based on histology and micro-computed tomography (μCT), there were no statistically significant difference in bone formation in the defect site between 4, 8 and 12 weeks, making it a suitable critical size defect. However, Bone grafting using bone morphogenetic proteins (BMP-2) based scaffolds in the established AC model[34] did not reveal any significant effect for BMP-2 on bone formation over 12 weeks.[35] Authors justified this because of burst release kinetics of BMP-2 from collagen scaffold and incompletely sealed oral tissue. But looking into the μCT images of the created alveolar defects,[34] communications between the created cleft defects and surrounding anatomical structures such as nasal cavity and periodontal ligament space of the incisor teeth were identified. This could result in substantial loss of BMP-2 with subsequent suboptimal BMP-2 concentration at the defect site. Toward this end, there is no reliable, reproducible and cost-effective animal model suitable for testing new bone grafting alternatives, which could explain the delays for developing alternative therapies for secondary bone grafting. Therefore, our study critically assessed and compared the current rodent models of cleft palate (MPC and AC) to identify the most reliable model. This study also proposed alterations in the design of two models based on preoperative virtual planning to avoid damage to surrounding anatomical structures. Finally, bone healing in the modified models was thoroughly evaluated over 8 weeks to confirm the critical size nature of the defects.

5.2 METHODS

A series of successive experiments is presented in this article. In the pilot study we attempted to reproduce the published 7×4×3 mm^3 AC model in 8 weeks old Sprague Dawley rats. However, this resulted in significant injury of the surrounding structures including the incisor teeth, nasal septum and palatine foramen. The same dimensions were then reproduced in 16 weeks old Sprague Dawley rats and damage to the same structures was again observed. We then compared the anteroposterior and transverse dimensions of the maxilla in 16 weeks old Sprague Dawley vs. Wistar rats (n=4/group). Subsequently, virtual planning for the appropriate design of MPC and AC defects was performed in 16 weeks old Wistar rats (n= 4). Finally, we conducted a comparative study to assess bone healing following employing the designed defects based on virtual planning in 16 weeks old Wistar rats weighing 375-400 g (n=6/group). Modified defects were designed to be at least 1 mm away from roots of the incisors to avoid damage to PDL, 1 mm away from the palatine foramen and 1 mm away from the zygomatic arch. Bone healing in the modified models was assessed by "in vivo" μCT (weeks 0, 4, and 8) and histology (week 8).

5.2.1 Animals and surgical procedures

The animal care committee at the University of Alberta approved the experimental protocol. Animals were housed in standard conditions (2 rats/cage at room temperature with 12 hour of light/dark cycle). Soft diet and liquid gel packs were provided for the animals 2 days preoperative and 1 week postoperative, and then advanced to a regular diet.

Rats were anesthetized by intra-peritoneal injections of Ketamine (75 mg/kg) and Domitor (0.5 mg/kg). Additionally, 0.25 ml of lidocaine 0.4% was injected at the surgical site. For MPC group, V-shaped incision was done at midline and extends bilaterally to the zygomatic arches. Using Bien Air surgical hand piece, MPC defects of 7×2.5×1 mm^3 were created in the premaxilla. For AC group, longitudinal incision was made at the alveolar crest and AC defects of 5×2.5×1 mm^3 were created. Mucosal flaps were closed using 4-0 polyglactin absorbable sutures. At the end of the surgery, animals were recovered by intra-peritoneal

injections of 1mg/kg revertor (atipamezole hydrochloride). Postoperative pain control included subcutaneous administration of Metacam at 2 mg/kg (once/day) and Butorphanol at 0.2mg/kg (twice/day). Rats were evaluated daily for two week postoperative for any indications of pain (e.g. reduced activity, porphyrin staining, lethargy, loss of appetite or weight loss).

5.2.2 *In vivo* µCT Assessment

Rat maxillae were scanned with µCT scan (Skyscan 1176 *in vivo* µCT, Skyscan NV, Kontich, Belgium). Isoflurane (2% in oxygen) was used to anesthetize the rats during µCT imaging. All µCT scans were conducted at 100 kV through 180º with a rotation step of 0.5º to produce serial cross-sectional images of isotropic 18 μm^3 voxels. All images were processed using bundled commercial software. Cross-sectional µCT images and 3D models were utilized for cleft defect size measurements as well as morphometric analysis.

5.2.3 Radiomorphometric analysis

Reconstructed 3D images were subjected to analysis using Mimics software (Materialise, Leuven, Belgium) to measure anteroposterior and transverse dimensions of the maxillae in non operated 16 weeks old Sprague Dawley vs. Wistar rats (n=4). For this purpose, we utilized landmarks established by Gomes et al.[166] in an axial viewing position (**Figure** 5-1). The distances from infraorbital foramen to incisal point (IF-IP) were measured bilaterally to represent the anteroposterior dimension while the distance between right and left IF was utilized for transverse measurements. Additionally, we used the same landmarks to compare maxillary growth over time between 16, 20 and 24 weeks old Wistar rats (n=4).

Subsequently, different 2D and 3D views of µCT data of the scanned maxillae of non operated 16 weeks old Wistar rats (n=4) were carefully evaluated to plan the appropriate dimension and position of MPC and AC defects. For MPC defect, the maximum defect length and width were measured on the ventral surface of the 3D reconstructed µCT images. Distance between IP and a point located 1 mm anterior to the palatine foramen was measured to represent the maximum length (anteroposterior dimension) of the defect. The distance was measured between

lines drawn 1 mm away from the right and left incisors and along the contour of palatine bone, representing the width of the defect. While, lateral surface of 3D reconstructed premaxilla was used to estimate the appropriate size of the AC defect that is 1 mm away from zygomatic arch, incisor root and palatine foramen. Additionally, 2D image μCT were used to measure the thickness of the palatine bone that represents the maximum depth for both MPC and AC defects. All measurements were completed and reassessed after one week by a single operator.

Following virtual planning, both MPC and AC defects with the modified dimensions were employed in 16 weeks old Wistar rats (n=6 per group). Bone healing of the developed defects was monitored overtime using *in vivo* μCT imaging. A fixed rectangular region of interest (ROI) was employed to sample a standardized volume of the palatine bone in the premaxilla in order to perform standardized morphometric analyses. Incisor roots were utilized as anatomical landmarks for consistent selection of the same region of palatine bone from all samples. Skyscan CT-Analyser software (CTAn 1.10.0.1, SkyScan, Kontich BE) was used to binarize 2D transverse images with a gray scale thresholding of 36/255 to measure bone volume (BV, mm^3). The difference between BV at W0 and subsequent time points (W4 and W8) was defined as bone filling volume, and the percentage ratio between the bone filling volume and initial defect volume at W0 was defined as percent bone filling.

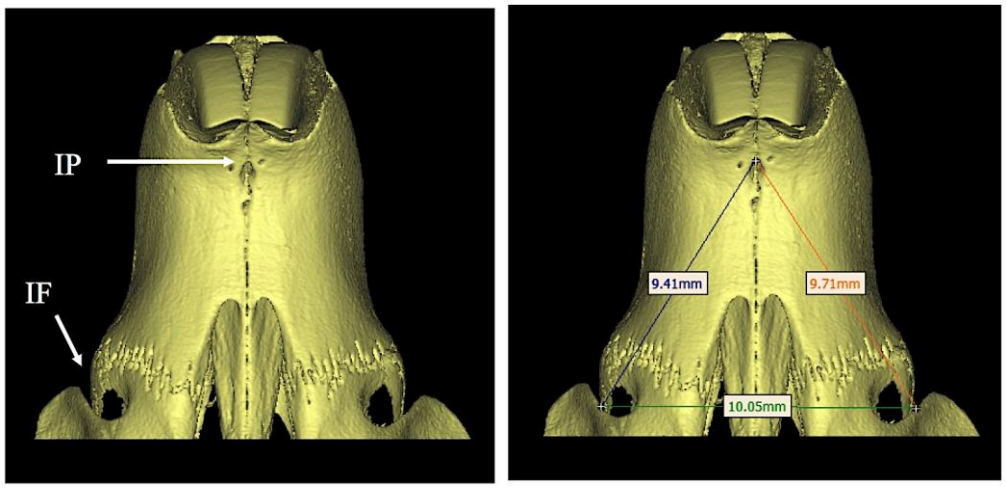

Figure 5-1: Axial view of 3D reconstruction of rat maxilla showing landmarks used for anteroposterior and transverse measurements. IP: Incisal point and IF: Infraorbital foramen

5.2.4 Histological assessment

At the end point (8 weeks) all rats were euthanized by CO2. Maxillae were dissected and stored in 10% paraformaldehyde. Then, samples were washed with phosphate buffered saline (PBS) and immersed in 10% Disodium Ethylene Diamine Tetra Acetic acid (EDTA) for decalcification for 3 weeks. Samples were sectioned and stained with Hematoxylin and eosin (H&E) stain to assess bone formation at the cleft defect site.

5.2.5 Statistics

Student t-test was performed to determine if there is significant difference between different data sets and p values <0.05 were considered significant. All µCT measurements were completed and reassessed after one week by a single operator. The intraclass correlation coefficient (ICC) was used to estimate the intra-rater reliability.

5.3 RESULTS

5.3.1 Validation of current cleft palate models

Our preliminary studies utilizing a 7×4×3 mm^3 AC defect in 8 weeks old Sprague Dawley rats resulted in injury of the surrounding structures including roots of incisors, zygomatic arch, and a clear communication with nasal cavity (**Figure** 5-2) based on gross examination of the dissected maxilla. In a subsequent study, we utilized older Sprague Dawley rats (16 weeks) for developing the AC defect. However the size of maxilla in the older rats (16 weeks) was not significantly different from the younger rats (8 weeks) and therefore the original alveolar defect measurements (7×4×3 mm^3) also resulted in damage to the surrounding structures. These findings were confirmed by µCT assessment shown in **Figure** 5-3. Following this experiment, we performed morphometeric analysis of rat maxillae to verify the reproducibility of the reported dimensions in the two published models (MPC and AC).[33, 34]

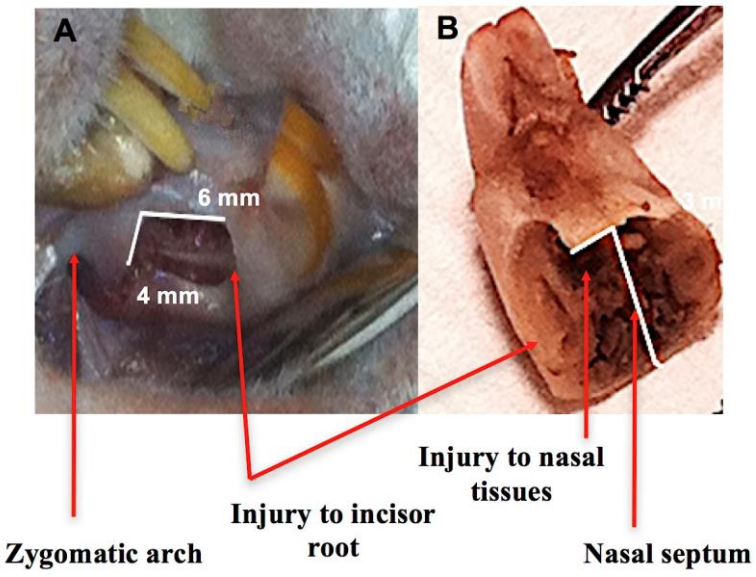

Figure 5-2: AC model (6×4×3 mm^3) created in a representative 8 weeks old Sprague Dawley rat. A- lateral view of the defect with rat placed in supine position, and B- coronal section of gross specimen at the defect site confirming injury to incisor root and nasal tissues.

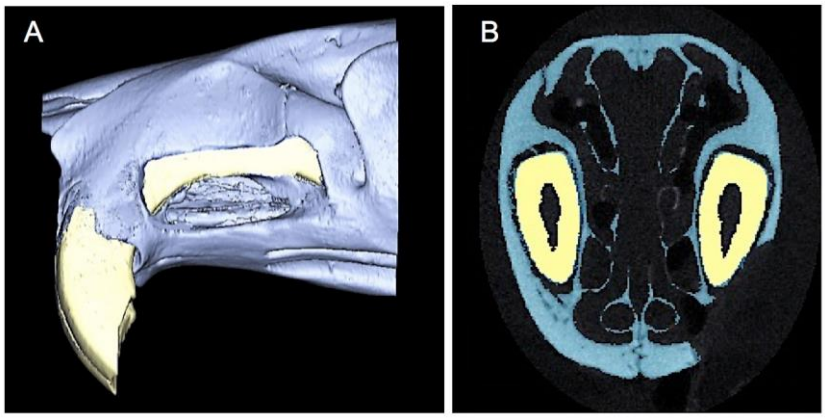

Figure 5-3: Representative µCT images of AC model (7×4×1 mm^3) created in 16 weeks old Sprague Dawley rats. Incisor segmentation was done to demonstrate the exposure of the incisor root (arc shaped) with these dimensions. A- Lateral view of representative 3D reconstructed premaxilla, and B-Coronal cross- sectional image

5.3.2 Radiographic morphometric analysis

Unpaired t-test was performed to determine if there is a difference in the size of the maxilla between Sprague Dawley and Wistar rats (16 weeks old). Two-tail p-value was 0.16 providing evidence that there were no differences in the anteroposterior and transverse dimensions two groups (**Table** 5-1). Furthermore, there was no significant difference in the anteroposterior dimensions between right and left side in each group (two-tail p-value was 0.47 and 0.65 for Sprague Dawley and Wistar rats, respectively) confirming palatal symmetry. Additionally, there were no significant differences in the anteroposterior or transverse dimensions measured in 16, 20, and 24 weeks old Wistar rats (**Table** 5-2).

Table 5-1: Mean values of anteroposterior and transverse measurements of maxillae of 16 weeks old Sprague Dawley and Wistar rats (n= 4/group)

Group	**Measurements**	
	IF-IP	IF-IF
Sprague Dawley rats	9.32±0.13 (right side) 9.43±0.17 (left side)	9.24±0.27
Wistar rats	9.11±0.57 (right side) 8.97±0.70 (left side)	9.83±0.56

Table 5-2: Mean values of anteroposterior and transverse measurements of maxillae of 16, 20 and 24 weeks old Wistar rats (n= 4/group)

Rat age	Measurements	
	IF-IP	IF-IF
16 weeks old	9.11±0.57 (right side) 8.97±0.70 (left side)	9.83±0.56
20 weeks old	9.67±0.92 (right side) 9.55±0.63 (left side)	10.33±0.26
24 weeks old	9.3±0.75 (right side) 9.60±0.68 (left side)	10.50±0.33

Virtual planning was performed in 16 weeks old Wistar rats based on preoperative μCT images (**Figure** 5-4). For MPC defects, the mean length (anteroposterior dimension) was 2.84±0.4 mm while the mean width (side-to-side) was 7.23±0.27 mm. While for AC defects, the mean length (anteroposterior dimension) was 5.48±0.22 mm and the mean width (dorsal-ventral dimension) was 2.43±0.13 mm. Finally, the mean depth for both models (palatine bone thickness) was 1±0.2 mm.

All μCT measurements were completed and reassessed after one week by a single operator. The intra-rater ICC for μCT measurements was high (0.99) with narrow confidence interval, indicating precision and reliability of the measurements.

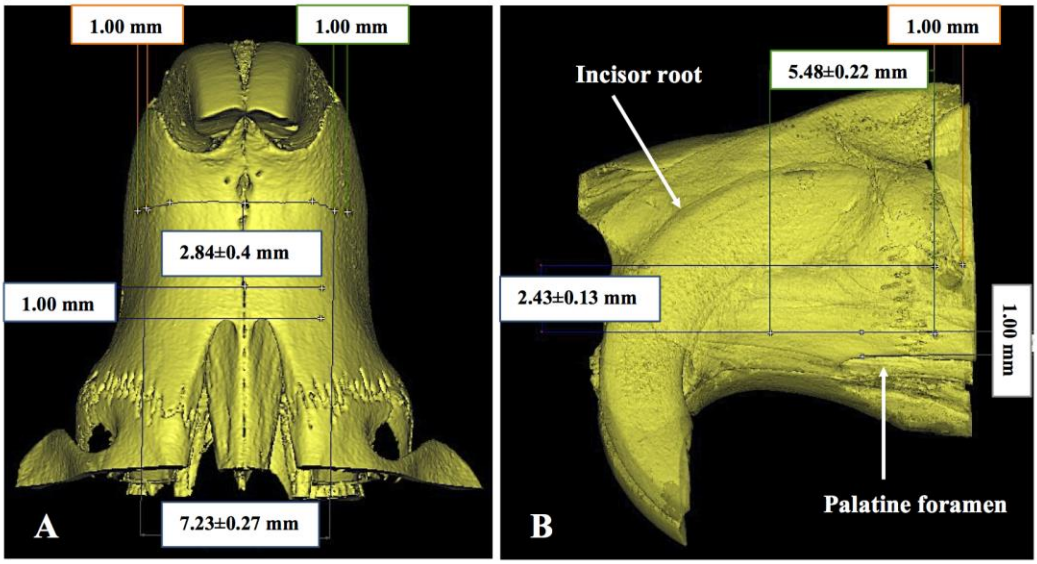

Figure 5-4: Preoperative virtual planning of the surgical defects using 3D reconstructed µCT images performed in 16 weeks old Wistar rats. A- Representative ventral view of 3D reconstructed premaxilla showing preoperative MPC defect position and dimensions, and B- Representative lateral view of 3D transparency renders of premaxilla showing preoperative AC position and dimensions.

5.3.3 Bone healing following modifications of current cleft palate models

There were no intraoperative or postoperative mortalities in both MPC and AC groups. Operated animals grew and increased in weight in a pattern similar to non operated group. Based on the activity, hair coat appearance and feeding behaviour, all rats in both groups experienced mild to moderate pain during the first postoperative week, which substantially reduced over time.

Preoperative virtual planning made significant contributions to customize the size and location of the surgical defects without damaging adjacent anatomical structures (**Figure** 5-5). The postoperative measurements were (7.2±0.3)×(2.6±0.2)×(1±0.2) mm^3 for MPC defects and (5.3±0.6)×(2.6±0.2)×(1±0.2) mm^3 for AC defects. The mean postoperative cleft size was 18.6±1.8 mm^2 in MPC group vs. 14.2±1.3 mm^2 in AC group.

Bone healing in the created defects was evaluated by µCT at weeks 0, 4, and 8. Both models demonstrated bone healing at the edges of the developed defects at

week 4 with no further significant healing at week 8 (**Figure** 5-6). There was no significant difference in percent bone filling between MPC group and AC group (29.43±6.51 vs. 36.36±15.13, respectively) at week 4 or at week 8 (37.73±12.00 vs. 38.78±9.89, respectively).

Histological assessments of bony defects at week 8 were confirmatory to the μCT results. New bone formation was found along the edges of the developed MPC (**Figure** 5-7) and AC defects (**Figure** 5-8). New bone had a woven appearance with osteoid depositions at its inner surface. Active bone remodelling was evidenced by the presence of calcification lines.

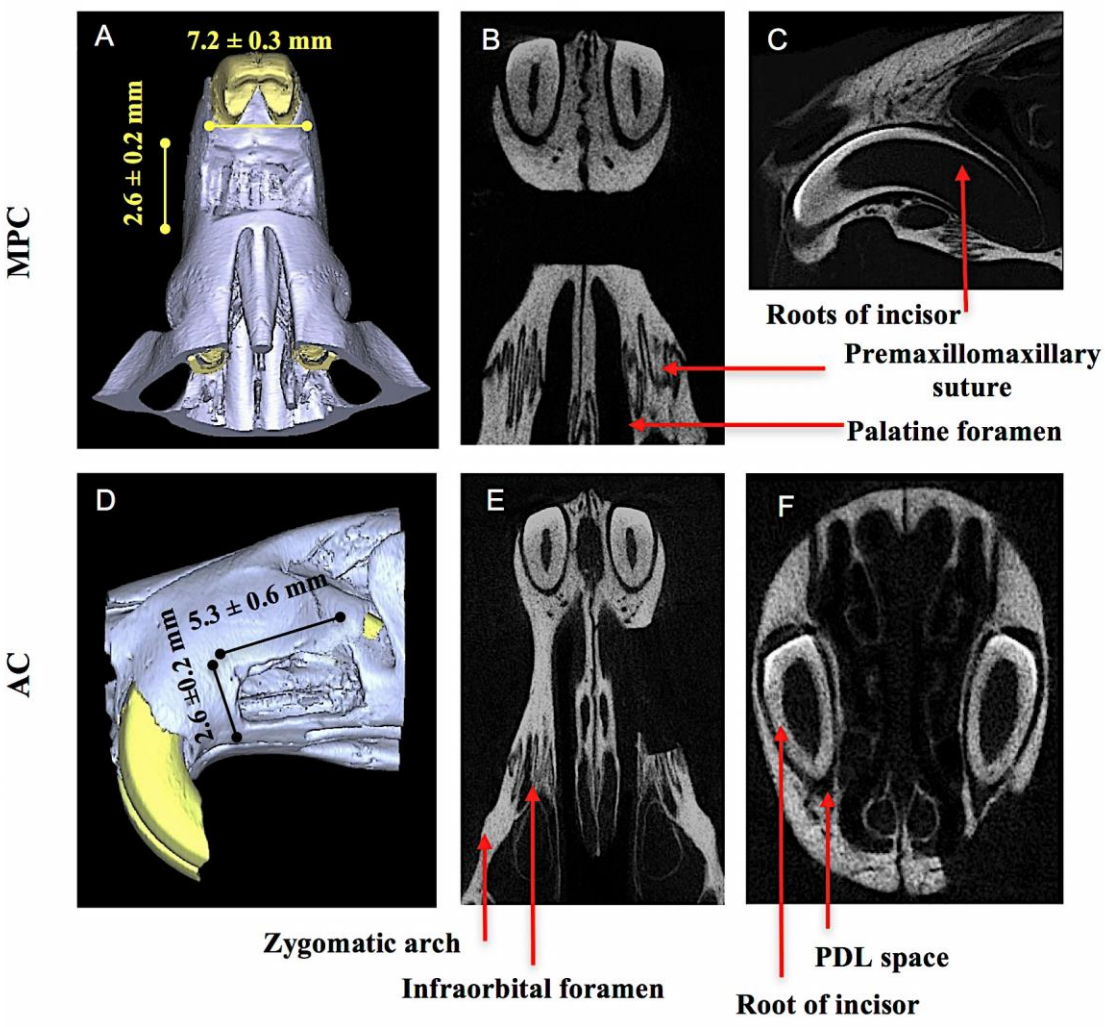

Figure 5-5: Representative µCT images comparing immediate postoperative dimensions and positions of the modified MPC and AC models developed in 16 weeks old Wistar rats. Surgical defects were created in rat premaxilla and designed to be at least 1 mm away from roots of the incisors and palatine foramen. Representative ventral view of 3D reconstructed premaxilla (A), axial cross-section (B), and sagittal cross-section (C) of MPC defect. Representative lateral view of 3D reconstructed premaxilla (D), axial cross-section (E), and coronal cross-section (F) of AC defect.

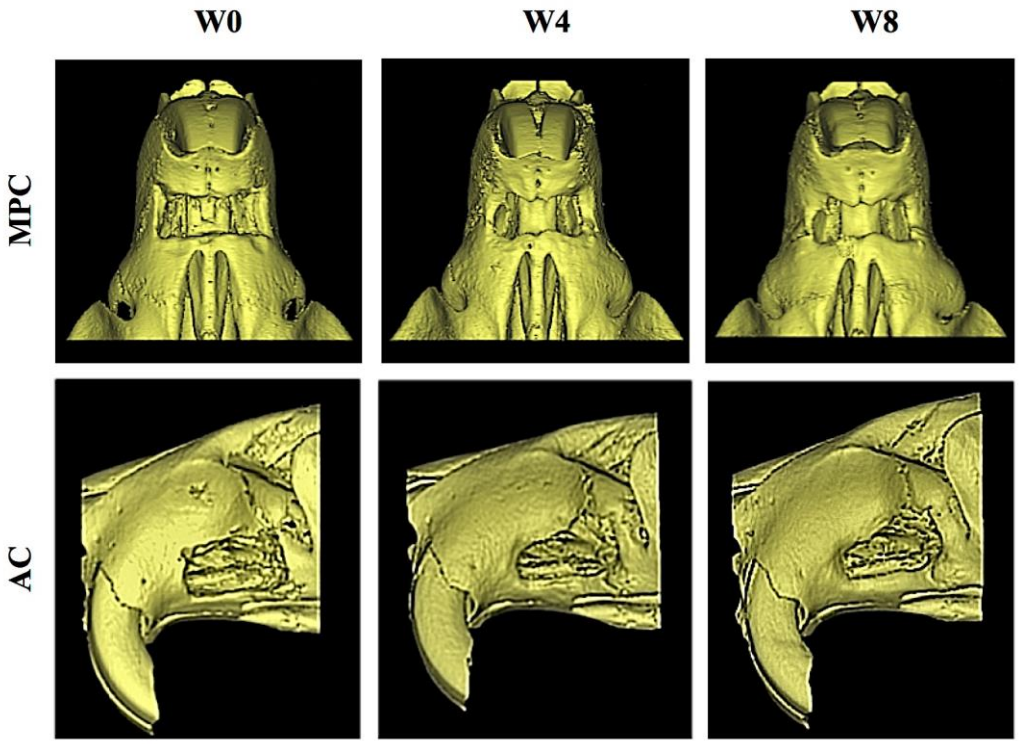

Figure 5-6: Representative µCT images comparing bone healing of MPC and AC models. Representative ventral view of 3D reconstructed µCT images showing bone healing in MPC model at week 0 (A), week 4 (B) and week 8 (C). Representative lateral view of 3D reconstructed µCT images showing bone healing in AC model at week 0 (D), week 4 (E) and week 8 (F). Note the persistent central defect in both models confirming critical size through week 8.

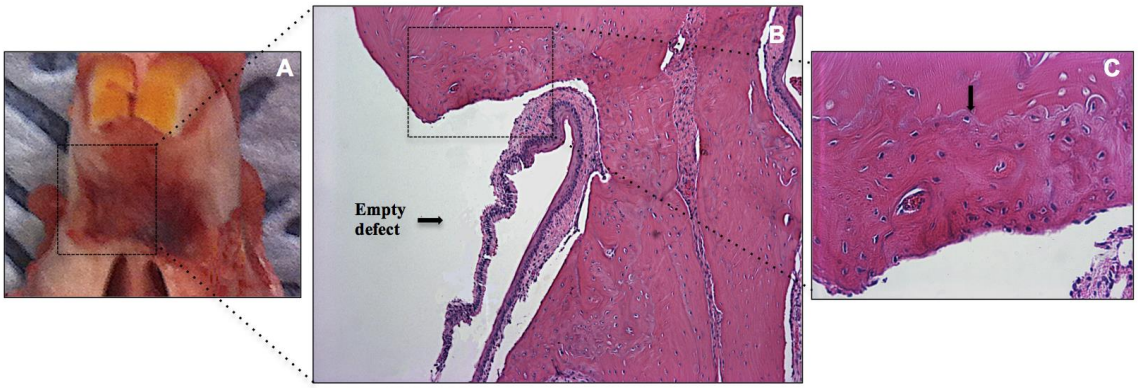

Figure 5-7: MPC model at week 8 postoperative: A- Gross specimen of the defect (Ventral view), B- Corresponding H&E stained axial section (10x) showing empty defect with new bone formation at the edges, and C- Higher magnification of the defect margin (40x) showing woven bone formation and calcification lines (black arrow).

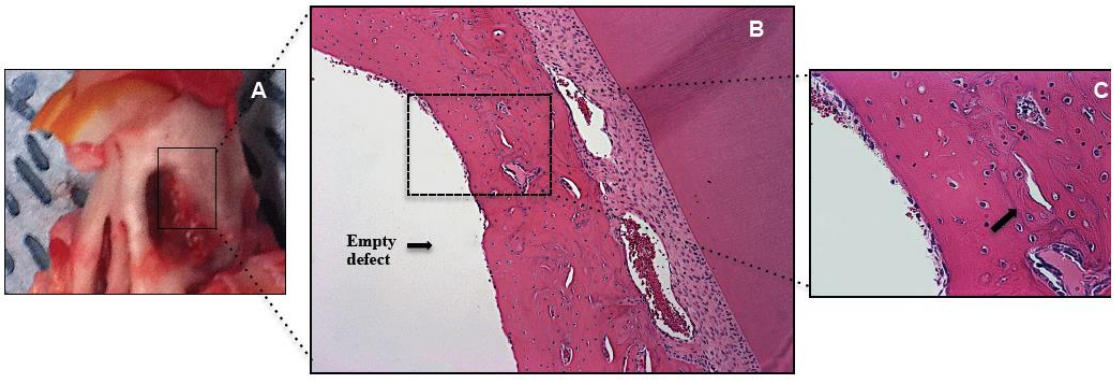

Figure 5-8: AC model at week 8 postoperative: A- Gross specimen of the defect (Lateral view), B- Corresponding H&E stained sagittal section (10x) showing empty defect with new bone formation at the edges, and C- Higher magnification of the defect margin (40x) showing woven bone formation and calcification lines (black arrow).

5.4 DISCUSSION

There has been considerable debate in the literature about the suitable animal model of cleft palate with critical size defect to simulate human cleft defects. Rodent models of cleft palate are available but have limitations: one lacked sufficient information about tested rats[33] and the other failed when utilized for testing bone grafting therapies based on BMP-2.[34, 35] Hence, in this study we modified the dimension of the current rodent models of cleft palate and assessed bone healing to improve their performance for bone grafting studies.

Our initial studies utilizing a 7×4×3 mm^3 AC defect in 8 and 16 weeks old Sprague Dawley rats revealed substantial injury to the surrounding structures including incisor roots and palatine foramen based on macroscopic and μCT examinations. These finding were consistent with the cross sectional μCT images presented in Nguyen et al. study.[34]

Comparing anteroposterior (IF-IP) and transverse dimensions (IF-IF) of the maxillae in 16 weeks old Sprague Dawley vs. Wistar rats, revealed no significant differences between the two species. Moreover, the IF-IP data collected in our study for 16, 20 and 24 weeks old Wistar rats were similar to the previously reported IF-IP dimensions in 12 weeks old Wistar rats.[166, 167] These findings signify the validity and reproducibility of those anatomical landmarks. It also supports our initial findings that size of maxilla is not significantly different in young rats (8 weeks old) vs. older rats (16 weeks old). It is also interesting to mention that rats have a complete set of teeth (i.e. dentally mature) by 6 weeks of age,[168] which could suggest that rat's maxilla reaches its maximum anteroposterior and transverse dimensions by this time with no significant changes afterwards. Nonetheless, more studies are needed to confirm these conclusions.

Dimension modifications employed in our study were aimed to improve the performance of the current cleft palate models[33, 34] when used for bone grafting studies.[35] We avoided the exposure of the incisor roots in the grafting area as it creates periodontal defect, which could complicate the outcomes of bone grafting or result in subsequent graft loss.[169] We also avoided communication with

palatine foramen as it could lead to substantial loss of osteoinductive molecules such as BMP-2[35] or leakage of BMP-2 with subsequent adverse effects on the associated nerves.[117] The depth of modified MPC and AC defects was limited to the thickness of the palatine bone to create oronasal communication, but we avoided damage to nasal tissue to further mimic the clinical situation. However, proper soft tissue (nasal and oral) handling will be required when the modified models are employed for testing different bone grafting techniques. We evaluated bone healing in the modified defects over 8 weeks, since Nguyen et al.[34] reported that bone healing plateaued after 4 weeks postoperative with no significant bone formation between 4 and 12 weeks. Taken together, we believe that modified MPC and AC models are appropriate for testing the efficacy of new biomaterials for secondary bone grafting.

Preoperative virtual planning of the modified MPC and AC surgical defects using μCT data provided accurate guide for surgical implementation after careful consideration of the anatomy. Planned dimensions vs. actual surgical dimensions were similar. For MPC defects, virtual planning resulted in a defect that is 7.23±0.27 mm long, 2.84±0.4 mm wide, and 1±0.2 mm deep while postoperative defects were (7.2±0.3)×(2.6±0.2)×(1±0.2) mm^3. For AC defects, the planned dimensions were 5.48±0.22 mm wide, 2.43±0.13 mm long, and 1±0.2 mm deep vs. postoperative defects dimensions of (5.3±0.6)×(2.6±0.2)×(1±0.2) mm^3. It is clear that preoperative virtual planning improved the potential for achieving successful postoperative surgical outcomes.

Mehrara et al.[33] reported complete bone healing in MPC defect (9×5×3 mm^3) by 12 weeks (i.e. not critical size defect). In our hands, bone healing in the modified MPC (7×2.5×1 mm^3) followed the peripheries of the defect leaving central defect confirming critical size nature of the defect. Moreover, percent bone filling was 29.43±6.51 at week 4 and 37.73±12.00 at week 8. It is important to mention that Mehrara et al.[33] did not report age or strain of the rats utilized in their study. Moreover, they assessed bone healing based on semi-quantitative assessment of 2D radiograph while our study used μCT for quantitative measurement. Limitations of 2D imaging include superimposition of structures,

variable magnification, and distortion.[113] While, CT scanning provides through evaluation of the anatomy and accurate quantitative measures for bone healing.[170]

Comparing the AC model presented in our study (16 weeks old rats) vs. Nguyen et al.[34] study (8 weeks old rats), we found similar bone healing occurring at the defect margin. Additionally, percent bone filling was similar in both studies at week 4 (36.36±15.13in our study vs. 43±5.6 in Nguyen's study) with no significant healing at week 8 (38.78±9.89 in our study vs. 53±8.3 in Nguyen's study), verifying the comparability of the two method of μCT quantitative analysis. Modifications employed to the AC defect made it more conservative and more clinically representative and yet a critical size defect. Lower percent bone healing reported in our study could be due to the utilization of older rats than those used by Nguyen et al.[34] Understandably, younger animals are expected to have superior bone healing potential as compared to older animals, which could be due to the increased proliferative capacity of younger cells. This is consistent with Ekeland et al.[171] findings, who reported that healing fractures in the young rats (3 weeks old rats) almost regained the mechanical properties of the normal bones after 4 weeks, whereas the mechanical strength of the femoral fractures in the adult rats (14 weeks old rats) approached normal values after 12 weeks.

To the best of our knowledge, this is the first study that provided careful assessment of μCT images that facilitated examination of the adjacent anatomy and proper virtual planning of the surgical defects. It also provided valid and reliable measures for defect width, height, and depth and made it possible to accurately calculate the cleft volume, bone filling volume, and bone filling percentage. The presented modifications for AC and MPC cleft models made them more reproducible, reliable, and practical as they simulate osseous defect in cleft palate patients. MPC represents a bilateral cleft defect, while; AC model represents a unilateral cleft defect. However, we found that the AC defects are more challenging to create as it is surrounded by incisor roots, palatine foramen and the zygomatic arch which introduced greater variability between animals in the initial cleft size and subsequent healing specially at week 4. Conversely, MPC defect had less anatomical challenges and larger residual defect volume as

compared to AC defect. Taken all together, we consider MPC model to be more appropriate for efficacy testing of new bone grafting therapies for cleft palate reconstruction, which would have a tremendous impact on reconstructive maxillofacial surgery.

Chapter 6

Cleft Palate Reconstruction Using Collagen and Nanofiber Scaffold Incorporating Bone Morphogenetic Protein In Rats

6.1 BACKGROUND

Secondary bone grafting is a fundamental step in the overall management of patients with cleft palate. Its objectives include closure of the residual oronasal fistula, support for permanent tooth eruption, and/or establishment of adequate bone for prosthodontic rehabilitation of the edentulous segment.[12] Autologous bone grafting is currently the preferred method for cleft palate reconstruction, but it is limited by donor site morbidity.[5] Therefore, several reported studies were undertaken to evaluate the effectiveness of various artificial bone grafts as demineralized bone matrix, hydroxyapatite, cadaveric bone grafts and methylmethacrylate, but the lack of bioactivity, mechanical weakness and susceptibility to infection limited their use.[16] To overcome those limitations, INFUSE® Bone Graft has been utilized for cleft palate reconstruction in an off-label capacity. [77-80, 82] It consists of an osteoconductive collagen scaffold and bone morphogenetic protein-2 (BMP-2) as an osteoinductive agent. Collagen is the backbone of native bone tissue where ~ 90% of extracellular matrix is composed of collagen type I.[22] Absorbable collagen scaffold (ACS) has low antigenicity, low toxicity and is biodegradable.[23] It also contains RGD (Arg-Gly-Asp) and non RGD domains that facilitate cell migration, attachment, proliferation, and differentiation.[24, 25] BMP-2 stimulates *de novo* bone formation when implanted in an appropriate environment. It attracts host stem cells to the grafting site and stimulates their differentiation into osteogenic lineages.[83]

The main benefit of BMP-2+ACS is to provide bone formation similar to autografts, but with significantly reduced donor site morbidity, hospital stay, and overall cost of the procedure.[77-80, 82] However to achieve those therapeutic effects when ACS is utilized, milligram doses (1.5 mg/ml) of BMP-2 are needed. Recently, a study employed a chemically cross-linked hydrogel and demonstrated moderate bone formation at a reduced BMP-2 concentration (250 μg/ml).[84] However, severe gingival inflammation and initial exposure of BMP-2+hydrogel construct occurred in two participants and therefore, the study was prematurely terminated. Reducing the effective BMP-2 concentration needed for bone formation is promising, as it will reduce adverse events and overall cost. But, an

appropriate carrier is also necessary to maximize the clinical outcomes and to reduce morbidity. The primary scaffold properties of concern are biocompatibility, biodegradability, cell adhesiveness and interconnectivity. Self-assembling peptide nanofiber (NF) based hydrogel $RADA_4$ $(Arg\text{-}Ala\text{-}Asp\text{-}Ala)_4$ is a biologically-inspired biomaterial that have been shown to meet these three criteria. NF hydrogel is made from natural amino acids, which can be metabolized naturally and safely by the body. Moreover, its 3D structure is similar to the natural extracellular matrix with fiber diameter of ~10 nm and pore size between 5–200 nm.[30] Studies reported that NF based scaffolds supported proliferation and osteogenic differentiation of osteoprogenitor cells, suggesting possible application for bone tissue engineering.[31, 32] Additionally, it provides a sustained release profile for incorporated growth factors and proteins due to its exceptional diffusion properties.[29] Extreme release profiles such as slow release of sub-therapeutic concentrations or rapid release of loaded proteins could adversely affect the therapeutic outcome.[172] Release profiles of loaded proteins within NF hydrogel can be adjusted by altering peptide concentrations.[88] Therefore, we hypothesized that retention of bioactive BMP-2 at the defect site together with the release of therapeutic amounts could influence chemotaxis, proliferation, and osteogenic differentiation of host MSCs leading to robust bone formation.

Towards that end, this study developed a NF based scaffold (within an ACS backbone) to control the release of BMP-2 for robust bone tissue induction in a rodent surgical model of cleft palate. But, the choice of the proper NF density is a critical factor that determines the release profile and the overall success of the delivery system *in vivo*. Therefore, the release profiles of BMP-2 from scaffolds with different NF densities were evaluated *in vitro* to explore the optimum NF density that could recapitulate physiological bone healing process. Subsequently, the designed scaffold with the appropriate NF density was implanted into the mid palatal cleft (MPC) model ($7\times2.5\times1$ mm^3) previously described in Chapter 5 and bone formation was assessed using micro-computed tomography (μCT) and histology. This study aimed to provide the necessary "proof-of-principle" for

developing and transferring this technology to the clinical setting, with the objective of improving the quality of life of patients with cleft palate.

6.2 MATERIALS AND METHODS

6.2.1 Materials

Phosphate Buffered Saline (PBS) and Distilled/deionized water (ddH2O) were acquired from Invitrogen (Grand Island, NY). ACS was purchased from BARD, Davol Inc. (Warwick, RI, USA). BioXclude™, placental resorbable membrane (PRM) was obtained from Citagenix Inc. (Laval, Qc, Canada). Self-assembling peptide RADA16-I was purchased from RS Synthesis, LLC. (Louisville, KY, USA) and used without further purification. Stock peptide solution was reconstituted in ddH_2O. Recombinant human BMP-2 was obtained from an E-coli expression system, and its activity has been testified in the literature.[130, 131] The BMP-2 stock solution was prepared in ddH_2O. Fluorescein isothiocyanate (FITC) was obtained from Sigma-Aldrich (St. Louis, MO, USA), and it was used to label the BMP-2 according to manufacturer's instructions.

6.2.2 *In vitro* release study

In an attempt to find the proper NF concentration suitable for sustained BMP-2 release *in vivo*, an *in vitro* diffusion experiments were conducted. Different working RADA16-I concentrations (1% and 2% w/v) were prepared by diluting stock peptide solution in PBS. Aliquots of 30 µl from the prepared NF solutions were applied onto 6 mm diameter ACS discs impregnated with 8µg of FITC labelled BMP-2 placed in 96 well plates. ACS discs infused with 8µg FITC labelled BMP-2 were used as control. Subsequently, the constructs were incubated overnight at 4°C to form the gel. Then, 200 µl of PBS was slowly added as a release media. At predetermined time points 40 µl of the supernatant was sampled and replaced with fresh PBS to determine the amount of BMP-2 released as a function of time using florescent spectroscopy ($\lambda_{Excitation}$= 495 nm and $\lambda_{Emission}$= 525 nm).

6.2.3 Bone grafting surgery

6.2.3.1 Steps for standardization and Scaffold Preparation

Several steps were completed to develop a standardized MPC surgical defect and to prepare scaffolds of standardized size for bone grafting, in order to minimize variation between the groups (**Figure** 6-1). An impression was taken of the rat maxillary arch with a prepared surgical defect of 7x2.5x1 mm^3 from which a stone model was fabricated and a surgical template was created using methyl methacrylate. Multiple templates were prefabricated, sterilized and used intraoperatively to standardize the MPC defect size for all of the animals in the study. Moreover, a customized rectangular punch measuring 7×2.5 mm^2 was developed and used to pre-cut sterile ACS and PRM into pieces of standardized size. Preparation of the ACS+BMP scaffold was completed using 12 μg of BMP-2 solution, applied to each rectangular ACS scaffold and allowed to dry for 30 min. Prefabricated rectangular molds (7×2.5 mm^2) were then used to prepare NF+ACS, and NF+ACS+BMP-2 scaffold of standardized size. Simply, ACS+PBS or ACS+BMP-2 scaffold were placed in the mold and rehydrated with 30 μl from aseptically prepared NF solution.

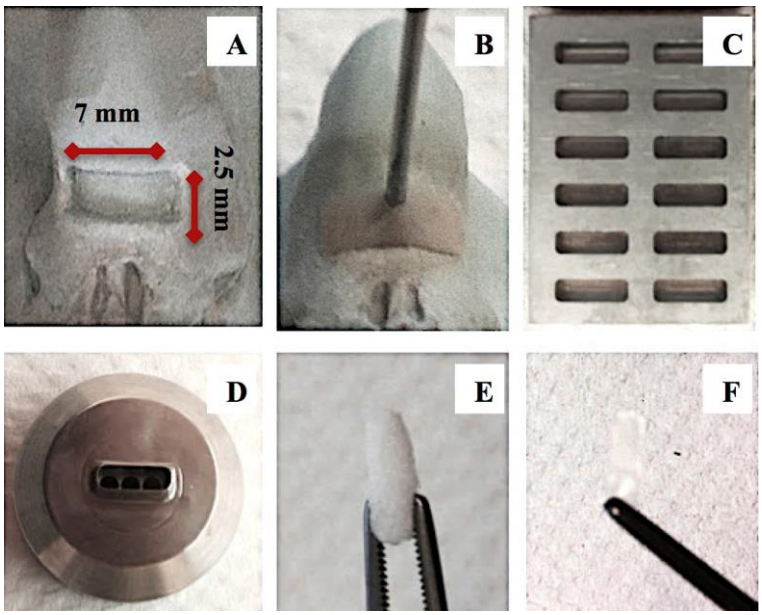

Figure 6-1: Tools developed to aid standardization for the grafting procedure. MPC preoperative defect was developed on a model of rat maxilla (A), methyl methacrylate surgical template was then fabricated (B), custom made rectangular molds was used for the preparation of NF scaffold (C), custom made rectangular punch (D) was used to cut ACS (E) and PRM (F).

6.2.3.2 Experimental setup

Animal care committee at the University of Alberta approved all experimental procedures. A total of thirty four 16 weeks old (375-400 g) Wistar rats were obtained from Charles River Laboratories International, Inc. (Wilmington, MA,USA). Animals were kept in standard environment (room temperature, 2 rats per cage with 12 hour light/dark cycle). Animals were provided with Soft diet and liquid gel packs 2 days preoperative and continued for 1 week postoperative, and then advanced to a regular diet.

6.2.3.3 Surgery

Intra-peritoneal (IP) injections of Ketamine (75 mg/kg) and Domitor (0.5 mg/kg) were used to anaesthetize animals before surgery. Lidocaine (0.25 ml of 0.4%) was also injected locally at the surgical site. Then, U-shaped incision was performed at maxillary midline and a full thickness mucoperiosteal flap was

elevated to expose the maxillary bone. The MPC defect of 7×2.5×1 mm^3 was then created using a No. 699 straight fissure and No. 4 round burs. The surgical template was utilized in all of the surgeries to ensure defect size standardization in all animals. Detailed description of the bone grafting technique is illustrated in **Figure** 6-2**.** Following hemostasis, PRM was placed to replace the nasal mucosa (in all groups except control) and the rats were randomly assigned to one of the following treatments groups (n=6 per group): control (no scaffold), ACS alone, ACS+BMP-2, NF+ACS, and NF+ACS+BMP-2. At the end of the surgery, the full thickness mucoperiosteal flap was closed in a primary fashion using 4-0 polyglactin absorbable sutures and the animals were injected with 1mg/kg revertor (atipamezole hydrochloride) via intra-peritoneal injection to reverse the sedative agent effects. Postoperative subcutaneous injections of Metacam at 2 mg/kg (once/day) and Butorphanol at 0.2mg/kg (twice/day) were performed for pain management. Subsequently, daily follow up and assessment was performed for one week, for evaluation of inadequate pain control, which could be assessed by reduced grooming, lethargy, porphyrin staining, loss of appetite or weight loss. Postoperative bone repair in the different treatment groups was assessed by µCT and histology.

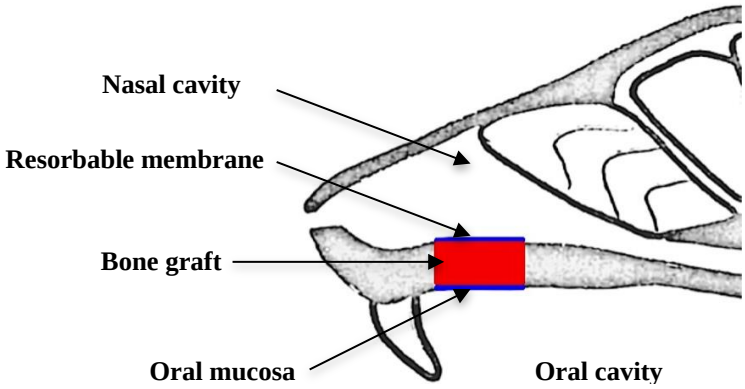

Figure 6-2: Diagram showing alveolar bone grafting technique viewed from sagittal aspect. PRM was placed as a lining for the nasal cavity, the scaffold was then placed into the developed MPC defect, and oral mucosa was closed with watertight sutures.

6.2.3.4 In vivo µCT imaging

In vivo µCT scans (Skyscan 1176 *in vivo* µCT, Skyscan NV, Kontich, Belgium) of the rat maxillae were performed at baseline (week 0), mid point (week 4), and at the experimental end point (week8). Rats were anesthetized with 2% isoflurane in oxygen administered through a nasal cone for the duration of µCT imaging. All µCT scans were done at 100 kV through 180º with a rotation step of 0.5º to produce serial cross-sectional images of 18 µm resolution. Projected images of the maxillae were reconstructed using Nrecon 1.6.1.5 software (SkyScan NV, Kontich, Belgium). Cross-sectional µCT images and 3D reconstructions were utilized for subsequent quantitative and morphometric analysis.

6.2.3.5 Quantitative and Radiomorphometric analysis

6.2.3.5.1 Assessment of bone healing

2D and 3D µCT images were utilized to assess bone healing in serial scans of the same animal overtime. A rectangular region of interest (ROI) of fixed size was used to section an identical volume of the palatine bone to perform standardized morphometric analyses. Incisor roots were utilized as anatomical landmarks for consistent sampling of the same region of palatine bone from all specimens. Skyscan CT-Analyser software package (CTAn 1.10.0.1, SkyScan NV, Kontich, Belgium) was used to binarize 2D coronal images with a gray scale thresholding of 36/255 to measure bone volume (BV, mm^3). Difference between BV at baseline (W0) and subsequent time points (W4 and W8) was described as bone filling volume, and the percentage ratio between the bone filling volume and initial defect volume at baseline was defined as percent bone filling

6.2.3.5.2 Growth measurements

Reconstructed 3D images were subjected to analysis using Mimics software (Materialise, Leuven, Belgium) to measure anteroposterior and transverse dimensions of the maxillae in operated animals (n=6/group). Non operated animals were used as control (n =4). We used the anatomical landmarks

established by Gomes et al.[166] in an axial viewing position. The distances between infraorbital foramen and incisal point (IF-IP) were measured bilaterally to represent the anteroposterior dimension while the distance between right and left IF was used for transverse dimensions. All µCT measurements were conducted and reassessed after one week by one examiner.

6.2.3.6 Histological analysis

All rats were euthanized at the end point (8 weeks) using by CO_2. Maxillae were dissected and fixed in 10% neutral buffered formalin (Fisher Scientific, USA). Then, samples were washed with PBS and immersed in decalcification solution (Cal-Ex II®, Fisher Scientific, USA) for 4 weeks. Samples were sectioned and stained with hematoxylin and eosin (H&E) stain and Masson's Trichrome stain (bone= dark blue, cortical bone= red)[173] to assess bone formation at the cleft defect site.

6.2.4 Statistics

In vitro release study was done in triplicate for each scaffold at each time point, while animal experiments were conducted in 6 animals/group. The results were expressed as mean ± standard deviation (SD). Statistical analysis was performed with one-way analysis of variance (ANOVA) using SPSS version 18.0 software package (SPSS, Chicago, IL, USA). Intergroup differences were identified by Tukey's HSD post-hoc test, and statistical significance was expressed as p-values <0.05. Additionally, the intraclass correlation coefficient (ICC) was used to estimate the intra-rater reliability for µCT measurements.

6.3 RESULTS AND DISCUSSION

6.3.1 *In vitro* release

In vitro release studies were aimed to explore the optimum NF density that could recapitulate physiological bone healing process. To mimic the clinical situation, BMP-2 was loaded using physical adsorption method on ACS scaffold

and NF hydrogel with different densities (1-2%) was then added to slow BMP-2 release. ACS was used as an adjuvant to provide structural integrity for the NF hydrogel, facilitate handling and to prevent them from migrating away from the defect site, which was closer to clinical application. The release of FITC labelled BMP-2 from the prepared NF scaffolds into PBS was evaluated at room temperature for 23 days (**Figure** 6-3). While, ACS alone (0% NF) was used as control. The release profile for the BMP-2 demonstrates a clear dose response relationship with increasing NF concentration (i.e., increasing NF concentration reduces BMP-2 release over time). The results demonstrate that modifying the nanofiber peptide density is capable of controlling the release of FITC-BMP-2. (**Figure** 6-4**A**) shows that ACS alone exhibited quick release of BMP-2 during the initial stage, and around (8.7%, 77.6 ng) of BMP-2 content was released during the first 2 h. This was followed by release of gradually decreasing amounts over the 23 days of the study. A total of 601 ng or 37% of the initial BMP2 loaded was released from ACS scaffold. On the other hand, hydrogel containing 1% and 2% NF released BMP-2 in a slower fashion, and only 9% and 3% of BMP-2 content was released after 24 h, respectively. NF with 1% density extended the time for maximum from 2 h to 24 h 55 ng or 9.3% is released within the first 24 h, followed by a gradual sustained release of BMP-2 over 23 days (**Figure** 6-4 **B**). By the end of the experiment 1% NF released 541 ng (34.58%) of its BMP-2 content over 23 days. Furthermore, inclusion of higher NF (2%) density into the scaffold further delayed the rate and extent of BMP-2 released (**Figure** 6-4 **C**). Scaffold containing 2% NF exhibited maximum BMP-2 release after 5 days (35.2 ng or 10.28% of initial BMP-2 content). After 23 days, 2% NF scaffold allowed only 25.55% of its BMP-2 content to be released. In general, the release profile of BMP-2 from nanofiber containing scaffolds followed the diffusional behaviour. This would suggest that the release of BMP-2 from this matrix is governed by the exchange of BMP-2 and the water molecules. After 23 days, almost 37%, 34% and 25% of BMP-2 was released from 0, 1, and 2% NF, respectively.

The time course of bone healing consists of a complex, sequential series of well-coordinated events including initial haematoma and inflammation, cellular

migration and subsequent repair processes, endochondral and/or intramembranous bone formation, and subsequent remodelling. The initial proinflammatory response of the haematoma lasts for 3-4 days. Dose dependent local soft tissue edema after BMP-2+ACS implantation peaked at 3 h for the subcutaneous implants and at 2 days for the intramuscular implants has been reported.[174] Following the inflammatory phase, the reparative phase is initiated by migration of MSCs to the defect site in response to growth factor release. MSCs then proliferate and differentiate into osteogenic lineages, which build woven bone (collagen type 1) throughout the defect.[53] Relating our release data to the bone healing process, we found that both 0 and 1% NF release larger quantities of BMP-2 during the inflammatory phase, which could in turn increase inflammation following *in vivo* implantation, that might adversely inhibit or delay the tissue regeneration process.[175] In contrast, constructs containing 2% NF, released minimal amounts of BMP-2 during the inflammatory phase. However, during the cell recruitment phase it maintained maximal BMP-2 concentrations. Therefore, subsequent animal studies utilized 2% NF concentration to ensure the sustained release capabilities of the scaffold during the study period.

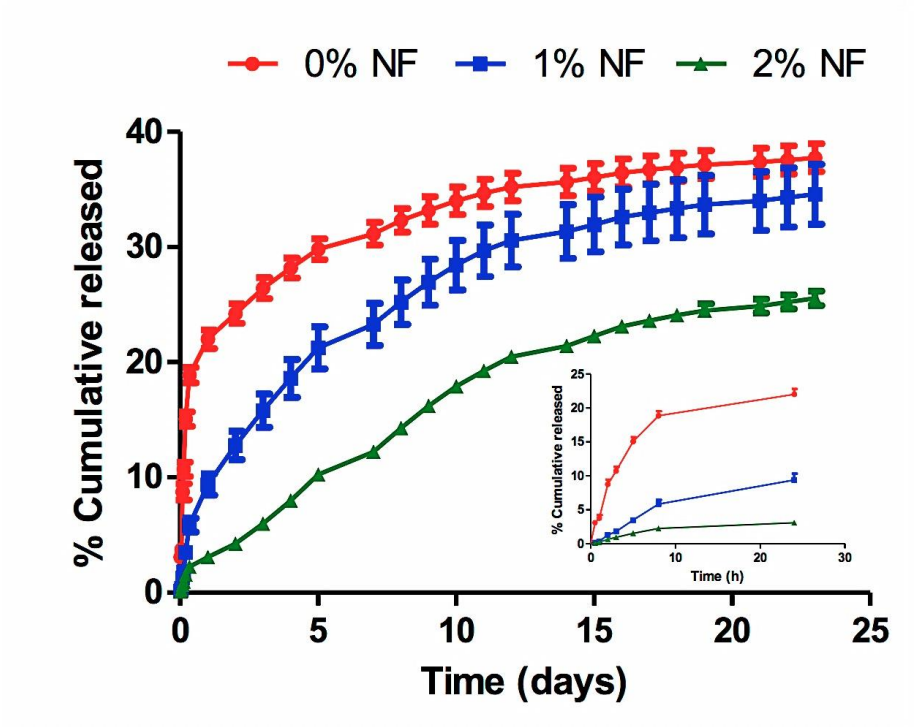

Figure 6-3: Release profile of FITC labelled BMP-2 from scaffolds with different NF densities (0-2% w/v) over 23 days. Release experiments were performed into PBS at room temperature. Data points represent the mean of % cumulative BMP-2 released ± SD (n=3). Inset: Release profile of FITC labelled BMP-2 from scaffolds having different NF densities (0-2% w/v) over first 24 hours

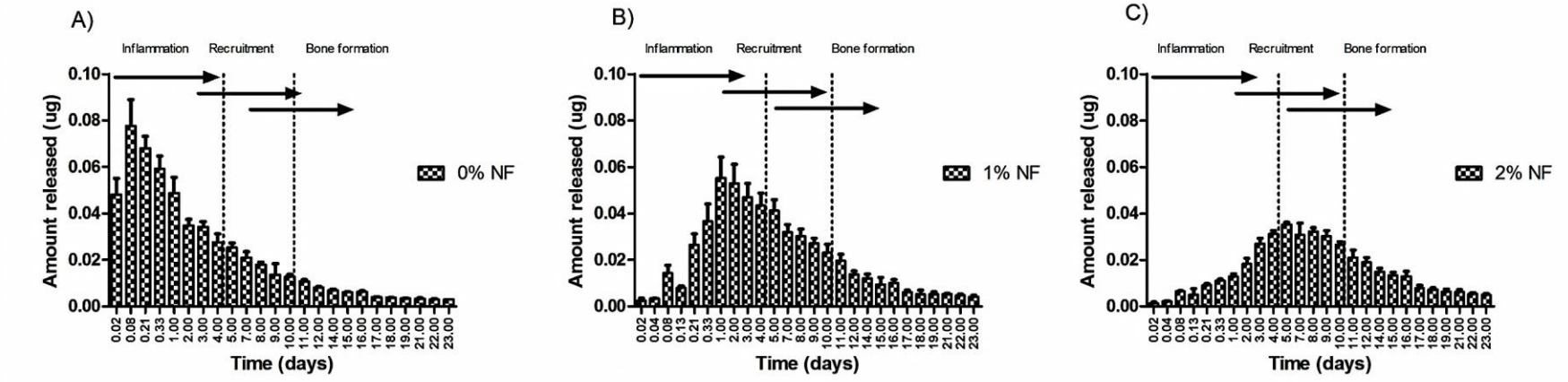

Figure 6-4: Release profile of FITC labelled BMP-2 from scaffolds having different NF densities A) 0% w/v B) 1% w/v C) 2 % w/v. Release experiments were performed into PBS at room temperature. Data points represent the mean amount of BMP-2 released ± SD (n=3).

6.3.2 *In vivo* bone grafting

6.3.2.1 Postoperative recovery

In general, operated rats tolerated the surgery and maintained normal body weight similar to non operated rats. Only one rat in the BMP-2 group died 3 days postoperative. But, there was no intraoperative or postoperative mortalities in the other groups. The mortality rate reported in our study (~4%) is still smaller than other studies investigated the development of alveolar cleft model[34] and MPC[33] that reported ~10% intraoperative death.

All operated rats were scored with mild to moderate pain during the first postoperative week based on the activity, hair coat appearance and feeding behaviour. This pain was considerably reduced overtime. Other studies utilizing rodent model of cleft palate[33-35] did not report evaluations of postoperative pain, which is an important addition with our study.

6.3.2.2 Bone healing following different treatments

Bone regeneration in the different treatment groups was monitored using *in vivo* μCT imaging which enabled the assessment of bone healing in sequential temporal scans of the same rat at weeks 0, 4 and 8 simulating clinical studies. Conversely, other studies[34, 35] euthanized the animals at 4, 8 and 12 weeks intervals.

Figure 6-5 illustrates the percent bone filling in the different treatment groups. While, **Figure** 6-6 demonstrates the healing of the surgical defects over 8 weeks in each group from 3D reconstructed μCT images. Bone healing occurred at the margins of the surgical defects in control, ACS, and NF+ACS groups over the 8 weeks of the study. No animals in these groups had complete closure of MPC defects. There were no significant differences in the percent bone filling between control, ACS, and NF+ACS groups at week 4 (29.43±6.51, 27.09±15.71, and 23.94±7.99, respectively) and week 8 (37.72±12.00, 40.14±15.12, and 22.43±5.98, respectively). Conversely, Nguyen et al.[35] reported significant increase in bone formation in groups treated with ACS as compared to untreated control based on percent bone formation at week 8 (79±9 vs. 53±8, respectively).

In this study,[35] they employed alveolar cleft model[34] and compared bone formations with the following treatments ACS, ACS+BMP-2, Hydroxyapatite tricalcium phosphate (HA-TCP), and HA-TCP plus BMP-2). However, Nguyen et al.[35] utilized 8 weeks old Sprauge Dawley rats while our study utilized 16 weeks old Wistar rats. Young animals are expected to have superior bone healing potential as compared to older animals, which could be due to the increased proliferative capacity of younger cells. This is consistent with the findings of Ekeland et al.[171] who reported that healing fractures in young rats (3 weeks old rats) almost regained the mechanical properties of the normal bones after 4 weeks, whereas the mechanical strength of femoral fractures in the adult rats (14 weeks old rats) approached normal values after 12 weeks.

Interestingly, the addition of BMP-2 considerably enhanced bone healing at the defect site as compared to other groups. Bone formation in ACS+BMP-2 treated group was only significantly different from control, ACS, and NF+ACS groups at week 8 ($p<0.05$) but not at week 4. Whereas, percent bone filling in animals treated with NF+ACS+BMP-2 was significantly higher than control, ACS, and NF+ACS groups at week 4 and 8 ($p<0.01$). Bone filling percentage in NF+ACS+ BMP-2 group was higher than ACS+ BMP-2 group at week 4 (75.31±10.86 vs. 54.29±18.90, respectively) and at week 8 (88.4±8.32 vs. 71.59±20.29, respectively). However, the difference between ACS+BMP-2 and NF+ACS+BMP-2 groups was not statistically significant ($p>0.05$).

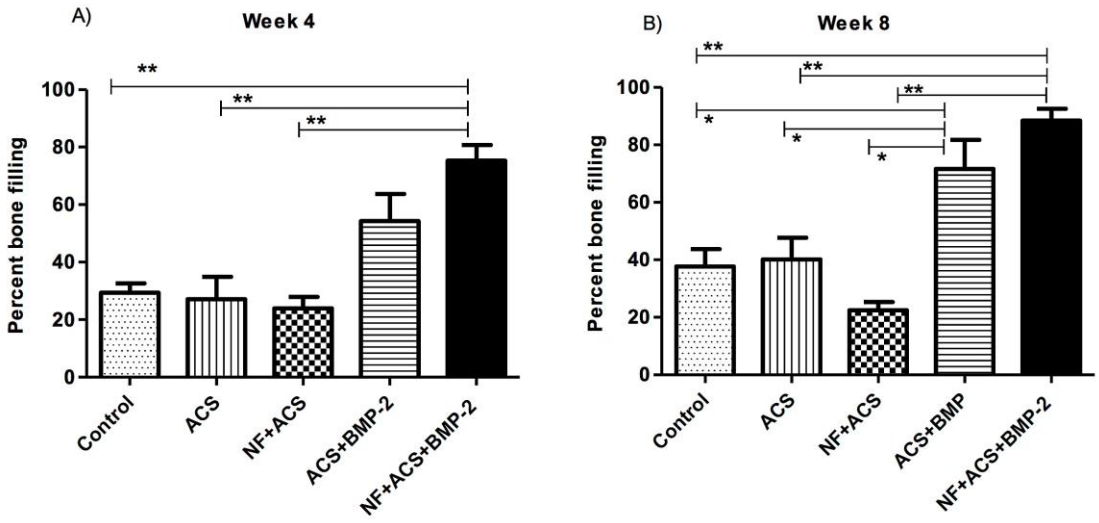

Figure 6-5: Percent bone filling following different treatments at week 4 (A) and week 8 (B). **: $p<0.01$ and *: $p<0.05$

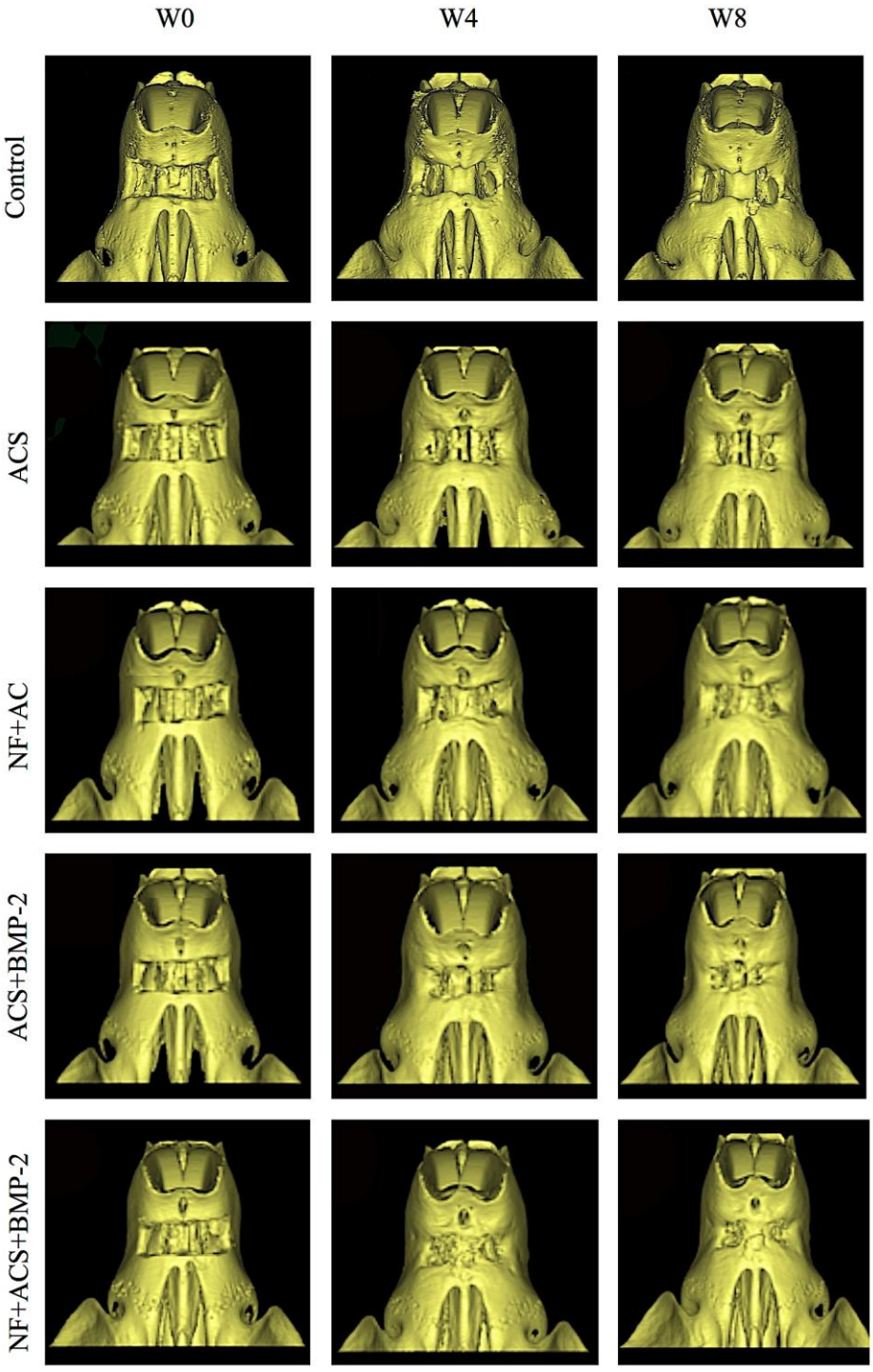

Figure 6-6: Representative ventral view of 3D reconstructed µCT images illustrating MPC defect healing over 8 weeks following different treatments.

Histological assessments of bony defects at week 8 confirmed the μCT results (**Figure** 6-7). H&E staining for ACS, and NF+ACS groups displayed fibrous tissue filling the defect with no bone formation within the defect and limited bone regrowth at peripheries of the defects. Scaffolding materials were degraded and defects remain widely patent. On the other hand, constructs containing BMP-2 exhibited osteoinductive properties. ACS+BMP-2 treatment resulted in partial closure of the surgical defect while NF+ACS+BMP-2 treatment showed central and peripheral bone formation within the region previously occupied by the scaffold. The thickness of the regenerated bone was greater in the later treatment group.

Masson trichrome staining (**Figure** 6-7) was also performed to further characterize the maturation of the newly formed bone. ACS+BMP-2 demonstrated both woven bone (blue) and mature bone (red), but NF+ACS+BMP-2 showed more mature bone formation, with an increased bone thickness in the regenerated area. NF+ACS+BMP-2 performed relatively well in the healing of bone defects.

Four of six clefts demonstrated bone bridging, which almost restored the osseous defects at week 8 with NF+ACS+BMP-2 treatment. The other two animals presented fibrous healing with minimal bone formations at the edges of the defect similar to ACS, and NF+ACS groups. With the ACS+BMP-2 group, three defects had substantial bone formation extending from each margin, albeit with a central residual defect whilst the other three defects progressed to fibrous healing similar to ACS, and NF+ACS groups. Based on histological evaluations, both H&E and trichrome staining, together with cross-sectional images (**Figure** 6-8) and 3D reconstructed μCT images, NF+ACS+BMP-2 treatment resulted in better and more consistent bone healing throughout the implanted scaffold when compared to ACS+BMP-2 group.

In contrast, Nguyen et al.[35] could not reveal any significant effect on bone formation over 12 weeks for BMP-2 (4.4 μg/implant) loaded on ACS and HA-TCP when compared to groups treated with ACS and HA-TCP alone. This could be due to burst release of BMP-2 from the scaffolds used, low BMP-2

concentration and/or ineffective handling of the soft tissue closure leading to substantial early loss of BMP-2. These shortcomings were addressed in our study through the utilization of NF hydrogel scaffold to sustain the release of BMP-2 to host osteoprogenitor cells. Our decision to utilize a higher BMP-2 concentration (12 μg/implant) was based on the osteoinductive concentrations used in other animal studies focusing on bone regeneration of maxillary and mandibular defects and normalized to the MPC cleft defect size.[75, 176, 177] The osteoinduction of the BMP-2 graft is also dependent on the effective soft tissue handling to maintain BMP-2 at the defect site and to prevent early loss of BMP-2 into nasal and/or oral cavities. Therefore, PRM was placed as a lining for the nasal cavity, the scaffold was then placed into the developed MPC defect, and oral mucosa was closed with watertight sutures to mimic the clinical scenario. These modifications appeared valid and enabled the appraisal of the osteoinductive potential BMP-2 loaded constructs. Although all of the experimental groups were implanted with PRM except controls, bone healing was similar between ACS and NF vs. untreated control. This finding rules out the possibility that PRM plays a role in enhancing bone formation and confirms that the main function of PRM is to provide a nasal seal to reduce early loss of BMP-2 into the nasal cavity. To our knowledge, this is the first animal report to address nasal communication and employ nasal seal to improve the outcomes of bone grafting.

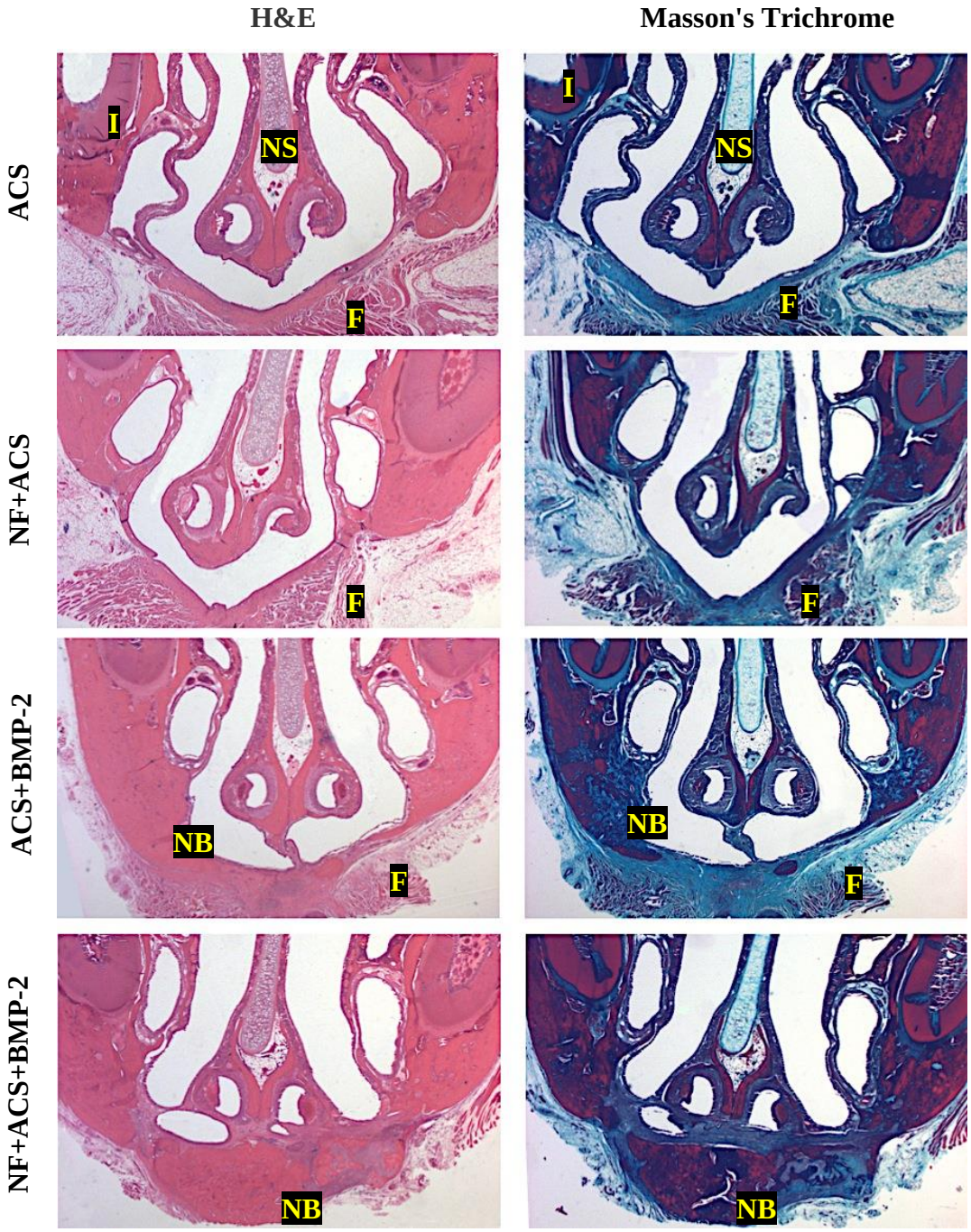

Figure 6-7: Representative coronal histological sections (1.6×) of MPC defect comparing bone healing between different treatments at week 8. Sections are stained with H&E and Masson's Trichrome stain (bone= dark blue, cortical bone= red). I: incisors, NS: nasal septum, F: fibrous tissue, and NB: new bone.

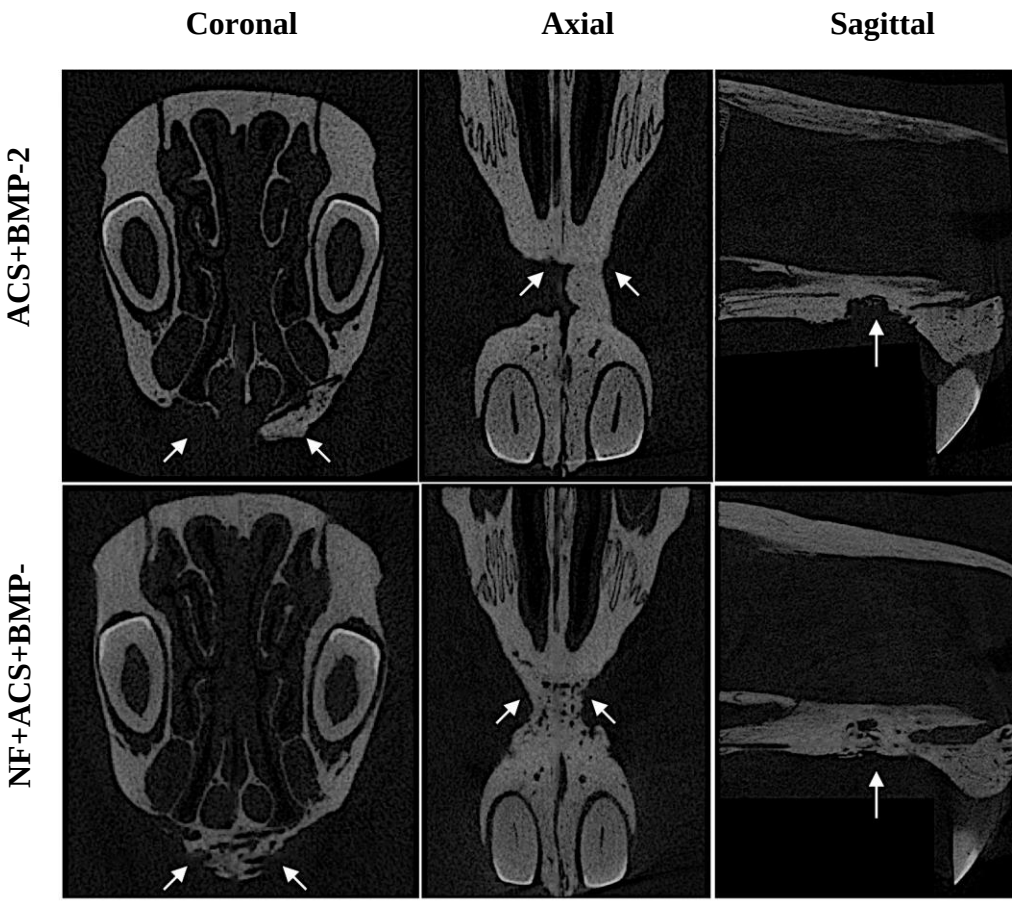

Figure 6-8: Representative µCT images comparing bone healing at week 8 in MPC defects (arrow) treated with ACS+BMP-2 and NF+ACS+BMP-2 in the 3 reference planes (coronal, axial and sagittal).

6.3.2.3 Effect of different treatments on Maxillary growth

Since the rats used in our study are dentally mature but skeletally immature,[168] we further assessed the effects of different bone grafts used in the study on the growth of the regenerated maxillary bone. Comparing the anteroposterior (IF-IP) and transverse dimensions (IF-IF) in operated rats with different bone grafts vs. non operated (control) rats revealed no differences over the 8 weeks of the study (**Table** 6-1). Additionally, there were no significant differences in the anteroposterior or transverse dimensions between week 0, 4, and 8 in each treatment group. Furthermore, there was no significant difference in the anteroposterior dimensions between right and left side in each group confirming

palatal symmetry following bone grafting of the created surgical defect. All dimensions were measured and re-examined after one week by one operator. The intra-rater ICC was 0.99 with narrow confidence interval, indicating accuracy and reliability of the measurement method.

The effects of BMP on craniofacial growth remain understudied. To our knowledge, only one study was completed in growing minipigs (2 months old) which compared bone healing in 2 × 4 cm parietal bone defects reconstructed with BMP-7+ ACS+ carboxymethyl cellulose vs. autografts.[178] That study reported that BMP-7 implantation did not disrupt cranial growth and development, which is in line with our results.

Table 6-1: Mean values of anteroposterior and transverse measurements of maxillae of operated and non operated rats at weeks 0, 4, and 8 postoperatively

Group	Measurements					
	W0		W4		W8	
	IF-IP	IF-IF	IF-IP	IF-IF	IF-IP	IF-IF
Non operated	9.11±0.57 (Right) 8.97±0.70 (Left)	9.83±0.56	9.67±0.91 (Right) 9.55±0.63 (Left)	10.34±0.26	9.33±0.75 (Right) 9.6±0.68 (Left)	10.50±0.33
ACS	9.18±0.53 (Right) 8.97±0.70 (Left)	9.60±0.27	9.47±0.24 (Right) 9.75±0.22 (Left)	10.05±0.28	9.69±0.28 (Right) 10.01±0.44 (Left)	9.85±0.35
NF+ACS	9.30±0.12 (Right) 9.04±0.10 (Left)	9.58±0.37	9.85±0.04 (Right) 9.50±0.20 (Left)	10.09±0.18	9.84±0.16 (Right) 9.48±0.06 (Left)	10.36±0.49
ACS+BMP-2	8.72±0.75 (Right) 9.09±0.74 (Left)	9.49±0.35	8.96±0.47 (Right) 9.16±0.73 (Left)	9.24±0.44	9.10±0.37 (Right) 9.42±0.48 (Left)	9.48±0.24
NF+ACS+BMP-2	9.35±0.10 (Right) 9.44±0.28 (Left)	9.49±0.08	9.60±0.20 (Right) 9.72±0.11 (Left)	10.16±0.20	9.73±0.48 (Right) 9.86±0.34 (Left)	10.24±0.13

6.4 Conclusion

The aim of this study was to develop NF based constructs with an ACS backbone as sustained release carriers for BMP-2 and to evaluate the osteoactivity of BMP-2 in the repair of cleft palate defects. The *in vitro* release results showed that scaffolds containing 2% NF exhibited a release profile conducive to stages of bone healing process and hence, it was utilized for subsequent *in vivo* studies. We did not directly assess the functionality of released BMP-2. However, our *in vivo* studies indicated that NF+ACS+BMP-2 treatment resulted in improved and more consistent bone defect filling when compared to ACS+BMP-2 group, supportive of its biological activity.

Every attempt was made in this study to simulate the clinical situation in order to facilitate future translation to human applications. Therefore, PRM was placed as a lining for the nasal cavity, the scaffold was then placed into the developed MPC defect, and oral mucosa was closed with watertight sutures to prevent early loss of BMP-2. Moreover, the *in vivo* μCT imaging allowed longitudinal analysis of bone regrowth. The modified MPC defect model appeared valid and enabled evaluation of the osteogenic potential of our osteoinductive scaffolds. NF and BMP-2 in the concentration and conditions utilized enhanced *de novo* bone formation. Additionally, based on anteroposterior and transverse measurements we found that BMP-2 implantation did not disrupt maxillary growth. In conclusion, NF+ACS+BMP-2 constructs exhibited oseoinductive properties together with incredible simplicity of the preparation, which makes it a novel approach for drug delivery for cleft palate reconstruction.

Chapter 7

General Discussion, Conclusions and Future Directions

7.1 GENERAL DISCUSSION

Bone reconstruction of the alveolar cleft is a fundamental part of the continuum of treatments needed for managing cleft palate patients, especially in children with complete clefts of the hard palate. Autograft is the gold standard therapy, however, it is limited by donor site morbidity and limited supply.[5] To overcome current grafting limitations this thesis focused on developing two tissue engineering therapies to provide effective and minimally invasive treatment options for cleft patients. One approach is to develop a cell-based therapy, using osteogenically induced mesenchymal stem cells (MSCs). MSCs were selected since they are readily available, can be easily expanded in standard culture, and have reliable osteogenic potential with no risk of immune rejection or tumorigenicity.[17] The second approach focused on the delivery of bone morphogenetic protein-2 (BMP-2) in a properly designed scaffold, to provide the necessary sustained activity after *in vivo* implantation. BMP-2 was selected since it is known for its osteoinductive potential. Thus, it acts as a morphogen (causing osteogenic differentiation of stem cells) if placed in the appropriate environment. The main benefits of these innovative therapies are reduced donor site morbidity, hospital stay duration, and overall procedure cost. This chapter (**Chapter 7**) provides a general discussion and summary of this dissertation. It also suggests future studies that could be done to further expand the knowledge of bone tissue engineering therapies.

Developing cell-based therapy for bone regeneration was elaborated in **Chapter 4**. The studies were conducted using human MSCs with a main focus on optimal approach for *in vitro* modification of the cells in order to assess their potential for developing cell-based therapy but no *in vivo* transplantations were done (to maintain project focus). A step-by-step approach was taken to clarify the role of specific osteogenic supplements, namely dexamethasone (Dex), vitamin D3 (Vit-D3), basic fibroblast growth factor (b-FGF), and BMP-2 on MSC differentiation. Osteogenic and adipogenic differentiation were evaluated concurrently in MSCs cultures exposed to range of concentrations and combinations of those osteogenic supplements (16 treatments in initial

experiments and 37 treatments in subsequent experiments presented in our study). Osteogenesis was assessed by alkaline phosphatase (ALP) activity, mineralization, and gene-expression of ALP, Runx2, bone sialoprotein (BSP), and osteonectin (ON). Adipogenesis was characterized by Oil Red O staining, gene-expression of peroxisome proliferator-activated receptor (PPARγ2) and adipocyte protein-2 (aP2). Finally, a comparison between osteogenesis and adipogenesis was then performed to determine the best osteogenic combination. Cultures treated with Dex (100 nM), Vit-D3 (10/50 nM) and BMP-2 (500 ng/mL) demonstrated maximal calcification and up-regulation of ALP and BSP expression. But, adipogenesis was up regulated parallel with osteogenesis in these cultures, as evidenced by the lipid formation and substantial up-regulation of PPARγ2 and aP2 gene-expression. Having adipogenesis in the induced cells is not desirable, since it might reduce the osteogenic cell pool at the transplant site resulting in poor outcomes and subsequent graft failure, hence, it is imperative to minimize this activity for cultures destined for clinical application. An optimal condition was obtained at Dex (10 nM) and BMP-2 (500 ng/mL) for mineralization without increasing adipogenesis-related markers. Dex was found to be essential for mineralization of MSCs. BMP-2 alone did not affect ALP activity and poorly induced *in vitro* calcification by h-MSCs. BMP-2 enhanced osteogenesis in Dex treated cultures and showed dose dependent mineralization in MSCs. While, b-FGF mitigated osteogenesis and enhanced adipogenesis. Vit-D3 appears essential for calcification only in the presence of b-FGF. It must be stated that this conclusion is based on addition of media supplements to h-MSCs simultaneously.

The concept of reconstructing craniofacial defects with MSCs from bone marrow was successfully validated in different animal models,[55, 154] with osteogenically induced cells yielding better bone induction in animal models.[155] However, the use of MSCs for bone reconstruction in humans remains understudied. Gimbel et al.[58] implanted collagen scaffolds seeded with bone marrow aspirates into human cleft defects and reduced morbidity compared to autologous grafts, but they did not report any quantitative measurement of bone

formation at defects. Behnia et al.[59] implanted MSCs combined with a demineralized bone mineral/calcium sulphate scaffold to obtain <50% bone fill. Both studies employed MSCs with no osteogenic conditioning. Hibi et al.,[61] on the other hand, employed osteogenically induced h-MSCs to repair an alveolar cleft in a 9 year old patient, which resulted in ~79% bone fill after 9 month post-operatively with successful eruption of lateral incisor and canine. The conditioning was attempted with platelet-rich plasma, whose osteogenic effects are difficult to dissect due to its various constituents. No attempts have been made to optimize the osteogenic conditioning of the cells using purified supplements similar to those utilized in this study before transplantation. Employing purified reagents may be a better approach, since it can provide better control over the potency and reproducibility of cellular differentiation. The outcome of cell-based therapies for bone regeneration could be accordingly optimized with such an approach, potentially providing an alternative therapy for autologous grafts. Our studies delineated the conditions for phenotypic differentiation of MSCs and it will be important to explore *in vivo* potential of phenotypically differentiated MSC for translation into clinics.

After optimizing the conditions for bone regeneration in culture, a reliable animal model of cleft palate was developed in **Chapter 5** to facilitate efficacy testing for the new biomaterials for secondary bone grafting. An appropriate animal model of cleft palate is needed to test new biomaterials for secondary bone grafting. Available animal models of cleft palate include both congenital and surgical clefts. Congenital models significantly enhanced our understanding of etiology and morphogenetic factors contributing to cleft development, but they were not utilized for development of new grafting therapies.[34] This could be due to the small maxilla size in mice models as well as the variability in cleft size and anatomical location. Therefore, surgical cleft models are considered more suitable. Surgical clefts were produced in primates,[73, 164] dogs,[74] and rabbits.[75, 165] But these models are limited by high operational and husbandry cost. This led to the development of rodent models of cleft palate. Two main rodent models of gingivoperiosteoplasty are published namely mid palate cleft (MPC) model[33]

(9×5×3 mm^3) and alveolar cleft (AC) model[34] (7×4×3 mm^3). However, both models have limitations: one was not a critically sized defect[33] and the other failed when utilized for testing bone grafting therapies based on BMP-2.[34, 35] Consequently, **Chapter 5** is focused on developing a reliable rodent model of cleft palate. The current rodent models of cleft palate were critically assessed and compared to identify the most reliable model. This was achieved through a series of successive experiments. Our initial studies utilizing a 7×4×3 mm^3 AC defect in 8 and 16 weeks old Sprague Dawley rats revealed substantial injury to the surrounding structures including incisor roots and palatine foramen based on macroscopic and micro-computed tomography (μCT) examinations. These finding were consistent with the μCT images presented in Nguyen et al. study.[34] Then, we compared the anteroposterior and transverse dimensions of the maxilla in non operated 16 weeks old Sprague Dawley vs. Wistar rats. For this purpose, we utilized landmarks established by Gomes et al.,[166] the distances from infraorbital foramen to incisal point (IF-IP) were measured bilaterally to represent the anteroposterior dimension while the distance between right and left IF was utilized for transverse measurements. There were no differences in IF-IP or IF-IF of the maxillae in 16 weeks old Sprague Dawley vs. Wistar. Moreover, our IF-IP data for 16, 20 and 24 weeks old Wistar rats were similar to the reported IF-IP dimensions in 12 weeks old Wistar rats.[166, 167] These findings signify the validity and reproducibility of those landmarks. It also supports our initial findings that size of maxilla is not significantly different in young rats (8 weeks old) vs. older rats (16 weeks old). Subsequently, virtual planning for the appropriate design of MPC and AC defects was performed in 16 weeks old Wistar rats. Defects were designed to be at least 1 mm away from roots of the incisors to avoid damage to PDL, 1 mm away from the palatine foramen and 1 mm away from the zygomatic arch Finally, we conducted a comparative study to assess bone healing following employing the designed defects based on virtual planning in 16 weeks old Wistar rats. Preoperative virtual planning of the modified MPC and AC surgical defects using μCT data provided accurate guide for surgical implementation after careful consideration of the anatomy. Planned dimensions vs. actual surgical dimensions

were similar. For MPC defects, virtual planning resulted in a defect that is 7.23±0.27 mm long, 2.84±0.4 mm wide, and 1±0.2mm deep while postoperative defects were (7.2±0.3)×(2.6±0.2)×(1±0.2) mm^3. For AC defects, the planned dimensions were 5.48±0.22 mm wide, 2.43±0.13 mm long, and 1±0.2 mm deep vs. postoperative defects dimensions of (5.3±0.6)×(2.6±0.2)×(1±0.2) mm^3. It is clear that preoperative virtual planning improved the potential for achieving successful postoperative surgical outcomes.

The presented modifications for AC and MPC cleft models made them more reproducible, reliable, and practical as they simulate bony defects in cleft palate patients. MPC represents a bilateral cleft defect, while; AC model represents a unilateral cleft defect. However, we found that the AC defects are more challenging to create as it is surrounded by incisor roots, palatine foramen and the zygomatic arch which introduced greater variability between animals in the initial cleft size and subsequent healing specially at week 4. Conversely, MPC defect had less anatomical challenges and larger residual defect volume as compared to AC defect. Consequently, we consider the MPC model to be more appropriate for efficacy testing of new bone grafting therapies for cleft palate reconstruction, which would have a tremendous impact on reconstructive maxillofacial surgery.

The second bone tissue engineering approach based on the delivery of BMP-2 in a properly designed scaffold was elaborated in **Chapter 6**. Despite successful bone formation through simple adsorption of BMP-2 on collagen scaffold, burst release of growth factors with fast reduction of biological activity and the lack of controlled release limits its utility.[27] As bone growth is temporal, the appropriate cells may not be attracted to the defect area until after considerable diffusion of BMP-2 from the site.[28] Hence, this chapter focused on the development, *in vitro*, and *in vivo* characterization of a carrier that provides sustained release of BMP-2 for enhanced bone formation. Initially, a nanofiber (NF) scaffold with collagen backbone was constructed to control the release of BMP-2. ACS was used as an adjuvant to provide structural integrity for the NF hydrogel, facilitate handling and to prevent them from migrating away from the defect site. To mimic the clinical situation, BMP-2 was loaded using physical adsorption method on

absorbable collagen scaffold (ACS) and NF hydrogel with different densities (1-2% w/v) was then added to slow BMP-2 release. Then, the release of FITC labelled BMP-2 from the prepared NF scaffolds into PBS was evaluated *in vitro* over 23 days to explore the optimum NF density that could recapitulate physiological bone healing process. Bone healing process consists of complex series of well-coordinated events including initial haematoma and inflammation for 3-4 days, followed by reparative processes and intramembranous bone formation. Relating our release data to the bone healing process, we found that both 0 and 1% NF released larger quantities of BMP-2 during the inflammatory phase which could increase inflammation following *in vivo* implantation, that could adversely inhibit or delay the tissue regeneration process.[175] While construct containing 2% NF, released minimal amounts of BMP-2 during the inflammatory phase and maintained its maximum BMP-2 concentrations during the cell recruitment phase.

To test the efficacy of the designed scaffold, NF+ACS+BMP-2 (2% w/v) scaffold was implanted into the previously developed MPC model ($7\times2.5\times1$ mm^3) and bone healing was assessed using μCT and histology over 8 weeks. Five treatment groups (n=6 per group) were tested: control (no scaffold), ACS alone, ACS+BMP-2, NF+ACS, and NF+ACS+BMP-2. Percent bone filling was similar in control, ACS, and NF+ACS groups at week 4 (29.43±6.51, 27.09±15.71, and 23.94±7.99, respectively) and week 8 (37.72±12.00, 40.14±15.12, and 22.43±5.98, respectively). Consistently, histological assessments of the defects at 8 weeks demonstrated that ACS, and NF+ACS groups displayed fibrous tissue filling the defect with no bone formation within the defect and limited bone regrowth at peripheries of the defects. Interestingly, the addition of BMP-2 considerably enhanced bone healing at the defect site as compared to other groups. Bone filling percentage in NF+ACS+ BMP-2 group was higher than ACS+BMP-2 group at week 4 (75.31±10.86 vs. 54.29±18.90, respectively) and at week 8 (88.4±8.32 vs. 71.59±20.29, respectively), this difference was not statistically significant ($p>0.05$). Based on histological evaluation, ACS+BMP-2 treatment demonstrated partial closure of the surgical defect while

NF+ACS+BMP-2 treatment showed central and peripheral bone formation within the region previously occupied by the scaffold. The thickness of the regenerated bone was larger in the later treatment group. Overall, histologic evaluations using both H&E and trichrome staining along with cross-sectional and 3D reconstructed μCT images, demonstrated that NF+ACS+BMP-2 treatment resulted in better and more consistent bone healing throughout the implanted scaffold when compared to the ACS+BMP-2 group.

In contrast, Nguyen et al.[35] could not reveal any significant effect for BMP-2 (4.4 μg/implant) on bone formation over 12 weeks when BMP-2 was loaded on ACS and HA-TCP as compared to groups treated with ACS and HA-TCP alone. This could be due to burst release of BMP-2 from the scaffolds used, low BMP-2 concentration and/or ineffective handling of the soft tissue closure leading to substantial early loss of BMP-2. These shortcomings were addressed in our animal study through the utilization of 2% NF hydrogel scaffold to sustain the release of BMP-2 to host osteoprogenitor cells. Moreover, we utilized a higher BMP-2 concentration (12 μg/implant) which was calculated based on the osteoinductive concentrations used in other animal studies,[14, 22, 23] focusing on bone regeneration of maxillary or mandibular defects, and normalized to the MPC cleft defect size. The osteoinduction of the BMP-2 graft is also dependent on the effective soft tissue handling to maintain BMP-2 at the defect site and to prevent early loss of BMP-2 into nasal and/or oral cavities. Therefore, a PRM was placed as a lining for the nasal cavity, the designed scaffold was then placed into the developed MPC defect, and oral mucosa was closed with watertight sutures to mimic the clinical scenario. These modifications appeared valid and enabled the appraisal of the osteoinductive potential BMP-2 loaded constructs. To our knowledge, this is the first animal report to address nasal communication and employ nasal seal to improve the outcomes of bone grafting. Based on histologic evaluations, both H&E and trichrome staining, together with cross-sectional and 3D reconstructed μCT images, NF+ACS+BMP-2 treatment resulted in better and more predictable bone healing throughout the graft as compared to ACS+BMP-2 group.

7.2 GENERAL CONCLUSIONS

In vitro characterization of osteogenically induced MSCs was presented in this thesis. *In vitro* and *in vivo* characterization of NF+ACS based scaffold for sustained BMP-2 delivery was also reported. Based on the outcomes presented in this thesis, the following conclusions can be drawn:

- Optimal condition for osteogenic differentiation of MSCs without increasing adipogenesis-related markers was obtained at Dex (10 nM) and BMP-2 (500 ng/mL). These findings could be employed in cultivation of MSCs for *in vivo* testing of cell-based strategies of cleft palate reconstruction.
- Dex was found to be essential for mineralization of MSCs. BMP-2 alone did not affect ALP activity and poorly induced *in vitro* calcification by h-MSCs. BMP-2 enhanced osteogenesis in Dex treated cultures and showed dose dependent mineralization in MSCs. While, b-FGF mitigated osteogenesis and enhanced adipogenesis. Vit-D3 appears essential for calcification only in the presence of b-FGF.
- The presented modifications for AC and MPC cleft models made them more reproducible, reliable, and practical as they simulate bony defects in cleft palate patients. However, MPC defect had less anatomical challenges and larger residual defect volume as compared to AC defect and hence we consider it more appropriate for efficacy testing of new bone grafting therapies for cleft palate reconstruction.
- The *in vitro* release results showed that scaffolds containing 2% NF exhibited an ideal release profile when related to stages of bone healing process and hence, it was utilized for subsequent *in vivo* studies.
- NF+ACS+BMP-2 constructs exhibited oseoinductive properties together with incredible simplicity of the preparation, which makes it a novel approach for drug delivery for cleft palate reconstruction.

7.3 FUTURE RECOMMENDATION

Our *in vitro* studies on osteogenic differentiation of MSCs presented balanced osteogenesis and adipogenesis data for several combinations of supplements and presented optimal conditions for osteogenesis with minimal induction of adipogenesis based on ALP activity, calcification and expression of specific osteogenic and adipogenic markers. However, it must be stated that this conclusion is based on simultaneous addition of media supplements to MSCs. It is likely that sequential addition of the media supplements might alter this picture and lead to different results. We can envision employing conditions that do not support osteogenesis initially (e.g., culture in BM+b-FGF supplementation) followed by exposure to osteogenic supplements (e.g., Dex and BMP-2) when sufficient cell expansion occurs.

Runt-related transcription factor-2 (Runx-2), osterix (Osx) and canonical Wnt signaling promotes osteogenic differentiation of MSCs into bone forming cells. BMP activates Smads, which interact with Runx-2 to induce expression of osteogenic genes.[47] Runx-2 maintains osteoblasts in immature stage and negatively controls osteoblast terminal differentiation.[48] While, Osx is the downstream gene of Runx-2, which promotes the differentiation of pre-osteoblasts to immature osteoblasts.[49] Osx forms a complex with the nuclear factor of activated T cells (NFAT). Then NFAT activates the Wnt signaling pathway, which controls osteoblastogenesis and bone mass.[50] During osteogenic differentiation of MSCs, Runx-2 inhibits adipogenic differentiation of MSCs through blocking Ccaat-enhancer-binding proteins (C/EBP) family and peroxisome proliferator-activated receptor gamma2 (PPAR-γ_2). Therefore, future studies identifying the pathways involved for specific differentiation events, and especially the critical molecules involved in phenotypic switch should be considered.

Quantitative PCR was a very beneficial technique that aided the understanding of osteogenesis and adipogenesis in MSCs treated with different combination of osteogenic supplements *in vitro*, but we did not perform this analysis at the *in vivo* animal study. Although μCT and the histology provided very valuable

information, *in situ* hybridization would provide with more details at the gene expression level, which could explain tissue reaction following implantation of different bone grafts. It could also explain the reason for graft failure reported in some treatment groups. Moreover, looking at the common inflammatory mediators like IL-1, IL-6 and TNF-alpha could characterize the inflammatory response to different grafts with or without BMP-2.

Additional studies exploring *in vivo* transplantation of osteogenically induced cells are also needed to determine if the induced cellular phenotypes could give a functional response (i.e. robust bone formation) in the developed MPC models. A comparison between cell-based vs. the developed BMP-2 based therapies could be pursed in the future to explore the most effective therapy. Future studies are needed to explore the synergistic effects of combining cell- and protein-based therapies that could further augment bone formation *in vivo*.

Another important area of investigation would be to assess the adjunctive use of Dex or b-FGF with optimized BMP-2 concentrations to test possibility of utilizing the synergistic effects of those combinations on bone regeneration. This is based on previous studies that demonstrated that BMP-7-induced ectopic bone formation was significantly improved with the application of Dex.[179] It is also reported that combinations of BMP-2 and b-FGF enhanced bone formation *in vivo.*[124]

New bone grafting therapies should be compared to autologous bone grafting that is the standard therapy in humans. But, animal studies reported inconsistent results from autografts.[180, 181] Therefore, future studies optimizing the outcomes of autografting would be beneficial to further characterize the efficacy of new bone grafting therapies.

It is important to mention that rats do not have canines or premolars,[168] so this model cannot be used to evaluate if the engineered bone can support tooth eruption. Therefore, a through biomechanical testing of the tissue-engineered bone should be the next step to validate new therapies for cleft palate reconstruction.

Assessment of postoperative complications is another essential aspect for evaluating BMP-2 based therapies. Therefore additional investigations will be required to gain further insight into systemic complications reported in the spine applications such as cancer risk, systemic toxicity, reproductive toxicity, immunogenicity, and effects on distal organs.[117] Moreover, the minimum effective BMP-2 dose for robust bone formation lower than what we used in the *in vivo* study needs to be identified. Reducing BMP-2 concentration is appealing, as it will reduce the cost and side effects of the therapy.

In conclusion, osteogenically induced MSCs and BMP-2 loaded in a properly designed scaffold are promising bone tissue engineering therapies, which could potentially treat cleft palate patient with minimal side effects and therefore increasing the quality of life for cleft palate patients. The work presented included a broad range of research techniques, from molecular understanding of therapeutic interventions to pre-clinical outcome measures in an animal model, which could potentially provide the scientific foundation for future human clinical trials.

REFERENCES

1. Gundlach KK, Maus C: Epidemiological studies on the frequency of clefts in Europe and world-wide. J Craniomaxillofac Surg 34 Suppl 2:1, 2006

2. Hupp JR, Ellis E, Tucker MR, Ellis E: Contemporary oral and maxillofacial surgery. Mosby Elsevier, 2008

3. Sadove AM, van Aalst JA, Culp JA: Cleft palate repair: art and issues. Clin Plast Surg 31:231, 2004

4. Murray JC: Gene/environment causes of cleft lip and/or palate. Clin Genet 61:248, 2002

5. Moreau JL, Caccamese JF, Coletti DP, Sauk JJ, Fisher JP: Tissue engineering solutions for cleft palates. J Oral Maxillofac Surg 65:2503, 2007

6. Waitzman NJ, Romano PS, Scheffler RM: Estimates of the economic costs of birth defects. Inquiry 31:188, 1994

7. Batsos C: An environmental scan of cleft lip and palate clinics and dental benefit programs in Canada. (ed. http://www.fptdwg.ca/assets/PDF/CleftPalate/1008-CleftLipAndPalateScan.pdf, 2010, p 1

8. Christensen K, Juel K, Herskind AM, Murray JC: Long term follow up study of survival associated with cleft lip and palate at birth. BMJ 328:1405, 2004

9. Precious DS: Primary cleft lip and palate. J Can Dent Assoc 65:279, 1999

10. Bajaj AK, Wongworawat AA, Punjabi A: Management of alveolar clefts. J Craniofac Surg 14:840, 2003

11. Craven C, Cole P, Hollier L, Jr., Stal S: Ensuring success in alveolar bone grafting: a three-dimensional approach. J Craniofac Surg 18:855, 2007

12. Vig KW: Alveolar bone grafts: the surgical/orthodontic management of the cleft maxilla. Ann Acad Med Singapore 28:721, 1999

13. Nandi SK, Roy S, Mukherjee P, Kundu B, De DK, Basu D: Orthopaedic applications of bone graft & graft substitutes: a review. Indian J Med Res 132:15, 2010

14. Kao ST, Scott DD: A review of bone substitutes. Oral Maxillofac Surg Clin North Am 19:513, 2007

15. Rawashdeh MA, Telfah H: Secondary alveolar bone grafting: the dilemma of donor site selection and morbidity. Br J Oral Maxillofac Surg 46:665, 2008

16. Cho YR, Gosain AK: Biomaterials in craniofacial reconstruction. Clin Plast Surg 31:377, 2004

17. Logeart-Avramoglou D, Anagnostou F, Bizios R, Petite H: Engineering bone: challenges and obstacles. J Cell Mol Med 9:72, 2005

18. Sharma B, Elisseeff JH: Engineering structurally organized cartilage and bone tissues. Ann Biomed Eng 32:148, 2004

19. Sanchez-Lara PA, Zhao H, Bajpai R, Abdelhamid AI, Warburton D: Impact of stem cells in craniofacial regenerative medicine. Front Physiol 3:188, 2012

20. Fiedler J, Roderer G, Gunther KP, Brenner RE: BMP-2, BMP-4, and PDGF-bb stimulate chemotactic migration of primary human mesenchymal progenitor cells. J Cell Biochem 87:305, 2002

21. Chen D, Zhao M, Mundy GR: Bone morphogenetic proteins. Growth Factors 22:233, 2004

22. Gelse K, Poschl E, Aigner T: Collagens--structure, function, and biosynthesis. Adv Drug Deliv Rev 55:1531, 2003

23. Friess W: Collagen--biomaterial for drug delivery. Eur J Pharm Biopharm 45:113, 1998

24. Heino J: The collagen family members as cell adhesion proteins. Bioessays 29:1001, 2007

25. Kleinman HK, Klebe RJ, Martin GR: Role of collagenous matrices in the adhesion and growth of cells. J Cell Biol 88:473, 1981

26. Axelrad TW, Einhorn TA: Bone morphogenetic proteins in orthopaedic surgery. Cytokine Growth Factor Rev 20:481, 2009

27. Schliephake H: Application of bone growth factors--the potential of different carrier systems. Oral Maxillofac Surg 14:17, 2010

28. Puleo DA: Dependence of mesenchymal cell responses on duration of exposure to bone morphogenetic protein-2 in vitro. J Cell Physiol 173:93, 1997

29. Nagai Y, Unsworth LD, Koutsopoulos S, Zhang S: Slow release of molecules in self-assembling peptide nanofiber scaffold. J Control Release 115:18, 2006

30. Gelain F, Bottai D, Vescovi A, Zhang S: Designer self-assembling peptide nanofiber scaffolds for adult mouse neural stem cell 3-dimensional cultures. PLoS One 1:e119, 2006

31. Horii A, Wang X, Gelain F, Zhang S: Biological designer self-assembling peptide nanofiber scaffolds significantly enhance osteoblast proliferation, differentiation and 3-D migration. PLoS One 2:e190, 2007

32. Bokhari MA, Akay G, Zhang S, Birch MA: The enhancement of osteoblast growth and differentiation in vitro on a peptide hydrogel-polyHIPE polymer hybrid material. Biomaterials 26:5198, 2005

33. Mehrara BJ, Saadeh PB, Steinbrech DS, Dudziak M, Grayson BH, Cutting CB, McCarthy JG, Gittes GK, Longaker MT: A rat model of gingivoperiosteoplasty. J Craniofac Surg 11:54, 2000

34. Nguyen PD, Lin CD, Allori AC, Ricci JL, Saadeh PB, Warren SM: Establishment of a critical-sized alveolar defect in the rat: a model for human gingivoperiosteoplasty. Plast Reconstr Surg 123:817, 2009

35. Nguyen PD, Lin CD, Allori AC, Schachar JS, Ricci JL, Saadeh PB, Warren SM: Scaffold-based rhBMP-2 therapy in a rat alveolar defect model: implications for human gingivoperiosteoplasty. Plast Reconstr Surg 124:1829, 2009

36. De La Pedraja J, Erbella J, McDonald WS, Thaller S: Approaches to cleft lip and palate repair. J Craniofac Surg 11:562, 2000

37. Dixon MJ, Marazita ML, Beaty TH, Murray JC: Cleft lip and palate: understanding genetic and environmental influences. Nat Rev Genet 12:167, 2011

38. Roberts TT, Rosenbaum AJ: Bone grafts, bone substitutes and orthobiologics: The bridge between basic science and clinical advancements in fracture healing. Organogenesis 8, 2012

39. Islam A: Bone marrow aspiration before bone marrow core biopsy using the same bone marrow biopsy needle: a good or bad practice? J Clin Pathol 60:212, 2007

40. Augello A, De Bari C: The regulation of differentiation in mesenchymal stem cells. Hum Gene Ther 21:1226, 2010

41. De Biase P, Capanna R: Clinical applications of BMPs. Injury 36 Suppl 3:S43, 2005

42. Rickard DJ, Sullivan TA, Shenker BJ, Leboy PS, Kazhdan I: Induction of rapid osteoblast differentiation in rat bone marrow stromal cell cultures by dexamethasone and BMP-2. Dev Biol 161:218, 1994

43. Jorgensen NR, Henriksen Z, Sorensen OH, Civitelli R: Dexamethasone, BMP-2, and 1,25-dihydroxyvitamin D enhance a more differentiated osteoblast phenotype: validation of an in vitro model for human bone marrow-derived primary osteoblasts. Steroids 69:219, 2004

44. Mostafa NZ, Fitzsimmons R, Major PW, Adesida A, Jomha N, Jiang H, Uludag H: Osteogenic differentiation of human mesenchymal stem cells cultured with dexamethasone, vitamin D3, basic fibroblast growth factor, and bone morphogenetic protein-2. Connect Tissue Res 53:117, 2012

45. McKay WF, Peckham SM, Badura JM: A comprehensive clinical review of recombinant human bone morphogenetic protein-2 (INFUSE Bone Graft). Int Orthop 31:729, 2007

46. Smith DM, Cooper GM, Mooney MP, Marra KG, Losee JE: Bone morphogenetic protein 2 therapy for craniofacial surgery. J Craniofac Surg 19:1244, 2008

47. Komori T: Regulation of bone development and maintenance by Runx2. Front Biosci 13:898, 2008

48. Marie PJ: Transcription factors controlling osteoblastogenesis. Arch Biochem Biophys 473:98, 2008

49. Celil AB, Hollinger JO, Campbell PG: Osx transcriptional regulation is mediated by additional pathways to BMP2/Smad signaling. J Cell Biochem 95:518, 2005

50. Koga T, Matsui Y, Asagiri M, Kodama T, de Crombrugghe B, Nakashima K, Takayanagi H: NFAT and Osterix cooperatively regulate bone formation. Nat Med 11:880, 2005

51. Baron R, Rawadi G, Roman-Roman S: Wnt signaling: a key regulator of bone mass. Curr Top Dev Biol 76:103, 2006

52. Gerstenfeld LC, Cullinane DM, Barnes GL, Graves DT, Einhorn TA: Fracture healing as a post-natal developmental process: molecular, spatial, and temporal aspects of its regulation. J Cell Biochem 88:873, 2003

53. Shapiro F: Bone development and its relation to fracture repair. The role of mesenchymal osteoblasts and surface osteoblasts. Eur Cell Mater 15:53, 2008

54. Wakitani S, Okabe T, Horibe S, Mitsuoka T, Saito M, Koyama T, Nawata M, Tensho K, Kato H, Uematsu K, Kuroda R, Kurosaka M, Yoshiya S, Hattori K, Ohgushi H: Safety of autologous bone marrow-derived mesenchymal stem cell transplantation for cartilage repair in 41 patients with 45 joints followed for up to 11 years and 5 months. J Tissue Eng Regen Med 5:146, 2011

55. Mankani MH, Kuznetsov SA, Wolfe RM, Marshall GW, Robey PG: In vivo bone formation by human bone marrow stromal cells: reconstruction of the mouse calvarium and mandible. Stem Cells 24:2140, 2006

56. Yang Y, Hallgrimsson B, Putnins EE: Craniofacial defect regeneration using engineered bone marrow mesenchymal stromal cells. J Biomed Mater Res A 99:74, 2011

57. Xu L, Lv K, Zhang W, Zhang X, Jiang X, Zhang F: The healing of critical-size calvarial bone defects in rat with rhPDGF-BB, BMSCs, and beta-TCP scaffolds. J Mater Sci Mater Med 23:1073, 2012

58. Gimbel M, Ashley RK, Sisodia M, Gabbay JS, Wasson KL, Heller J, Wilson L, Kawamoto HK, Bradley JP: Repair of alveolar cleft defects: reduced morbidity with bone marrow stem cells in a resorbable matrix. J Craniofac Surg 18:895, 2007

59. Behnia H, Khojasteh A, Soleimani M, Tehranchi A, Khoshzaban A, Keshel SH, Atashi R: Secondary repair of alveolar clefts using human mesenchymal stem cells. Oral Surg Oral Med Oral Pathol Oral Radiol Endod 108:e1, 2009

60. Castano-Izquierdo H, Alvarez-Barreto J, van den Dolder J, Jansen JA, Mikos AG, Sikavitsas VI: Pre-culture period of mesenchymal stem cells in osteogenic media influences their in vivo bone forming potential. J Biomed Mater Res A 82:129, 2007

61. Hibi H, Yamada Y, Ueda M, Endo Y: Alveolar cleft osteoplasty using tissue-engineered osteogenic material. Int J Oral Maxillofac Surg 35:551, 2006

62. Behnia H, Khojasteh A, Soleimani M, Tehranchi A, Atashi A: Repair of alveolar cleft defect with mesenchymal stem cells and platelet derived growth factors: a preliminary report. J Craniomaxillofac Surg 40:2, 2012

63. Marden LJ, Hollinger JO, Chaudhari A, Turek T, Schaub RG, Ron E: Recombinant human bone morphogenetic protein-2 is superior to demineralized bone matrix in repairing craniotomy defects in rats. J Biomed Mater Res 28:1127, 1994

64. Cowan CM, Aalami OO, Shi YY, Chou YF, Mari C, Thomas R, Quarto N, Nacamuli RP, Contag CH, Wu B, Longaker MT: Bone morphogenetic protein 2 and retinoic acid accelerate in vivo bone formation, osteoclast recruitment, and bone turnover. Tissue Eng 11:645, 2005

65. Lindholm TC, Lindholm TS, Marttinen A, Urist MR: Bovine bone morphogenetic protein (bBMP/NCP)-induced repair of skull trephine defects in pigs. Clin Orthop Relat Res 263, 1994

66. Takahashi Y, Yamamoto M, Yamada K, Kawakami O, Tabata Y: Skull bone regeneration in nonhuman primates by controlled release of bone morphogenetic protein-2 from a biodegradable hydrogel. Tissue Eng 13:293, 2007

67. Liu HC, E LL, Wang DS, Su F, Wu X, Shi ZP, Lv Y, Wang JZ: Reconstruction of alveolar bone defects using bone morphogenetic protein 2 mediated rabbit dental pulp stem cells seeded on nano-hydroxyapatite/collagen/poly(L-lactide). Tissue Eng Part A 17:2417, 2011

68. Marukawa E, Asahina I, Oda M, Seto I, Alam M, Enomoto S: Functional reconstruction of the non-human primate mandible using recombinant human bone morphogenetic protein-2. Int J Oral Maxillofac Surg 31:287, 2002

69. Choi Y, Lee JS, Kim YJ, Kim MS, Choi SH, Cho KS, Jung UW: Recombinant human BMP-2 stimulates the osteogenic potential of the Schneiderian membrane. Tissue Eng Part A, 2013

70. Lee J, Susin C, Rodriguez NA, de Stefano J, Prasad HS, Buxton AN, Wikesjo UM: Sinus augmentation using rhBMP-2/ACS in a mini-pig model: relative efficacy of autogenous fresh particulate iliac bone grafts. Clin Oral Implants Res 24:497, 2013

71. Kao DW, Kubota A, Nevins M, Fiorellini JP: The negative effect of combining rhBMP-2 and Bio-Oss on bone formation for maxillary sinus augmentation. Int J Periodontics Restorative Dent 32:61, 2012

72. Choi Y, Yun JH, Kim CS, Choi SH, Chai JK, Jung UW: Sinus augmentation using absorbable collagen sponge loaded with Escherichia coli-expressed recombinant human bone morphogenetic protein 2 in a standardized rabbit sinus model: a radiographic and histologic analysis. Clin Oral Implants Res 23:682, 2012

73. Boyne PJ, Nath R, Nakamura A: Human recombinant BMP-2 in osseous reconstruction of simulated cleft palate defects. Br J Oral Maxillofac Surg 36:84, 1998

74. Mayer M, Hollinger J, Ron E, Wozney J: Maxillary alveolar cleft repair in dogs using recombinant human bone morphogenetic protein-2 and a polymer carrier. Plast Reconstr Surg 98:247, 1996

75. Sawada Y, Hokugo A, Nishiura A, Hokugo R, Matsumoto N, Morita S, Tabata Y: A trial of alveolar cleft bone regeneration by controlled release of bone morphogenetic protein: an experimental study in rabbits. Oral Surg Oral Med Oral Pathol Oral Radiol Endod 108:812, 2009

76. Michael S, Mark M: Animal Models for Bone Tissue Engineering of Critical-sized Defects (CSDs), Bone Pathologies, and Orthopedic Disease States. *Bone Tissue Engineering*, (ed., CRC Press, 2004, p 217

77. Dickinson BP, Ashley RK, Wasson KL, O'Hara C, Gabbay J, Heller JB, Bradley JP: Reduced morbidity and improved healing with bone morphogenic protein-2 in older patients with alveolar cleft defects. Plast Reconstr Surg 121:209, 2008

78. Alonso N, Tanikawa DY, Freitas Rda S, Canan L, Jr., Ozawa TO, Rocha DL: Evaluation of maxillary alveolar reconstruction using a resorbable collagen sponge with recombinant human bone morphogenetic protein-2 in cleft lip and palate patients. Tissue Eng Part C Methods 16:1183, 2010

79. Canan LW, Jr., da Silva Freitas R, Alonso N, Tanikawa DY, Rocha DL, Coelho JC: Human bone morphogenetic protein-2 use for maxillary reconstruction in cleft lip and palate patients. J Craniofac Surg 23:1627, 2012

80. Herford AS, Boyne PJ, Rawson R, Williams RP: Bone morphogenetic protein-induced repair of the premaxillary cleft. J Oral Maxillofac Surg 65:2136, 2007

81. Fallucco MA, Carstens MH: Primary reconstruction of alveolar clefts using recombinant human bone morphogenic protein-2: clinical and radiographic outcomes. J Craniofac Surg 20 Suppl 2:1759, 2009

82. Herford AS, Boyne PJ, Williams RP: Clinical applications of rhBMP-2 in maxillofacial surgery. J Calif Dent Assoc 35:335, 2007

83. Chin M, Ng T, Tom WK, Carstens M: Repair of alveolar clefts with recombinant human bone morphogenetic protein (rhBMP-2) in patients with clefts. J Craniofac Surg 16:778, 2005

84. Neovius E, Lemberger M, Docherty Skogh AC, Hilborn J, Engstrand T: Alveolar bone healing accompanied by severe swelling in cleft children treated with bone morphogenetic protein-2 delivered by hydrogel. J Plast Reconstr Aesthet Surg 66:37, 2013

85. Haidar ZS, Hamdy RC, Tabrizian M: Delivery of recombinant bone morphogenetic proteins for bone regeneration and repair. Part B: Delivery systems for BMPs in orthopaedic and craniofacial tissue engineering. Biotechnol Lett 31:1825, 2009

86. Zhang Z, Hu J, Ma PX: Nanofiber-based delivery of bioactive agents and stem cells to bone sites. Adv Drug Deliv Rev 64:1129, 2012

87. Kohgo T, Yamada Y, Ito K, Yajima A, Yoshimi R, Okabe K, Baba S, Ueda M: Bone regeneration with self-assembling peptide nanofiber scaffolds in tissue engineering for osseointegration of dental implants. Int J Periodontics Restorative Dent 31:e9, 2011

88. Hauser CA, Zhang S: Designer self-assembling peptide nanofiber biological materials. Chem Soc Rev 39:2780, 2010

89. Garreta E, Genove E, Borros S, Semino CE: Osteogenic differentiation of mouse embryonic stem cells and mouse embryonic fibroblasts in a three-dimensional self-assembling peptide scaffold. Tissue Eng 12:2215, 2006

90. Misawa H, Kobayashi N, Soto-Gutierrez A, Chen Y, Yoshida A, Rivas-Carrillo JD, Navarro-Alvarez N, Tanaka K, Miki A, Takei J, Ueda T, Tanaka M, Endo H, Tanaka N, Ozaki T: PuraMatrix facilitates bone regeneration in bone defects of calvaria in mice. Cell Transplant 15:903, 2006

91. Tcacencu I, Karlstrom E, Cedervall J, Wendel M: Transplanted Human Bone Marrow Mesenchymal Stem Cells Seeded onto Peptide Hydrogel Decrease Alveolar Bone Loss. Biores Open Access 1:215, 2012

92. Nakahara H, Misawa H, Yoshida A, Hayashi T, Tanaka M, Furumatsu T, Tanaka N, Kobayashi N, Ozaki T: Bone repair using a hybrid scaffold of self-assembling peptide PuraMatrix and polyetheretherketone cage in rats. Cell Transplant 19:791, 2010

93. McKay WF, Peckham SM, Marotta JS: The Science of RhBMP-2. Quality Medical Pub., 2006

94. Friede H, Enemark H: Long-term evidence for favorable midfacial growth after delayed hard palate repair in UCLP patients. Cleft Palate Craniofac J 38:323, 2001

95. Lindaman LM: Bone healing in children. Clin Podiatr Med Surg 18:97, 2001

96. Caplan AI, Reuben D, Haynesworth SE: Cell-based tissue engineering therapies: the influence of whole body physiology. Adv Drug Deliv Rev 33:3, 1998

97. Williams A, Semb G, Bearn D, Shaw W, Sandy J: Prediction of outcomes of secondary alveolar bone grafting in children born with unilateral cleft lip and palate. Eur J Orthod 25:205, 2003

98. Long RE, Jr., Spangler BE, Yow M: Cleft width and secondary alveolar bone graft success. Cleft Palate Craniofac J 32:420, 1995

99. van der Meij A, Baart JA, Prahl-Andersen B, Kostense PJ, van der Sijp JR, Tuinzing DB: Outcome of bone grafting in relation to cleft width in unilateral cleft lip and palate patients. Oral Surg Oral Med Oral Pathol Oral Radiol Endod 96:19, 2003

100. Wehby GL, Cassell CH: The impact of orofacial clefts on quality of life and healthcare use and costs. Oral Dis 16:3, 2010

101. Guo J, Li C, Zhang Q, Wu G, Deacon SA, Chen J, Hu H, Zou S, Ye Q: Secondary bone grafting for alveolar cleft in children with cleft lip or cleft lip and palate. COCHRANE DB SYST REV CD008050, 2011

102. van Hout WM, Mink van der Molen AB, Breugem CC, Koole R, Van Cann EM: Reconstruction of the alveolar cleft: can growth factor-aided tissue engineering replace autologous bone grafting? A literature review and systematic review of results obtained with bone morphogenetic protein-2. Clin Oral Investig 15:297, 2011

103. Evans D: Hierarchy of evidence: a framework for ranking evidence evaluating healthcare interventions. J Clin Nurs 12:77, 2003

104. Slavin RE: Best-evidence synthesis: An alternative to meta-analytic and traditional reviews. Educational Researcher 15:5, 1986

105. Phillips B, Ball C, Sackett D, Badenoch D, Straus S, Haynes B, Dawes M:Oxford Centre for Evidence-based Medicine Levels of Evidence 1998:Updated by Jeremy Howick March 2009: http://www.cebm.net/?o=1116

106. Salyer KE: Primary reconstruction of alveolar clefts using recombinant human bone morphogenic protein-2: clinical and radiographic outcomes. J Craniofac Surg 20 Suppl 2:1765, 2009

107. Chin M: Primary reconstruction of alveolar clefts using recombinant human bone morphogenetic protein-2: clinical and radiologic outcomes. J Craniofac Surg 20 Suppl 2:1766, 2009

108. Epstein NE: Pros, cons, and costs of INFUSE in spinal surgery. Surg Neurol Int 2:10, 2011

109. Bergland O, Semb G, Abyholm FE: Elimination of the residual alveolar cleft by secondary bone grafting and subsequent orthodontic treatment. Cleft Palate J 23:175, 1986

110. Witherow H, Cox S, Jones E, Carr R, Waterhouse N: A new scale to assess radiographic success of secondary alveolar bone grafts. Cleft Palate Craniofac J 39:255, 2002

111. Kindelan JD, Nashed RR, Bromige MR: Radiographic assessment of secondary autogenous alveolar bone grafting in cleft lip and palate patients. Cleft Palate Craniofac J 34:195, 1997

112. Nightingale C, Witherow H, Reid FD, Edler R: Comparative reproducibility of three methods of radiographic assessment of alveolar bone grafting. Eur J Orthod 25:35, 2003

113. Ahmad M, Jenny J, Downie M: Application of cone beam computed tomography in oral and maxillofacial surgery. Aust Dent J 57 Suppl 1:82, 2012

114. Scarfe WC, Farman AG, Sukovic P: Clinical applications of cone-beam computed tomography in dental practice. J Can Dent Assoc 72:75, 2006

115. Chan HL, Misch K, Wang HL: Dental imaging in implant treatment planning. Implant Dent 19:288, 2010

116. Roberts JA, Drage NA, Davies J, Thomas DW: Effective dose from cone beam CT examinations in dentistry. Br J Radiol 82:35, 2009

117. Carragee EJ, Hurwitz EL, Weiner BK: A critical review of recombinant human bone morphogenetic protein-2 trials in spinal surgery: emerging safety concerns and lessons learned. Spine J 11:471, 2011

118. Devine JG, Dettori JR, France JC, Brodt E, McGuire RA: The use of rhBMP in spine surgery: is there a cancer risk? Evid Based Spine Care J 3:35, 2012

119. Waite PD, Waite DE: Bone grafting for the alveolar cleft defect. Semin Orthod 2:192, 1996

120. Zuk PA: Tissue engineering craniofacial defects with adult stem cells? Are we ready yet? Pediatr Res 63:478, 2008

121. Deifenderfer DL, Osyczka AM, Reilly GC, Leboy PS: BMP responsiveness in human mesenchymal stem cells. Connect Tissue Res 44:305, 2003

122. Jaiswal N, Haynesworth SE, Caplan AI, Bruder SP: Osteogenic differentiation of purified, culture-expanded human mesenchymal stem cells in vitro. J Cell Biochem 64:295, 1997

123. Hanada K, Dennis JE, Caplan AI: Stimulatory effects of basic fibroblast growth factor and bone morphogenetic protein-2 on osteogenic differentiation of rat bone marrow-derived mesenchymal stem cells. J Bone Miner Res 12:1606, 1997

124. Wang L, Huang Y, Pan K, Jiang X, Liu C: Osteogenic responses to different concentrations/ratios of BMP-2 and bFGF in bone formation. Ann Biomed Eng 38:77, 2010

125. Takita H, Tsuruga E, Ono I, Kuboki Y: Enhancement by bFGF of osteogenesis induced by rhBMP-2 in rats. Eur J Oral Sci 105:588, 1997

126. Fujimura K, Bessho K, Okubo Y, Kusumoto K, Segami N, Iizuka T: The effect of fibroblast growth factor-2 on the osteoinductive activity of recombinant human bone morphogenetic protein-2 in rat muscle. Arch Oral Biol 47:577, 2002

127. van Driel M, Pols HA, van Leeuwen JP: Osteoblast differentiation and control by vitamin D and vitamin D metabolites. Curr Pharm Des 10:2535, 2004

128. Beresford JN, Joyner CJ, Devlin C, Triffitt JT: The effects of dexamethasone and 1,25-dihydroxyvitamin D3 on osteogenic differentiation of human marrow stromal cells in vitro. Arch Oral Biol 39:941, 1994

129. van Driel M, Koedam M, Buurman CJ, Roelse M, Weyts F, Chiba H, Uitterlinden AG, Pols HA, van Leeuwen JP: Evidence that both 1alpha,25-dihydroxyvitamin D3 and 24-hydroxylated D3 enhance human osteoblast differentiation and mineralization. J Cell Biochem 99:922, 2006

130. Kirsch T, Nickel J, Sebald W: BMP-2 antagonists emerge from alterations in the low-affinity binding epitope for receptor BMPR-II. Embo J 19:3314, 2000

131. Ruppert R, Hoffmann E, Sebald W: Human bone morphogenetic protein 2 contains a heparin-binding site which modifies its biological activity. Eur J Biochem 237:295, 1996

132. Frank O, Heim M, Jakob M, Barbero A, Schafer D, Bendik I, Dick W, Heberer M, Martin I: Real-time quantitative RT-PCR analysis of human bone marrow stromal cells during osteogenic differentiation in vitro. J Cell Biochem 85:737, 2002

133. Anderson HC: Mechanism of mineral formation in bone. Lab Invest 60:320, 1989

134. Varkey M, Kucharski C, Doschak MR, Winn SR, Brochmann EJ, Murray S, Matyas JR, Zernicke RF, Uludag H: Osteogenic response of bone marrow stromal cells from normal and ovariectomized rats treated with a low dose of basic fibroblast growth factor. Tissue Eng 13:809, 2007

135. Fromigue O, Marie PJ, Lomri A: Differential effects of transforming growth factor beta2, dexamethasone and 1,25-dihydroxyvitamin D on human bone marrow stromal cells. Cytokine 9:613, 1997

136. Chaudhary LR, Hofmeister AM, Hruska KA: Differential growth factor control of bone formation through osteoprogenitor differentiation. Bone 34:402, 2004

137. Kim IS, Song YM, Cho TH, Park YD, Lee KB, Noh I, Weber F, Hwang SJ: In vitro response of primary human bone marrow stromal cells to recombinant human bone morphogenic protein-2 in the early and late stages of osteoblast differentiation. Dev Growth Differ 50:553, 2008

138. Piek E Fau - Sleumer LS, Sleumer Ls Fau - van Someren EP, van Someren Ep Fau - Heuver L, Heuver L Fau - de Haan JR, de Haan Jr Fau - de Grijs I, de Grijs I Fau - Gilissen C, Gilissen C Fau - Hendriks JM, Hendriks Jm Fau - van Ravestein-van Os RI, van Ravestein-van Os Ri Fau - Bauerschmidt S, Bauerschmidt S Fau - Dechering KJ, Dechering Kj Fau - van Zoelen EJ, van Zoelen EJ: Osteo-transcriptomics of human mesenchymal stem cells: accelerated gene expression and osteoblast differentiation induced by vitamin D reveals c-MYC as an enhancer of BMP2-induced osteogenesis.

139. Donahue HJ, Li Z, Zhou Z, Yellowley CE: Differentiation of human fetal osteoblastic cells and gap junctional intercellular communication. Am J Physiol Cell Physiol 278:C315, 2000

140. Hankemeier S, Keus M, Zeichen J, Jagodzinski M, Barkhausen T, Bosch U, Krettek C, Van Griensven M: Modulation of proliferation and differentiation of human bone marrow stromal cells by fibroblast growth factor 2: potential implications for tissue engineering of tendons and ligaments. Tissue Eng 11:41, 2005

141. Varkey M, Kucharski C, Haque T, Sebald W, Uludag H: In vitro osteogenic response of rat bone marrow cells to bFGF and BMP-2 treatments. Clin Orthop Relat Res 443:113, 2006

142. Nuttall ME, Patton AJ, Olivera DL, Nadeau DP, Gowen M: Human trabecular bone cells are able to express both osteoblastic and adipocytic phenotype: implications for osteopenic disorders. J Bone Miner Res 13:371, 1998

143. Bernlohr DA, Angus CW, Lane MD, Bolanowski MA, Kelly TJ, Jr.: Expression of specific mRNAs during adipose differentiation: identification of an mRNA encoding a homologue of myelin P2 protein. Proc Natl Acad Sci U S A 81:5468, 1984

144. Ross SR, Graves RA, Greenstein A, Platt KA, Shyu HL, Mellovitz B, Spiegelman BM: A fat-specific enhancer is the primary determinant of gene expression for adipocyte P2 in vivo. Proc Natl Acad Sci U S A 87:9590, 1990

145. Bellows CG, Wang YH, Heersche JN, Aubin JE: 1,25-dihydroxyvitamin D3 stimulates adipocyte differentiation in cultures of fetal rat calvaria cells: comparison with the effects of dexamethasone. Endocrinology 134:2221, 1994

146. Mikami Y, Lee M, Irie S, Honda MJ: Dexamethasone modulates osteogenesis and adipogenesis with regulation of osterix expression in rat calvaria-derived cells. J Cell Physiol 226:739, 2011

147. Shen B, Wei A, Whittaker S, Williams LA, Tao H, Ma DDF, Diwan AD: The role of BMP-7 in chondrogenic and osteogenic differentiation of human bone marrow multipotent mesenchymal stromal cells in vitro. J Cell Biochem 109:406, 2010

148. Neumann K, Endres M, Ringe J, Flath B, Manz R, Haupl T, Sittinger M, Kaps C: BMP7 promotes adipogenic but not osteo-/chondrogenic differentiation of adult human bone marrow-derived stem cells in high-density micro-mass culture. J Cell Biochem 102:626, 2007

149. Akita S, Fukui M, Nakagawa H, Fujii T, Akino K: Cranial bone defect healing is accelerated by mesenchymal stem cells induced by coadministration of bone morphogenetic protein-2 and basic fibroblast growth factor. Wound Repair Regen 12:252, 2004

150. Prockop DJ: Marrow stromal cells as stem cells for nonhematopoietic tissues. Science 276:71, 1997

151. Komori T: Regulation of bone development and extracellular matrix protein genes by RUNX2. Cell Tissue Res 339:189, 2010

152. Setzer B, Bachle M, Metzger MC, Kohal RJ: The gene-expression and phenotypic response of hFOB 1.19 osteoblasts to surface-modified titanium and zirconia. Biomaterials 30:979, 2009

153. Titorencu I, Jinga VV, Constantinescu E, Gafencu AV, Ciohodaru C, Manolescu I, Zaharia C, Simionescu M: Proliferation, differentiation and characterization of osteoblasts from human BM mesenchymal cells. Cytotherapy 9:682, 2007

154. Bidic SM, Calvert JW, Marra K, Kumta P, Campbell P, Mitchell R, Wigginton W, Hollinger JO, Weiss L, Mooney MP: Rabbit calvarial wound healing by means of seeded Caprotite scaffolds. J Dent Res 82:131, 2003

155. Burastero G Fau - Scarfi S, Scarfi S Fau - Ferraris C, Ferraris C Fau - Fresia C, Fresia C Fau - Sessarego N, Sessarego N Fau - Fruscione F, Fruscione F Fau - Monetti F, Monetti F Fau - Scarfo F, Scarfo F Fau - Schupbach P, Schupbach P Fau - Podesta M, Podesta M Fau - Grappiolo G, Grappiolo G Fau - Zocchi E, Zocchi E: The association of human mesenchymal stem cells with BMP-7 improves bone regeneration of critical-size segmental bone defects in athymic rats. 2010

156. Skoog T: The use of periosteal flaps in the repair of clefts of the primary palate. Cleft Palate J 2:332, 1965

157. Santiago PE, Grayson BH, Cutting CB, Gianoutsos MP, Brecht LE, Kwon SM: Reduced need for alveolar bone grafting by presurgical orthopedics and primary gingivoperiosteoplasty. Cleft Palate Craniofac J 35:77, 1998

158. De Riu G, Meloni SM, Raho MT, Gobbi R, Tullio A: Delayed iliac abscess as an unusual complication of an iliac bone graft in an orthognathic case. Int J Oral Maxillofac Surg 37:1156, 2008

159. Melnick M, Jaskoll T, Slavkin HC: Corticosteroid-induced cleft lip in mice: a teratologic, topographic, and histologic investigation. Am J Med Genet 10:333, 1981

160. Gong SG, White NJ, Sakasegawa AY: The Twirler mouse, a model for the study of cleft lip and palate. Arch Oral Biol 45:87, 2000

161. Juriloff DM, Harris MJ: Mouse genetic models of cleft lip with or without cleft palate. Birth Defects Res A Clin Mol Teratol 82:63, 2008

162. Yamada T, Mishima K, Fujiwara K, Imura H, Sugahara T: Cleft lip and palate in mice treated with 2,3,7,8-tetrachlorodibenzo-p-dioxin: a morphological in vivo study. Congenit Anom (Kyoto) 46:21, 2006

163. Schmitz JP, Hollinger JO: The critical size defect as an experimental model for craniomandibulofacial nonunions. Clin Orthop Relat Res 299, 1986

164. Boyne PJ: Use of marrow-cancellous bone grafts in maxillary alveolar and palatal clefts. J Dent Res 53:821, 1974

165. Puumanen K, Kellomaki M, Ritsila V, Bohling T, Tormala P, Waris T, Ashammakhi N: A novel bioabsorbable composite membrane of Polyactive 70/30

and bioactive glass number 13--93 in repair of experimental maxillary alveolar cleft defects. J Biomed Mater Res B Appl Biomater 75:25, 2005

166. Gomes FE, Moraes RB, Luz JG: Effects of temporal muscle detachment and coronoidotomy on facial growth in young rats. Braz Oral Res 26:348, 2012

167. Cruz DZ, Rodrigues L, Luz JG: Effects of detachment and repositioning of the medial pterygoid muscle on the growth of the maxilla and mandible of young rats. Acta Cir Bras 24:93, 2009

168. Hebel R, Stromberg MW: Anatomy and embryology of the laboratory rat. BioMed Verlag, 1986

169. El Deeb M, Messer LB, Lehnert MW, Hebda TW, Waite DE: Canine eruption into grafted bone in maxillary alveolar cleft defects. Cleft Palate J 19:9, 1982

170. Worthington P, Rubenstein J, Hatcher DC: The role of cone-beam computed tomography in the planning and placement of implants. J Am Dent Assoc 141 Suppl 3:19S, 2010

171. Ekeland A, Engesoeter LB, Langeland N: Influence of age on mechanical properties of healing fractures and intact bones in rats. Acta Orthop Scand 53:527, 1982

172. Bessa PC, Casal M, Reis RL: Bone morphogenetic proteins in tissue engineering: the road from laboratory to clinic, part II (BMP delivery). J Tissue Eng Regen Med 2:81, 2008

173. Aghaloo T, Cowan CM, Zhang X, Freymiller E, Soo C, Wu B, Ting K, Zhang Z: The effect of NELL1 and bone morphogenetic protein-2 on calvarial bone regeneration. J Oral Maxillofac Surg 68:300, 2010

174. Lee KB, Taghavi CE, Murray SS, Song KJ, Keorochana G, Wang JC: BMP induced inflammation: a comparison of rhBMP-7 and rhBMP-2. J Orthop Res 30:1985, 2012

175. Ratanavaraporn J, Furuya H, Tabata Y: Local suppression of pro-inflammatory cytokines and the effects in BMP-2-induced bone regeneration. Biomaterials 33:304, 2012

176. Jovanovic SA, Hunt DR, Bernard GW, Spiekermann H, Wozney JM, Wikesjo UM: Bone reconstruction following implantation of rhBMP-2 and guided bone regeneration in canine alveolar ridge defects. Clin Oral Implants Res 18:224, 2007

177. Hunt DR, Jovanovic SA, Wikesjo UM, Wozney JM, Bernard GW: Hyaluronan supports recombinant human bone morphogenetic protein-2 induced bone reconstruction of advanced alveolar ridge defects in dogs. A pilot study. J Periodontol 72:651, 2001

178. Springer IN, Acil Y, Kuchenbecker S, Bolte H, Warnke PH, Abboud M, Wiltfang J, Terheyden H: Bone graft versus BMP-7 in a critical size defect--cranioplasty in a growing infant model. Bone 37:563, 2005

179. Spiro AS, Beil FT, Schinke T, Schilling AF, Eulenburg C, Rueger JM, Amling M: Short-term application of dexamethasone enhances bone morphogenetic protein-7-induced ectopic bone formation in vivo. J Trauma 69:1473, 2010

180. Prata CA, Lacerda SA, Brentegani LG: Autogenous bone graft associated with enamel matrix proteins in bone repair. Implant Dent 16:413, 2007

181. Donos N, Kostopoulos L, Karring T: Augmentation of the mandible with GTR and onlay cortical bone grafting. An experimental study in the rat. Clin Oral Implants Res 13:175, 2002